Multiple axes of inter-organ signaling regulate organ scaling

A Dissertation
SUBMITTED TO THE FACULTY OF
UNIVERSITY OF MINNESOTA
BY

AMBUJ UPADHYAY

IN PARTIAL FULFILLMENT OF THE REQUIREMENTS
FOR THE DEGREE OF
DOCTOR OF PHILOSOPHY

Advisor
MICHAEL B. O'CONNOR

August 2019

Acknowledgements

First and foremost, I would like to thank Michael O'Connor for allowing me to conduct my graduate work in his lab. I am forever indebted for to him for being an incredible mentor and a friend. His patience has allowed me to craft my own project, and develop my own ideas which has been the best training anyone could ask for.

I would like to also thank the past and present members of the O'Connor lab for their support in and especially out of the lab. Going to work was never a chore because of the friendly and engaging atmosphere that they all created. Their selflessness and eagerness to collaborate was an essential aspect of producing this body of work. In particular I would like to thank Aidan Peterson, Mary-Jane O'Connor, Myung-Jun Kim, and Lindsay Moss-Taylor for their contributions to this work.

Thank my committee members: Jeff Simon, Thomas Neufeld, Jim Ervasti, Jeongsik Yong, and Laura Gammill. Thank you for the support, criticisms, and scientific guidance throughout my graduate training.

This work was funded in part by the Ray Anderson Fellowship from the GCD department, and NIH grants.

A very special thank you to my friends in the graduate program. Especially the MCSB class of 2012. I came to Minnesota knowing nobody, and in a matter of 2 weeks at Itasca, I made some lifelong friends. Our social fabric is what kept me going year after year, and without you this work would not be possible.

Lastly, I would like to thank my family for always supporting my career goals and encouraging me no matter how uncertain the paths are. As they say, If I have seen further, it is by standing on the shoulder of giants. Without you all, I would not be able to achieve this accomplishment.

Dedication

This dissertation is dedicated to my parents

Urmila Upadhyay
&
Sankat Haran Upadhyay

Abstract

The mechanisms governing static allometry of organ size has long been enigmatic. A central hypothesis predicts that during animal growth, body size is perceived by organs via inter-organ signals, which directs organ growth to match body size. Ligands of the Transforming Growth Factor β (TGFβ) superfamily are prime candidates for mediating this coordination of organ-body size. In *Drosophila*, multiple ligands of the Activin-like subfamily (Myoglianin, Activin-β, and Dawdle) signal via the only type-I receptor Baboon (Babo). Similar to defects in insulin signaling, null mutants of *babo* result in small imaginal discs and small overall body size. This is in part due to metabolic defects caused by defects in Daw signaling. In this dissertation I report how Activin-β and Myoglianin regulate body size and organ growth respectively. In Chapter one, I review known mechanisms governing growth in *Drosophila.* In Chapter two, I show that Activin-β signaling via Babo in the muscles is required for muscle growth and proper body size, but not imaginal disc growth. Remarkably, it is the motoneurons in the central brain secretes Activin-β necessary for body size. In Chapter three, I show that Myoglianin regulates imaginal disc growth which express specific combination of receptors that make the cells sensitive to only one ligand. Additionally, it is the larval muscles secrete Myoglianin which regulates imaginal disc growth but not body size. In chapter four, I speculate as to how such inter-organ signaling mechanisms can ensure proper allometry within species, and suggest additional experiments that would test this emerging model.

Table of Contents

ACKNOWLEDGEMENTS ..... **I**

DEDICATION ..... **II**

ABSTRACT ..... **III**

TABLE OF CONTENTS ..... **IV**

LIST OF FIGURES ..... **VII**

CHAPTER I **1**

INTRODUCTION **1**

1.1 INTER-ORGAN COMMUNICATION 2

1.2 ALLOMETRY 4

1.3 *DROSOPHILA MELANOGASTER* AS A MODEL FOR STUDYING GROWTH 7

1.4 DROSOPHILA LIFE CYCLE 7

1.5 SYSTEMIC REGULATORS OF BODY SIZE IN DROSOPHILA 9

1.5.1 Insulin/IGF-1 signaling 9

1.5.2 TOR signaling 10

1.5.3 Ecdysone and Juvenile Hormone regulate growth 12

1.6 SIGNALING PATHWAYS REGULATING ORGAN GROWTH 14

1.6.1 Ras/Raf/MAPK signaling pathway 14

1.6.2 JNK signaling 16

1.6.3 Hippo signaling 17

1.6.4 Other signaling pathways 18

1.7 TGF Β - SUPERFAMILY 19

1.7.1 Core *Drosophila* TGF-β Family Signaling Components 20

1.7.2 TGF-β family signaling in the wing imaginal disc 24

1.7.3 Models of Dpp gradient formation in the wing disc 25

1.7.4 Modifiers of the Dpp gradient 27

1.7.5 Transcriptional responses to BMP signaling in the wing disc 28

1.7.6 Role of Dpp in regulating tissue growth 30

1.7.7 BMP signaling in pupal wing development 32

1.7.8 Mad is a focal point for integration of cross-pathway signals 33
1.7.9 BMP signaling in other imaginal discs 35
1.7.10 TGF-β family signaling in the nervous system 38
1.7.11 Activin signaling stimulates neuroblast proliferation 43
1.7.12 Activin signaling and axon guidance and target selection 44
1.7.13 Activin signaling and neuronal remodeling 46
1.7.14 Role of TGF-β family signaling in physiological and metabolic homeostasis 48
1.7.15 TGF-β family signaling in metabolic homeostasis 49
1.7.16 TGF-β family signaling regulates hormonal control of Drosophila development. 54
1.8 STATEMENT OF THESIS WORK 56
CHAPTER I FIGURES 57

CHAPTER II 64

MOTONEURON-DERIVED ACTIVINB REGULATES DROSOPHILA BODY SIZE AND TISSUE-SCALING DURING LARVAL GROWTH AND ADULT DEVELOPMENT 64

SUMMARY 65
INTRODUCTION 66
RESULTS 71
Actβ is required for adult viability, normal body size, and correct tissue scaling 71
Actβ disproportionately affects larval muscle and certain polyploid tissue sizes 73
Actβ mutants feed normally but grow slowly 74
Overexpression of Actβ in its normal pattern produces larger and slower-growing larvae 77
Tissue and cell-type specific rescue experiments identify several potential sources of Actβ for controlling body size. 78
Motoneuron-derived Actβ regulates body size and viability 80
Motoneuron derived Actβ signals through the canonical Babo/dSmad2 pathway to control muscle and body size. 83
DISCUSSION 85
Localized versus systemic effects of Actβ 85
Mechanisms of Actβ control of tissue size 88
Larval versus Adult requirements for Actβ 89
Body-appendage scaling 91

TGFβ control of body size in other animals 94
MATERIALS AND METHODS 96
CHAPTER II FIGURES 103
CHAPTER III 121
MUSCLE-DERIVED MYOGLIANIN REGULATES IMAGINAL DISC GROWTH 121
SUMMARY 122
INTRODUCTION 123
RESULTS 127
Myoglianin is required for proper discs growth 127
Myo signals canonically via dSmad2 130
Myo signaling in imaginal discs requires a specific isoform of Baboon 131
Babo-a, Punt, and Plum mediate non-canonical signaling in wing imaginal discs 133
Muscle derived myoglianin signals to the wing disc 136
Overexpression of Myo in muscle or fat body rescues myo mutant disc growth 138
DISCUSSION 139
Only Myo regulates imaginal disc size 140
Plum and Punt are required for efficient Babo-A signaling to dSmad2 in the wing disc 141
Intrinsic (intra-organ) vs extrinsic (inter-organ) mode of Myo signaling 143
Significance of inter-organ communication 144
MATERIALS AND METHODS 146
CHAPTER III FIGURES 150
CHAPTER IV 165
CONCLUDING REMARKS & FUTURE DIRECTIONS 165
Brief summary 166
Significance of brain - muscle and muscle - wing communication 166
Future directions 169
REFRENCES 171

List of Figures

FIGURE 1-1. STATIC ALLOMETRY OF ORGAN SIZE WITHIN AND AMONG SPECIES.....58
FIGURE 1-2. LIMB XENOGRAFT EXPERIMENTS BY TWITTY AND SCHWIND. 59
FIGURE 1-3. CORE TRANSFORMING GROWTH FACTOR B (TGF-B) FAMILY SIGNALING COMPONENTS IN DROSOPHILA.....60
FIGURE 1-4. TGFB FAMILY ACCESSORY FACTORS IN *DROSOPHILA* 61
FIGURE 1-5. DPP SIGNALING IN *DROSOPHILA* WING DEVELOPMENT. 62
FIGURE 1-6. BMP AND ACTIVIN SIGNALING AT THE NEUROMUSCULAR JUNCTION 63
FIGURE 2-1. *ACTB* NULL MUTANTS EXHIBIT A SMALL BODY SIZE AND LATE PUPAL LETHALITY. 103
FIGURE 2-2. *ACTB* MUTANT ADULT ESCAPERS HAVE A DISPROPORTIONATELY SMALLER ABDOMEN COMPARED TO HEAD, THORAX, LEG, OR WING. 104
FIGURE 2-3. ACTB DISPROPORTIONATELY AFFECTS THE SIZE OF LARVAL BODY WALL MUSCLES AND FAT BODY NUCLEI SIZE. 105
FIGURE 2-4. *ACTB* MUTANT LARVAE GROW SLOWLY BUT DO NOT EXHIBIT DIFFERENCES IN CRITICAL WEIGHT OR DEVELOPMENTAL TIMING. 106
FIGURE 2-5. ACTB OVEREXPRESSION INCREASES BODY SIZE AND DELAYS DEVELOPMENTAL TIMING. 108
FIGURE 2-6. ANALYSIS OF *ACTB-GAL4* DRIVER EXPRESSION PATTERN (GREEN) IN L3 LARVAE. 109
FIGURE 2-7. EXPRESSION OF ACTB FROM SPECIFIC CELL TYPES DIFFERENTIALLY RESCUES ACTB MUTANT PHENOTYPES.....112
FIGURE 2-8. MOTOR NEURON DERIVED ACTB SIGNALING THROUGH BABO AND DSMAD2 CONTROLS BODY SIZE. 113
FIGURE 2-9 *ACTB* DOES NOT AFFECT MUSCLE NUCLEI NUMBER 114
FIGURE 2-10 SIZE OF VARIOUS POLYPLOID NUCLEI IN *ACTB* MUTANTS.....115
FIGURE 2-11 RNA *IN SITU* HYBRIDIZATION OF *ACTB* SHOWS EXPRESSION IN VARIOUS TISSUES 116
FIGURE 2-12 OVEREXPRESSION OF *ACTB* IN MOTONEURONS OR NEUROENDOCRINE CELLS INCREASES ADULT BODY SIZE. 117

FIGURE 2-13 HYPERACTIVATION OF ACTIVIN SIGNALING IN MUSCLES BUT NOT FATBODY IS LARVAL LETHAL 118
FIGURE 2-14 OK372-GAL4 IS NOT EXPRESSED IN DIMM+ NEUROENDOCRINE CELLS.....119
FIGURE 2-15 MUSCLE SPECIFIC ACTIVATION OF ACTIVIN SIGNALING INCREASES BODY SIZE BUT NOT WING SIZE.....120
FIGURE 3-1. *MYOGLIANIN* REGULATES SIZE OF IMAGINAL DISCS BY AND ACTIVATES DSMAD2. 151
FIGURE 3-2. BABOON-A REGULATES WING DISC GROWTH.....153
FIGURE 3-3. BABO-A AND PUNT ARE REQUIRED FOR NON-CANONICAL SILENCING OF *BRK.* .155
FIGURE 3-4. MUSCLE DERIVED MYO IS REQUIRED FOR NON-CANONICAL BABO ACTIVATION IN IMAGINAL DISCS. 157
FIGURE 3-5. OVEREXPRESSION OF *MYO* IN MUSCLES AND FAT-BODY RESCUES WING DISC SIZE OF *MYO* MUTANTS. 158
FIGURE 3-6. *MYO* MUTANTS SHOW NO DEFECTS IN CELL DEATH OR CELL GROWTH. 159
FIGURE 3-7 QPCR ANALYSIS OF *BABO* ISOFORM EXPRESSION IN LARVAL TISSUES 160
FIGURE 3-8. RNAI FOR *BABO-A* RESCUES WING DISC OVERGROWTH DUE TO *DSMAD2 RNAI.* 162
FIGURE 3-9. *PLUM* IS REQUIRED FOR NON-CANONICAL BABO ACTIVITY. 163
FIGURE 3-10. MUSCLE OVEREXPRESSION OF *MYO* INCREASES WING SIZE.....164
FIGURE 4-1. MODEL OF WING/MUSCLE SCALING VIA MYO SIGNALING 170

Chapter I

Introduction

Section 1.7 of this introduction is modified from a previously published work in which several co-authors contributed equally (Upadhyay et al., 2017) In particular Arpan C. Ghosh generated figure 1-3 and 1-4. Myung-Jun Kim generated figure 1-6. I generated figure 1-5.

1.1 INTER-ORGAN COMMUNICATION

Early in evolution life evolved from a heterogeneous soup of chemical reactions into a more specialized compartmentalization of cellular function known as organelles. Subsequent evolution of multicellularity, specialized cells, tissues, and organs has given rise to complex lifeforms we know today. Communication between every level of this hierarchy (from organelles to organs) is essential for the survival of the organism. Certain forms of communication like intra-cellular signaling are ubiquitous. For example, virtually in every cell adenosine triphosphate and adenosine diphosphate (ATP/ADP) levels signal to phosphofrucktokinase to regulate glycolysis and energy homeostasis. Communication between cells and organs are just as important. Organs have acquired specialized tasks and coordination among them are necessary for proper function as a whole.

Depending on the context, mechanisms for inter-organ communication can vary dramatically from small molecules, and proteins to even mechanical forces. One of the most obvious types of inter-organ communication involves the nervous systems and muscles. Motoneurons signal to the skeletal muscles via the neuromuscular junction to induce muscle contraction. When a wave of chemical potential from the neuron cell body reaches the axon terminal, small synaptic vesicles containing neurotransmitters such as acetylcholine are released by the neurons into the junction which are taken up by the muscles

triggering contraction (Kuo and Ehrlich, 2015). In humans, some muscles lining the internal vital organs can also signal back to the brain via the vagus nerve (Chambers et al., 2013). Among the many different inputs into the vagus nerve, stretching of smooth muscles in the stomach walls stimulates the nerve which is thought to trigger satiety (Williams et al., 2016; Zagorodnyuk et al., 2001). Another common type of inter-organ communication occurs via protein ligands. Probably the most widely recognized protein ligand involved in inter-organ communication is Insulin. In humans, nutrient uptake causes a spike in circulating sugar levels which then induces Insulin secretion from the pancreas (Quianzon and Cheikh, 2012). Circulating insulin triggers sugar uptake in most tissues, but also has other roles in different peripheral tissues (Quianzon and Cheikh, 2012; Rosenfeld, 2002). Defects in insulin signaling leads to numerous physiological complications collectively known as metabolic syndrome (Eckel et al., 2005).

The examples above highlight how different organs are linked in order to maintain energy homeostasis. Such mechanisms are widely conserved because they provide the basic building blocks for organisms to grow and maximize fitness (Nylin and Gotthard, 1998). Accompanying overall growth, is the growth of individual organs. During animal development, different organs are specified at different stages and grow at different rates (Penzo-Méndez and Stanger, 2015). This raises the question of how growth among different organs coordinated. Is organ growth controlled passively by regulating nutrient uptake then differential

processing in peripheral tissues? Or do organs communicate their size status with one another to regulate growth? As with most biological questions, the answer could possibly be both. Even though we know at great detail how regulation of nutrient metabolism affects organ growth, it remains less clear whether different organs in the body directly communicate to regulate each other's growth.

1.2 ALLOMETRY

When discussing inter-organ coordination of growth, the term allometry comes to mind (Huxley, 1932). In the broadest sense, allometry refers to the scaling relationship between a specific trait/parameter (e.g. metabolic rate or organ size) to body size (Garland and Carter, 1994; Gould, 1966; Schmidt-Nielsen, 1984; Spence, 2009). In this manuscript, allometry will generally refer to the scaling of organs to body size. Allometric relationships can be characterized in three different ways: ontogenetic allometry refers to the variation in organ size through development of an individual, static allometry refers to variations in organ to body size among individuals in a population, and phylogenetic allometry refers to variation across multiple species and/or taxa (Frankino et al., 2009; Stern and Emlen, 1999). With regard to organ/body size, it is well known that within species animals tend to have a stereotypic ratio of organ to body size, i.e. static allometry. However, allometry varies significantly among taxa, phylogenetic

allometry (Frankino et al., 2009; Spence, 2009). This has been one of the greatest mysteries in evolutionary developmental biology; how does limited variability within species coincide with high variability across taxa? To comprehend this idea, two fundamental questions must be investigated. First, what is the mechanism of morphological allometry among individuals within a specie and second, how does it evolve?

The first step to asking the larger question of evolution of allometry is determining the how organs scale with body size within a specie. Static morphological allometry can be assessed by measuring variation of organ/body size in the wild population (genetic allometry), or in the laboratory by altering environmental inputs such as temperature and nutrition (environmental allometry) (Frankino et al., 2009). Such quantitative measurements can be summarized by the equation $y = bx^a$, where x represents body size, y represents the size of a specific body part, and a rep resents the allometric coefficient (Frankino et al., 2009; Huxley, 1932). Log transformation of the data results in a linear relationship between organ and body size where a is the slope of the regression line (Figure 1-1 A) (Frankino et al., 2009). Comparing the static allometry of related species can sometimes reveal different coefficients for each group (Figure 1-1 B,C) (Frankino et al., 2009; Gould, 1966; Spence, 2009).

Identifying the allometric coefficient for different groups doesn't really identify the underlying mechanism governing allometry. That requires experimentation to test the system. Before the modern day genetic and

molecular techniques, in the early 20th century Twitty and Schwind made one of the seminal findings in the field using tissue grafting experiments in salamanders (Twitty and Schwind, 1931). Since perturbing overall body size independent of other body parts is challenging, the reverse was the only feasible experiment, and luckily some salamanders are highly amenable to grafting body parts. They obtained two salamanders, *Amblystoma punctatum* and *Amblystoma trigrinum*, which develop to significantly different body size that have proportionally sized limbs. Then they grafted a limb primordium from the large salamander onto the body of the small animal, and vice versa. Surprisingly, they found that the grafted limbs grew to match the size of the donor animal not the host (Figure 1-2) (Twitty and Schwind, 1931). In essence they had disrupted the allometric relationship of the limb size to overall body. But more importantly, their experiments along with numerous others from different animal models suggests that the final organ size is largely determined by tissue intrinsic factors (Bryant and Simpson, 1984). Thus, the body provides permissive signals for growth, such as nutrition and hormones, and the organs provide their own growth signals to determine the final organ size.

Modern day research aims to identify the molecular players that regulate overall body size as well as organ size. How these mechanisms affect growth locally and systemically in the animal will shed light on how static allometry is attained. Furthermore, phylogenetic analysis of the molecular players may help answer the larger question of how allometry evolves to give rise to the diversity

we see today. To help answer some of these questions we need a powerful animal model system. Below I will discuss the *Drosophila melanogaster* model and our current understanding of how body and organ size is regulated in this system.

1.3 *DROSOPHILA MELANOGASTER* AS A MODEL FOR STUDYING GROWTH

Drosophila melanogaster, commonly known as the fruit fly or vinegar fly, was established as model organism over a century ago by Thomas Hunt Morgan lab at Columbia University. Initially used to study heredity, today the portfolio of research using *D. melanogaster* is vast, and has claimed 8 Nobel Prizes as of 2018. Many of the disease associated genes in Humans have orthologs in *Drosophila*, making them a great model system to study molecular function (Chien et al., 2002). Furthermore, the use of an extensive and powerful genetic toolkit allows researchers to rapidly test hypothesis and identify the associated molecular mechanism.

1.4 DROSOPHILA LIFE CYCLE

D. melanogaster are a part of the order Diptera, and are holomatabolous insects that undergo complete metamorphosis via a pupal stage, as opposed to

hemimatabolous meaning incomplete metamorphosis. Adults sexually reproduce, and after mating females begin to lay eggs. At 25 degree Celsius egg development takes ~24 hours followed by three larval instar stages which lasts a total of four days and are demarcated by cuticle molting events between each stage. During the larval period larvae grows approximately 200 fold, the bulk of which occurs during the third instar stage lasting 48 hours (Church and Robertson, 1966). At the end of the larval stage the animal stops growing and forms a pupae to begin metamorphosis. During the 4-5 day pupal stage, many of the larval tissues undergo histolysis and new adult structures are formed from 19 imaginal discs that developed during the larval stage (Hales et al., 2015). The term imaginal comes from the Latin word *imago* meaning image which refers to the adult fly stage, and they are called disc because they resemble a flat round structure (Aldaz and Escudero, 2010). After the adults emerge from the pupal case, they mature and are reproductively active within several hours to complete the life cycle. Important to note that although the adults feed during their lifetime, they do not grow in either length or mass. This makes the larval growth period incredibly important for accumulating as much energy/mass as possible in order to survive the non-feeding pupal stage as well as maximizing reproductive fitness.

1.5 SYSTEMIC REGULATORS OF BODY SIZE IN DROSOPHILA

As mentioned above, growth occurs only during the larval stages, both in terms of the overall body size and also for the individual organs like the imaginal discs. Below I will briefly discuss what is known about how overall body size is regulated.

1.5.1 Insulin/IGF-1 signaling

The major regulator of growth in Drosophila is the Insulin/Insulin-like Growth Factor (IGF) signaling (IIS) pathway. In vertebrates insulin mediates metabolic functions and the IGF signaling promotes cell and tissue growth (Nakae et al., 2001). However, in Drosophila the two pathways are not distinct because they use the same ligands and receptors and mediate both metabolic and growth functions (Boulan et al., 2015). Upon feeding, in *Drosophila* free sugar in the hemolymph stimulates secretion of Insulin-like peptides (Dilps) from the Insulin producing cells (IPCs) in the brain (Colombani et al., 2003). Circulating Dilps travel to peripheral tissues and bind to Insulin receptor (InR), which then activates phosphoinositide-3-kinase (PI3K) (Boulan et al., 2015). PI3K activation leads to Akt activation which then regulates a host of different pathways, mainly Ras/Raf/Mapk, FOXO, and TOR pathways, all of which converge to regulate growth at transcription and translation levels (Boulan et al., 2015; Gokhale and Shingleton, 2015; Teleman, 2009). In *Drosophila* mutations that inhibit IIS, such as *Dilp*, *InR*, and *chico* knockouts, results in dramatically

smaller animals (Böhni et al., 1999; Grönke et al., 2010). Conversely ectopic activation of the pathway, such as *Dilp* overexpression, results in larger animals (Ikeya et al., 2002). Tissue specific perturbation of IIS signaling by FOXO expression leads to differential growth of the organs, which explains why different organs are more or less sensitive to external inputs like nutrition (Tang et al., 2011). Important to note that perturbing IIS pathway ubiquitously, such as whole animal mutants, affects both the overall body size as well as individual organ size, like the wing, in the same direction (Gokhale and Shingleton, 2015; Ikeya et al., 2002). This suggests that in the absence of Insuling signaling, static allometry is preserved. Therefore, even though IIS pathway is important for growth, it does not regulate static allometry of organ size (Mirth and Shingleton, 2012).

1.5.2 TOR signaling

Similar to IIS pathway, nutrient uptake provides the initial input to activate Target of Rapamycin (TOR) signaling which is conserved from yeast to mammals (Boulan et al., 2015). TOR gets its name from loss of function mutants that are resistant to the growth suppressing properties of Rapamycin, an anticancer drug (Heitman et al., 1991; Sabatini, 2017). Upon feeding and digestion, free amino acids in the hemolymph are taken up the peripheral tissues and activate TOR signaling (Boulan et al., 2015; Wolfson and Sabatini, 2017). TOR exists in two different complex, TORC1 and TORC2, however TORC1 is the primary regulator

of nutrient dependent growth (Boulan et al., 2015; Wolfson and Sabatini, 2017). TORC1 activity is requires Rheb, mutants of which are significantly smaller (Saucedo et al., 2003; Stocker et al., 2003). Recently, several amino acid molecular sensors have been identified in mammalian cell culture models that activate TORC1 (Wolfson and Sabatini, 2017). These include arginine sensors SLC38A9 and CASTOR1 that localize to lysosomes and cytosol respectively, and leucine sensor Sestrin2 that is also cytosolic (Chantranupong et al., 2016; Wang et al., 2015; Wolfson et al., 2016; Wyant et al., 2017). In *Drosophila*, only Sestrin2 is available to detect amino acids (Wolfson and Sabatini, 2017). In addition to amino acids, TORC1 activity can also be regulated by AKT signaling (see section 1.5.1 above). AKT activity inhibits TSC1/2, which in turn inhibits Rheb activity (Boulan et al., 2015; Wolfson and Sabatini, 2017). Ultimately TORC1 regulates growth by activating S6 Kinase (S6K) and inhibiting 4E-BP which promotes protein synthesis (Boulan et al., 2015). Therefore under normal conditions nutrient uptake by the larvae results in both IIS pathway activation as a result of free sugars and TOR pathway activation as a result of free amino acids, both of which converge to positively regulate tissue growth and overall all size.

1.5.3 Ecdysone and Juvenile Hormone regulate growth

Developmental checkpoints and timing of metamorphosis are critical aspects of insect biology which are regulated by the steroid hormone Ecdysone and a sesquiterpenoid Juvenile Hormone (JH) (Rewitz et al., 2013). Both of these hormones are synthesized in the Ring gland, but by different sub-compartments. Ecdysone is synthesized by the Prothoracic gland and JH by the corpus allatum (Rewitz et al., 2013). Ecdysone is the master regulator of developmental checkpoints in insects.

Ecdysone is secreted in pulses during the larval growth period that induces molting transitions between larval instar stage as well as the induction of pupal stage metamorphosis the end of larval growth (Riddiford, 1993). The process of molting is essential for growth, because it allows the larvae to shed its constrictive outer cuticle. The ecdysone peak at the end of third instar is also important, because it marks the end of the growth period (Rewitz et al., 2013). Multiple inputs regulate ecdysone production in the PG. The main effectors of ecdysone production and secretion are IIS (see section 1.5.1), TOR (see section 1.5.2), and Prothoracicotophic hormone (PTTH) signaling pathways (see reviews (Boulan et al., 2015; Rewitz et al., 2013). PTTH is a peptide ligand that is produced in a discrete set of neurons in the brain which synapses onto the PG cells (Gilbert, 2004; McBrayer et al., 2007). In the PG, PTTH activates MAPK pathway via its receptor Torso (Rewitz et al., 2009). Loss of function mutants of PTTH, Torso, Ras/MAPK, or genetically ablating the PTTH neurons result in

larger animals because of a failure to produce ecdysone at the correct time, hence the larvae continues to feed and grow (Caldwell et al., 2005; McBrayer et al., 2007; Rewitz et al., 2009; Shimell et al., 2018).

PG secreted ecdysone acts systemically via the hemolymph and regulates target gene expression in peripheral tissues (King-Jones and Thummel, 2005). Once Ecdysone is taken up by peripheral tissues, it is converted to its active version 20-hydroxyecdysone (20E) which then binds to cytosolic Ecdysone Receptor (EcR) and Ultraspiracle (Usp), and regulates transcription of target genes (Thomas et al., 1993; Uyehara and McKay, 2019; Yao et al., 1993). Interestingly, ecdysone signaling in different tissues results in drastically different outcomes. Ecdysone signaling in imaginal discs promotes growth and differentiation by repressing 4E-BP (see 1.5.2) and derepressing patterning genes such as *wg* (Herboso et al., 2015; Mirth et al., 2009). Additionally, ecdysone signaling results in lower levels of systemic IIS, which is rescued by EcR knockdown specifically in the fat-body (Boulan et al., 2015). It turns out the basal levels of ecdysone inhibits Myc activity which then affects *Dilp* expression and secretion from the IPCs through an unknown mechanism (Delanoue et al., 2010).

JH signaling plays a minor role in regulating growth. JH is expressed throughout larval development and is rapidly destroyed before the onset of pupariation (Browder et al., 2001; Riddiford et al., 2010). The role of JH in *Drosophila* is unclear however, in other model systems it is thought to be

required for Ecdysone production and secretion (Browder et al., 2001). In *Drosophila* neither ablation of the corpus allatum or exogenous JH is able to alter the timing of Ecdysone dependent puparium formation (Nijhout et al., 2014; Riddiford et al., 2010). However, JH depleted animals do have a slower growth rate and are smaller (Riddiford et al., 2010). In summary fine tuning of ecdysone and JH signaling throughout larval development not only affects organ growth directly but also body size by regulating systemic insulin signaling and developmental checkpoints.

1.6 SIGNALING PATHWAYS REGULATING ORGAN GROWTH

The previous sections highlight systemic factors circulating in the hemolymph which affect growth globally. In the following sections, I will discuss tissue intrinsic factors and signaling pathways that are crucial for regulating organ growth.

1.6.1 Ras/Raf/MAPK signaling pathway

Throughout wing imaginal disc development, multiple growth factors signal in the wing imaginal disc which converge onto the Ras/Raf/MAPK signaling pathway. These include EGF, FGF, and to a lesser extent Dilps (see section 1.5.1) which activate their respective receptor tyrosine kinases on the plasma

membrane. Ligand activation ultimately leads to the activation of the small G-protein Ras. GTP bound Ras activates Raf kinase and which activates MEK1/2 which then activates MAPK. Activated MAPK then translocates to the nucleus where it phosphorylates several transcription factors which regulate expression of hundreds of genes. For a detailed review of the Ras/Raf/MAPK signaling pathway, see reviews (Keshet and Seger, 2010; Sopko and Perrimon, 2013).

Ras/Raf/MAPK signaling regulates growth in multiple larval tissues. Overexpression of activated Ras in wing disc cell leads to cell autonomous myc activation and together they upregulate the cell cycle regulator cyclinE which induces G1/S transition and cell growth (Prober and Edgar, 2000). Consequently this ectopic Ras activation also leads to non-autonomous cell death of neighboring cells, probably due to lack of myc in the dying cells (Karim and Rubin, 1998). EGF signaling in the disc may also regulate growth by helping in patterning dorso-ventral boundary which positions the expression of an important morphogen *wingless* (Zecca and Struhl, 2002). Furthermore, two rounds of EGF secreted from the visceral muscles of the larval midgut is required to attain the proper number of intestinal stem cells, first during the early larval stages and second to induce production of adult midgut progenitors (Jiang and Edgar, 2009). In virtually every Drosophila tissue that has been analyzed Ras/Raf/MAPK signaling pathway is the focal point for the cross-talk between Insulin signaling and receptor tyrosine kinase pathway. Feedback from AKT as well as myc further complicates how a cell responds to Ras activity (Keshet and Seger, 2010). In

summary although Ras/Raf/MAPK pathway has a clear role in regulating cell and tissue growth, it is often challenging to accurately ascribe what percent each of the initial signal contributes to the final output.

1.6.2 JNK signaling

The Jun N-terminal Kinase (JNK) is part of the MAPK signaling family. *Drosophila* genome contains only one JNK called, *basket* (*bsk*). After Bsk is activated by upstream MAPK, it subsequently activates transcription factors Jun and Fos, which then regulates expression of target genes (Pinal et al., 2019). The role of JNK signaling in regulating tissue growth has predominantly been studied in the wing disc context. Here JNK signaling remarkably can play dual roles of inducing apoptosis and proliferation of “looser cells” and neighboring cells respectively (Pinal et al., 2019). Under normal conditions low levels of JNK activity along the anterior-posterior axis of the wing disc is thought to be required for normal proliferation of cells nearby (Willsey et al., 2016). However, under stressful conditions such as tissue damage or irradiation, a pulse of reactive oxygen species (ROS) signaling induces JNK activity which is necessary for repairing the tissue (Santabárbara-Ruiz et al., 2015). A key step in the process is removing the damaged cells, which requires caspase activation. In these dying “looser cells” JNK signaling is required for proper activation of caspase mediated cell death (Ryoo et al., 2004; Shlevkov and Morata, 2012). Furthermore, similar

to EGF/Ras signaling, JNK signaling is also required in the surrounding “winner cells” to repair the damaged tissue. In these cells JNK activity upregulates mitogenic factors such as *wg* and *dpp* which provides the cues for proliferation (Ryoo et al., 2004). For a more detail on JNK signaling in the wing disc, see review (Pinal et al., 2019).

1.6.3 Hippo signaling

One of the most striking organ size phenotypes results from perturbing the Hippo signaling pathway. Multiple inputs converge on the core kinases in the pathway, Hippo (Hpo) and Warts (Wts). Loss of function of *hpo* or *wts* in imaginal disc clones results in dramatic overgrowth in a cell autonomous manner (Wu et al., 2003b). Activated Hpo phosphorylates Wts, which in turn phosphorylates Yorki (Yki), preventing it from localizing to the nucleus and activing target genes. Under the Hpo inactive state, dephosphorylated Yki localizes to the nucleus and binds to the transcription factor Scalloped (Sd), and upregulates target genes such as *cyclinE* (cell cycle regulator), *myc* (cell growth), *diap1* (apoptosis inhibitor), and *bantam* (aids proliferation) (Halder and Johnson, 2011). Hence, overexpression of *yki* or loss of *hpo*/*wts* leads to dramatic overgrowth of the tissue. Thus, under wild type conditions, Hippo pathway actually limits proliferation and also induces apoptosis when cells overgrow their normal spatial boundaries (Halder and Johnson, 2011; Hariharan, 2015; Oh and Irvine, 2010).

How does Hippo signaling activated? Turns out that many of the inputs originate at the plasma membrane where transmembrane proteins ensure proper cell-cell contacts, which detects the integrity of an epithelial tissue (Halder and Johnson, 2011; Hariharan, 2015). Upon disruption of the cell-cell contacts, transmembrane proteins Fat and Crumbs and the basolateral complex of Scribble/Lethal giant larvae/Disc large is unable to activate Hpo/Wts which leads to Yki mediated cell proliferation (Halder and Johnson, 2011). Furthermore, it has been suggested that mechanical forces that cells exert on each other during tissue growth regulate Hippo signaling (Rauskolb et al., 2014). Surprisingly, as the wing imaginal disc grows, cells experience lower levels of tension which negatively affects Hpo (Rauskolb et al., 2014). Thus, as the imaginal disc approaches its final size at the end of larval development, low tension turns off Hippo signaling and halts tissue growth.

1.6.4 Other signaling pathways

Several other signaling pathways also play a role in regulating growth, albeit in very specific contexts. The Janus kinase (JAK) and signal transducer and activators of transcription (STAT) pathway acts generally like a stress sensor in hematopoietic cells as well the eye. In the wing disc, JAK/STAT signaling is required for proliferation and fate specification during early larval development however, later in development it acts predominantly to JNK signaling to sense

apoptotic cells (Recasens-Alvarez et al., 2017). For more details see review (Arbouzova and Zeidler, 2006).

Wingless (Wg) signaling is another pathway that plays an important role in regulating organ growth. The fascination with Wg is due to the vertebrate ortholog Wnt, mutants of which has been known to drive cancers. Wg in drosophila is important for fate specification both in embryos and in the imaginal discs (Swarup and Verheyen, 2012). Certain *wg* null mutants fail to specify the wing pouch portion of the imaginal disc, which gives rise to adults with only the notum portion of the thorax (Morata and Lawrence, 1977; Sharma and Chopra, 1976). Furthermore, ectopic *wg* expression in the notum of the imaginal wing disc result in the formation of a secondary wing (Ng et al., 1996). For more details see review (Swarup and Verheyen, 2012).

Two additional signaling pathways that regulate organ growth in *Drosophila* are worth mentioning. They belong to the Transforming Growth Factor β (TGF-β) superfamily, which includes the Bone Morphogenetic Protein (BMP) subfamily and the TGF/Activin subfamily. Since they are the central focus of this dissertation, they are discussed in detail below.

1.7 TGF β - SUPERFAMILY

The TGF-β family signaling pathway is conserved and ubiquitous in animals. In Drosophila, fewer representatives of each signaling component are

present compared to vertebrates, simplifying mechanistic study of the pathway. Although there are fewer family members, the TGF-β family pathway still regulates multiple and diverse functions in Drosophila.

1.7.1 Core *Drosophila* TGF-β Family Signaling Components

As in mammals, the Drosophila TGF-β family signaling pathway has two branches, activins and bone morphogenetic proteins (BMP), initiated by different ligands, that are defined by sequence conservation within families and the downstream signal transduction components that they use (Figure 1-3). In both branches, canonical signaling begins upon extracellular ligand binding to a heteromeric receptor complex composed of two molecules each of type I and type II transmembrane serine/threonine kinases. Formation of this ligand-receptor complex results in phosphorylation of the GS domain within the type I receptor by the constitutively active type II receptor kinase. This phosphorylation event activates the type I receptor kinase and enables it to phosphorylate an appropriate receptor-activated Smad (R-Smad) substrate, either dSmad2 for the activin branch, or Mad for the BMP branch. The phosphorylated R-Smad then forms a complex with the Drosophila common-Smad (co-Smad), Medea, and this complex translocates to the nucleus where it can regulate transcriptional responses with a variety of cofactors. Some TGF-β signal transduction components, such as the type II receptors Punt and Wishful thinking (Wit) and

the co-Smad Medea, are shared between the activin and BMP branches and often act redundantly, while others, such as the type I receptors and the R-Smads, are restricted to signaling within a single subfamily branch. Many accessory factors interact with core TGF-β components and are discussed below (Figure 1-4).

In the BMP signaling branch, three ligands - Decapentaplegic (Dpp), Glass bottom boat (Gbb), and Screw (Scw) - signal through two type I receptors - Thickveins (Tkv) and Saxophone (Sax) - and either of two type II receptors - Wit or Punt. Although loss-of-function mutations in either tkv or sax are lethal, tkv over-expression can rescue sax mutants (Brummel et al., 1994), suggesting that it may be the primary BMP type I receptor, while Sax, in most cases, fine-tunes signaling levels. Downstream of the receptors, Mad is the primary R-Smad that appears to transduce all BMP signals in combination with the co-Smad Medea. One inhibitory Smad, Dad, appears to act specifically to modulate BMP signaling (Kamiya et al., 2008).

Within the activin subfamily, three ligands – Activin-β (Actβ), Dawdle (Daw), and Myoglianin (Myo) – signal through the single type I receptor Baboon (Babo) and either Wit or Punt, and this branch uses dSmad2 as the R-Smad transcriptional transducer. In this pathway, each ligand appears to have unique functions, but double mutants have not yet been analyzed in detail to determine whether they also act redundantly. Consistent with the unique functional activities of the three ligands, three isoforms of Babo have been identified. Each differs in

the ligand-binding domain and is produced through alternative splicing of a single exon (Jensen et al., 2009). Signaling assays in S2 cells demonstrate that Daw signals through BaboC (Jensen et al., 2009), while subsequent in vivo work indicates that Myo signals preferentially through BaboA (Awasaki et al., 2011; Zhu et al., 2008). It remains to be shown if Actβ signals through BaboB and if there is any promiscuity in ligand binding to the different receptor isoforms. A handful of genes have been shown to be expressed downstream of dSmad2 in specific contexts (Bai et al., 2013; Gibbens et al., 2011; Zheng et al., 2003) but only one, Atg8a, is known to be a direct target, although a fully validated dSmad2 consensus binding sequence has not yet been determined.

Unlike in vertebrates, only two non-Smad signaling pathways have been described in Drosophila. One involves the activin branch, where Rho-like GTPases and Lim kinase act downstream of Babo to limit mushroom body axon extension (Ng, 2008) and the other is Lim kinase acting downstream of BMP signaling to regulate neuromuscular junction (NMJ) growth (Eaton and Davis, 2005; Piccioli and Littleton, 2014).

In addition to non-Smad-dependent signaling, one example of cross-pathway Smad activation has also been documented in Drosophila (Figure 1-3). In this case, the activin receptor Babo can phosphorylate the BMP transducer Mad in cell culture and also in vivo when over-expressed together with Mad (Gesualdi and Haerry, 2007; Peterson et al., 2012). However, whether this occurs under endogenous conditions is unknown. As discussed below, loss of

dSmad2 protein does lead to enhanced Mad activity in vivo, but it is not clear whether this comes about as a result of enhanced C-terminal phosphorylation of Mad or through some other modifications that happen only in the absence of dSmad2 (Peterson and O'Connor, 2013).

As in vertebrates, many accessory factors regulate ligand production and availability and several are highlighted in Table 1. For example Drosophila follistatin (fs) can modulate ligand activity of both BMP and activin pathway ligands; inhibiting Dpp and Actβ while enhancing Daw activity (Bickel et al., 2008; Pentek et al., 2009). The BMP heterodimer Dpp-Scw binds to a complex of Short gastrulation and Twisted gastrulation (Sog/Tsg) and, as described below, is required for shuttling of the Dpp-Scw heterodimer during embryonic dorsal patterning (Shimmi et al., 2005). Numerous potential co-receptors have also been identified.

Differential processing can also dramatically affect ligand signal range and activity. Furin proteases facilitate maturation of the disulfide-linked ligand dimer by processing the inactive pro-protein at any one of several potential "maturation sites". For Dpp, three furin cleavage sites are processed in distinct ways producing ligands with different N-terminal sequences. These alternatively processed ligands have different activities, such as long-range or short-range diffusion, and variable stabilities (Künnapuu et al., 2009; Sopory et al., 2010). They can also affect interactions with extracellular matrix (ECM) proteins, such as the Drosophila glypican Division abnormally delayed (Dally), through inclusion

or exclusion of heparan sulfate proteoglycan (HSPG) binding sites (Akiyama et al., 2008). In some cases, additional cleavage within the upstream prodomain is needed to fully release the prodomain from the mature ligand, and in the two Drosophila examples, this processing is performed by a Tolloid/BMP-1 type protease (Künnapuu et al., 2014; Serpe and O'Connor, 2006). Lastly, there is an example where cleavage of the BMP-type ligand Gbb does not take place at the normal maturation site, but instead at an upstream site leading to production of a very long mature ligand that, surprisingly, has bioactivity. The choice of maturation site seems to be tissue context-specific (Akiyama et al., 2012; Fritsch et al., 2012).

1.7.2 TGF-β family signaling in the wing imaginal disc

Drosophila larvae contain fifteen distinct sac-like tissues called imaginal discs, which are mitotic and give rise to adult structures. Here, we will primarily focus on the wing imaginal disc because it is the most well characterized system for understanding TGF-β signaling. Growth and patterning of imaginal discs is largely controlled by Dpp signaling (Hamaratoglu et al., 2014; Restrepo et al., 2014). In contrast, activin signals play a modest role in cell proliferation but not patterning (Brummel et al., 1999; Hevia and de Celis, 2013; Peterson and O'Connor, 2013). In the wing disc, as in the embryo, Dpp functions as a morphogen to specify different cell fates. In this tissue, Dpp is secreted from a

narrow strip of cells abutting the A/P boundary and spreads to both compartments, forming a gradient that regulates the expression of several target genes in a concentration-dependent manner (Campbell and Tomlinson, 1999; Jaźwińska et al., 1999; Lecuit et al., 1996; Minami et al., 1999; Nellen et al., 1996). The spatially defined expression of Dpp target genes governs both growth and size, as well as patterning of the adult wing veins. Below, I will focus on how the Dpp gradient is formed, interpreted, and translated to produce a functional wing.

1.7.3 Models of Dpp gradient formation in the wing disc

Francis Crick initially proposed that morphogen gradients can form by simple diffusion (Crick, 1970). To examine the role of Dpp diffusion in the wing disc, a Dpp-green fluorescent protein (GFP) fusion was created allowing the morphogen gradient to be directly visualized (Entchev et al., 2000; Teleman and Cohen, 2000). Surprisingly, fluorescent recovery after photobleaching (FRAP) experiments using this Dpp-GFP suggested a diffusion coefficient that was too slow to account for production of the observed gradient in the wing disc (Kicheva and González-Gaitán, 2008). This result led to the development of two alternative models, one involving multiple rounds of receptor-mediated ligand uptake and re-secretion, termed transcytosis (Kicheva and González-Gaitán, 2008), and a

second based on directed transport of Dpp along extended actin based filipodia, termed cytonemes (Ramírez-Weber and Kornberg, 1999; Roy et al., 2011).

Although the final resolution of the true mechanism may not be fully settled, single molecule imaging of tagged Dpp in the wing disc has allowed for measurements of the diffusion coefficient, revealing two distinct populations of Dpp that diffuse at different rates (Zhou et al., 2012). A significant portion of Dpp diffuses extremely slowly, as predicted for ligand bound to cell surface proteins such as receptors, and another pool of Dpp diffuses much more rapidly, consistent with free diffusion that is hindered only by the viscosity of the extracellular fluid and the tortuosity of intercellular paths (Zhou et al., 2012). Theoretical calculations suggest that this highly mobile pool of Dpp is sufficient to form the observed gradient in the disc. Furthermore, wild-type cells can sense Dpp even when completely surrounded by cells lacking Tkv. This observation argues against the need for receptor-mediated transcytosis (Schwank et al., 2011). To date, no strong support for cytoneme-mediated dispersal of Dpp throughout the wing disc has been reported, although it does appear that cytonemes convey Dpp from the wing disc to other interacting tissues such as the trachea (Roy et al., 2011; Roy et al., 2014).

1.7.4 Modifiers of the Dpp gradient

Since the FRAP studies and other microscopy techniques highlighted above suggest that most of the Dpp appears to be bound to the cell surface, it is likely that any molecule regulating ligand-receptor interactions will dramatically affect either gradient formation or the signaling output. Indeed, genetic approaches identified the products of the genes *division abnormally delayed* (*dally*) and *dally-like protein* (*dlp*), which encode two members of the HSPG family, as proteins that potentially affect Dpp gradient formation and/or signal output (Akiyama et al., 2008; Belenkaya et al., 2004; Fujise et al., 2003). However, the theoretical calculations now suggest that HSPGs do not restrict the fast free diffusion of Dpp (Zhou et al., 2012). Instead, they exert their primary effect on signaling output and not gradient formation, likely by facilitating Dpp-receptor interactions (Kuo et al., 2010).

Another less well understood aspect of morphogen gradients is their ability to scale according to size of the tissue (Wartlick et al., 2011b). A novel secreted factor, *Pentagone* (*Pent*), has been shown to be important for Dpp gradient scaling as the wing disc grows during the larval stages (Hamaratoglu et al., 2011; Vuilleumier et al., 2010). Pent contains follistatin-like, thyroglobulin type I and EF hand calcium-binding domains and interacts with HSPGs to alter the slope of the Dpp signaling output (Vuilleumier et al., 2010).

Since *pent* expression is negatively regulated by Dpp signaling, cells along the flanks sense less Dpp as the disc grows in size, and begin to produce Pent, which then through feedback, appears to facilitate Dpp gradient expansion (Ben-Zvi et al., 2011; Vuilleumier et al., 2010). The ability of Pent to facilitate internalization of Dally and Dlp has been proposed to modify the ability of cells to trap and transduce BMP by fine-tuning the levels of the BMP reception system at the plasma membrane (Norman et al., 2016).

1.7.5 Transcriptional responses to BMP signaling in the wing disc

The morphogen model predicts that target genes of BMP signaling should be differentially expressed within the morphogen gradient field. Indeed, early on *spalt* (*sal*), *optomoter blind* (*omb*), and *brinker* (*brk*) were identified as likely BMP-responsive genes (Figure 1-5, A) that are differentially expressed along the A/P axis (Campbell and Tomlinson, 1999; Jaźwińska et al., 1999; Lecuit et al., 1996; Minami et al., 1999; Nellen et al., 1996). Both *omb* and *sal* encode transcription factors that are required for proper patterning and cell survival in the central region of the disc, while *brk* encodes a repressor that is expressed in the lateral regions of the disc. *brk* expression is negatively regulated in the center of the disc by silencer elements (SE) that bind a heteromeric complex of transcription factors composed of pMad and Medea, together with another transcription factor, Schnurri (Affolter and Basler, 2007; Kim et al., 1997). Surprisingly, the induction

of *omb* and *sal* by Dpp actually occurs by repressing *brk*, which is itself a repressor of *omb* and *sal*. The result is that high levels of Dpp signaling directly silences *brk* in the center of the disc so that its expression pattern is an inverse complement to that of the Dpp gradient, low in the middle and high at the edges (Figure 1-5, A). The graded expression of *brk* in the more central regions of the disc in turn gives rise to the nested expression patterns of *omb* and *sal* (Figure 1-5, A).

Although expression of *omb* and *sal* are indirectly controlled by Dpp signaling, direct targets have also been identified, including *dad* which codes for an inhibitory Smad (Tsuneizumi et al., 1997). Dad affects the robustness of the Dpp signaling gradient (Ogiso et al., 2011) by blocking Tkv-meditated phosphorylation of Mad and oligomerization of pMad (Inoue et al., 1998). Within the central region of the disc, dad expression is controlled by an activating element (AE) in its regulatory sequences that directly responds to Dpp signals. The AE DNA sequence is similar to that of the SE and recruits a trimeric pMad-Medea complex, but it differs at certain nucleotide positions, such that the AE does not recruit Schnurri (Weiss et al., 2010). As a result, it is able to promote transcription rather than repress it. The lateral boundary of dad activation is controlled by Brk repression. The combined activities of AE and SE elements, together with Brk binding sites, appears to explain the bulk of BMP response gene expression patterns so far identified in the wing disc.

1.7.6 Role of Dpp in regulating tissue growth

In addition to controlling patterning within the wing disc, Dpp also regulates tissue growth. Loss of *dpp* leads to very small discs (Spencer et al., 1982; Zecca et al., 1995) while gain of Dpp signaling throughout the disc produces overgrowth (Martín-Castellanos and Edgar, 2002; Nellen et al., 1996). Even expressing extra dpp within its normal source using *dpp*-Gal4 causes a mild enlargement of the larval wing disc with some extra vein defects (Entchev et al., 2000; Teleman and Cohen, 2000). When expressed locally in clones, it can also lead to the formation of an entirely new secondary winglet attached to a normal wing (Zecca et al., 1995).

How BMP signaling can regulate both growth and patterning in the wing disc has been an enigma for quite some time. The dilemma arises because cell proliferation within the wing disc is uniform (Milán et al., 1996) and patterning is clearly coupled to gradient formation and interpretation. Explaining how uniform proliferation can be produced by a graded pattern of Dpp has proved difficult. Several hypotheses have been put forth including the idea that proliferation depends on the slope of the Dpp gradient (Day and Lawrence, 2000), the rate of change in Dpp signal reception (Wartlick et al., 2011a), and the 'growth equalization model' (Restrepo et al., 2014). At present the mechanism for producing uniform growth is unclear since all the models have some conflicts with certain observations. The major conflict arises from analysis of *brk* mutants and expression. That Brk plays a central role in regulating wing disc growth was

initially revealed by analysis of loss-of-function clones, which in the flanks of the disc also leads to winglet formation similar to gain of BMP signaling (Campbell and Tomlinson, 1999). Subsequently, it was found that increased expression of *brk* in the entire disc leads to a severe reduction in disc size (Martín et al., 2004; Schwank et al., 2008) similar to loss of *dpp*. The real surprise, however, was that wing discs not only grow, but actually overgrow if they lose both *brk* and *dpp* (Campbell and Tomlinson, 1999; Schwank et al., 2008). This observation suggests that neither the slope model nor the temporal dynamics model is correct. One alternative is that Dpp and Brk do not directly regulate proliferation of wing disc cells, but instead modulate an underlying non-uniform proliferation pattern that is the result of other growth promoting signals such as insulin-TOR and/or the Hippo, and other Activin like signaling pathways (Restrepo et al., 2014).

Two additional studies employing novel independent reagents, suggest that the Dpp gradient is not required for uniform growth (Akiyama and Gibson, 2015; Hamaratoglu et al., 2011). In the first study *dpp* is deleted from the Dpp producing cells in the wing disc, using a UAS>GAL4/FRT system (Akiyama and Gibson, 2015). Surprisingly, these discs proliferates uniformly resulting in a normal size tissue, even though *brk* expression is up-regulated in the wing pouch. This result argues against the Dpp-gradient and the growth equalization model and instead supports the temporal dynamics model perhaps due to other non-A/P boundary disc cells that still produce Dpp. In the second method, Dpp

diffusion is restricted by a nanobody trapping method and once again there is uniform disc growth, supporting the growth equalization model (Harmansa et al., 2015). Going forward it will be important to reconcile these observations. Furthermore, if and how Gbb signaling contributes to disc growth in the absence of a Dpp-gradient will be interesting to explore.

1.7.7 BMP signaling in pupal wing development

Dpp and Gbb also play important roles in vein specification and positioning, which begins in late larval stages and continues throughout pupal development (de Celis, 2003; O'Connor et al., 2006). During the late larval stages, induction of the BMP targets, *sal* and *omb*, dictate where some of the longitudinal veins (LV) will form (de Celis, 2003; de Celis et al., 1997). Soon after pupariation, *dpp* expression is lost at the A/P boundary and becomes localized to cells that form the LVs, and high levels of pMad are detected in these pre-vein cells (Conley et al., 2000). Intriguingly, the posterior crossvein (PCV), that forms slightly later at about 20 hours after puparium formation, also requires BMP signaling, but *dpp* is not expressed in primordial PCV cells. Nevertheless, these cells receive high levels of BMP signal as evidenced by strong pMad staining (Ralston and Blair, 2005). The mechanism appears to be similar to that used in the embryo where Dpp or a Dpp-Gbb heterodimer is shuttled away from the primordial LVs and concentrated at the site of the future PCV (Matsuda and

Shimmi, 2012). This shuttling process requires several extracellular BMP modulators including *sog*, *CV*-2, *CV*-1 (a *tsg* homolog) and *tlr* (a *tld* homolog) (Figure 1-5, B) (O'Connor et al., 2006). Another factor, *crossveinless-D* which encodes a vittelogenin-like lipoprotein appears to regulate PCV formation by modulating Dpp movement as part of a lipid–Dpp–lipoprotein complex (Chen et al., 2012).

1.7.8 Mad is a focal point for integration of cross-pathway signals

Dpp signals are integrated with numerous other growth and patterning signals during imaginal disc development. In many cases, this interaction occurs through Mad, and two important points of integration within the wing disc involve the Hippo (see section 1.6.3) and Wingless (see section 1.6.4) signaling pathways (reviewed in (Baena-Lopez et al., 2012). The microRNA *bantam* (*ban*) is particularly interesting since it also responds to Dpp signaling (Martín et al., 2004) and a direct link between the control of ban levels by Dpp and Hippo has been established (Oh and Irvine, 2011). On its own, Yki is not able to bind DNA but can do so when in a complex with other transcription factors. Mad can form a complex with Yki, and this complex is mediated through a PPXY motif located in the linker region between the Mad homology 1 (MH1) DNA binding domain of Mad and the C-terminal MH2 domain, a more typical site of regulatory interaction between Mad and other proteins (Oh and Irvine, 2010). The Mad-Yki complex

was also shown to bind to a novel enhancer element in the *ban* promoter to augment ban transcription, thus providing an integration point for these two growth promoting signals (Oh and Irvine 2010).

Mad is also the focal point of interaction with the canonical Wg pathway (Eivers et al., 2009; Eivers et al., 2011). Both in vivo and in vitro studies demonstrated that unphosphorylated Mad forms a complex with Armadillo (homologue of vertebrate β-catenin) to regulate wg target genes in both the embryo and wing disc. Upon Dpp signaling, Mad is titrated away from Armadillo, resulting in Wg-reporters being significantly down-regulated (Eivers et al., 2011). Once again, the linker region between the MH1 and MH2 domains of Mad plays an important role in mediating regulatory interactions between the two pathways. The linker region possesses several serines and tyrosines, which are phosphorylated by various kinases to control Mad stability (Alarcón et al., 2009; Kretzschmar et al., 1997; Pera et al., 2003). In particular, glycogen synthase kinase-3 (GSK3)-mediated phosphorylation of the linker is important for initiating Mad degradation via Smurf1 and it was proposed that both the Wg and Dpp functions of Mad are terminated by GSK3 phosphorylation of the linker (Eivers et al., 2011).

A third signal intersection converging on Mad takes place between the Activin and the BMP signaling branches in the wing disc. Although these two branches appear to have diverged from one another long ago, the Activin-specific type I receptor Babo retains an ability to activate Mad by C-terminal

phosphorylation (Peterson et al., 2012). Whether this C-terminal Mad phosphorylation activity is utilized during normal development is still not clear, but results from using a *dSmad2* null mutant further supports the idea that cross-signaling by the Activin pathway impinges on Mad activity (Peterson and O'Connor, 2013; Sander et al., 2010). Interestingly, when dSmad2 protein is absent, Babo sends an ectopic signal that leads to pronounced overgrowth of the wing disc. The excessive growth is caused by down-regulation of *brk*, and this down-regulation requires binding of a Mad-Medea-Schnurri complex to the *brk* silencer elements. However, there was no detectable increase of C-terminal Mad phosphorylation, leading to the intriguing unresolved issue of how Mad is hyper-activated by Babo in the absence of dSmad2 (Peterson and O'Connor, 2013). Taken together, these studies indicate that Mad is clearly at the nexus of integrating numerous signaling events that control wing growth and patterning.

1.7.9 BMP signaling in other imaginal discs

So far, our discussion has focused on the role of BMP signaling in wing disc growth and patterning since it is the best studied of the imaginal tissues. Not surprisingly, however, BMP signals also play important roles in the development of all imaginal discs. In fact, the name decapentaplegic indicates that all 15 (decapenta) discs are defective (plegic) (Spencer et al., 1982). Here, we briefly examine the role of BMP signaling in the leg, eye and genital imaginal discs.

More detailed reviews cover the development of the eye (Curtiss and Mlodzik, 2000), leg (Estella et al., 2012) and genital discs (Estrada et al., 2003; Sánchez et al., 2001).

In the leg disc, Dpp synergizes with Wg to give proximal/distal (PD) positional information the tissue with distal being the center (Estella and Mann, 2008; Lecuit and Cohen, 1997). Along the A/P boundary of the leg disc *dpp* is expressed in the dorsal compartment and *wg* in the ventral. This creates a zone in the center of the disc where both ligands are present at high concentrations, which is required to induce the expression of the distal marker *distal less* (*dll*). Cells surrounding the *dll* expression domain sense moderate levels of Dpp and Wg and turn on *dachshund* (*dac*), a medial leg marker. Cells in the periphery give rise to proximal domains of the leg and sense low levels of the ligands leading to expression of *homothorax* and *teashirt*. Patterning of *dll* and *dac* are thought to result from *brk* repression, a mechanism that poses striking similarity with the wing disc (Estella and Mann, 2008). Thus, while the details of patterning in the leg disc are different from those in the wing, the basic function of Dpp as a morphogen that functions, in part, through the repression of *brk*, is nevertheless the same in both tissues.

In the eye imaginal disc, the responses to Dpp are notably different from those in other discs. In this tissue, *dpp* is expressed only in the morphogenetic furrow, which migrates posterior to anterior during late larval stages (Baker, 2001). The Dpp signaling response varies depending on the position of the cells

relative to the furrow. Cells anterior of the furrow are stimulated to proliferate, while cells in and abutting the furrow undergo cell cycle arrest (Baker, 2001). Cell cycle arrest is necessary for proper eye differentiation since mutant clones defective in Dpp signaling are delayed in entering G1 arrest and do not fully differentiate (Firth et al., 2010; Horsfield et al., 1998). Although the mechanism for the dual nature of Dpp signaling to induce both cell proliferation and G1 arrest is unresolved, it is likely that multiple signaling pathways, including those activated by Wg, Hh, Notch, and EGF (see section 1.6.1), finely tune this process (Amore and Casares, 2010).

Dpp signaling also plays an important role in genital disc development, which gives rise to the adult internal and external genitalia and analia. Several distinguishing characteristics of this disc set it apart from the others. It is the only disc that is located medially, formed by the fusion of cells originating from three embryonic segments, it is an unpaired disc (i.e. not one for each side of the larva,) and it is sexually dimorphic (Estrada et al., 2003; Sánchez and Guerrero, 2001). Nevertheless, the genital disc has some similarity to other discs, such as the leg, in the sense that *hh* expression in the posterior compartment induces expression of *dpp* and *wg* in the anterior compartment, which in turn induces *dll* expression that is required for development of the disc in both males and females (Sánchez and Guerrero, 2001; Sánchez et al., 2001).

1.7.10 TGF-β family signaling in the nervous system

The Drosophila NMJ, a collection of synapses made on body wall muscles by motor neurons, has long served as an excellent model for studying synapse formation and function. The NMJ grows substantially during larval life to accommodate the rapidly growing body wall muscles, and several trans-synaptic signaling pathways have been shown to play important roles in coordinating the pre- and postsynaptic development at the larval NMJ (Dani and Broadie, 2012). Both branches of TGF-β family signaling have important roles at the NMJ (Figure 1-6), and BMP signaling has been particularly well studied. The primary ligand involved is Gbb, which is expressed in the muscles and the central nervous system (CNS) beginning at the embryonic stage (McCabe et al., 2003). Mutations in *gbb* cause a loss of pMad accumulation in motor neuron nuclei as well as a reduced NMJ size, aberrant presynaptic ultrastructure, and defective neurotransmission (McCabe et al., 2003). The defective synaptic growth of *gbb* null mutants is only fully rescued when *gbb* expression is restored in muscles and not in the CNS. These observations suggest that the Gbb signal acts in a retrograde fashion to control presynaptic growth in the motor neurons (McCabe et al., 2003).

Similar phenotypes in pMad level, NMJ size, neurotransmitter release, and synaptic ultrastructure were also observed in mutations of the type II receptor *wit* (Aberle et al., 2002; Marqués et al., 2002). The expression of *wit* is restricted to motor neurons in the neuromuscular system and restoration of wit in

the motor neurons rescues synaptic size, supporting the idea that Wit acts as the primary type II receptor for Gbb in motor neurons. Likewise, null mutations in all other BMP signal transduction components, including *tkv*, *sax*, *mad* and *medea*, phenocopy the *gbb* and *wit* null mutations indicating that canonical BMP signaling is the main regulator of synaptic growth at the NMJ (McCabe et al., 2004; Rawson et al., 2003).

The identities of target genes in motor neurons that regulate synaptic growth is largely unknown. However, recent studies utilizing molecular genetic tools that allow for temporal regulation of Gbb signaling at the NMJ identified some molecular mechanisms through which Gbb affects synapse structure and function. These studies demonstrated that synaptic structure and function use genetically separate pathways with an early transient embryonic signal needed for synaptic growth, while continuous Gbb signaling is required for maturation of neurotransmitter release properties (Berke et al., 2013). One BMP target gene required for regulating synaptic growth is *trio*, which encodes a guanine nucleotide exchange factor (GEF) that acts on Rac GTPases (Ball et al., 2010). Since previous studies demonstrate that GTPases control axon growth and guidance through alterations in the actin cytoskeleton (Dickson, 2001; Fan et al., 2003), it was postulated that Trio could promote synaptic growth also by modulation of the actin cytoskeleton via Rac (Ball et al., 2010). However, a direct relationship between Rac activation and changes in actin filaments is yet to be demonstrated. In parallel to stimulating *trio* expression, Wit signaling also leads

to stimulation of Lim domain kinase 1 (Limk1) activity through a non-canonical pathway. Since Lim kinase is implicated in rapid bouton budding in response to elevated synaptic activity and synaptic stabilization (Eaton and Davis, 2005; Piccioli and Littleton, 2014), this may be yet another means by which the Gbb signal influences synaptic growth.

In addition to promoting NMJ growth and presynaptic structural maturation, BMP signaling also plays a pivotal role in regulating synaptic transmission at the NMJ. Strong BMP pathway mutants display reductions in the amplitude of evoked junctional potential (EJP) and the frequency of miniature EJPs (mEJP) (Aberle et al., 2002; Marqués et al., 2002; McCabe et al., 2003; Rawson et al., 2003). Unlike synaptic growth that is predominantly regulated by retrograde BMP signaling, the defective synaptic transmission phenotypes of *gbb* mutants are only completely rescued when *gbb* expression is restored by a pan-neuronal driver (Aberle et al., 2002; McCabe et al., 2003), indicating that presynaptic Gbb is required for proper neurotransmission. The smaller magnitude of EJPs has also implied that homeostatic regulation of synaptic efficacy is compromised in the BMP pathway mutants. It was later demonstrated that BMP signaling is continuously required in the motor neurons to confer competence for the rapid induction of synaptic homeostasis (Goold and Davis, 2007). In terms of the effects on neurotransmission, the only BMP-responsive target gene identified to date is *twit*, which encodes a Ly6 neurotoxin-like molecule. Restoring *twit* expression in *wit* mutant motor neurons partially rescues

neurotransmitter release defects, although the molecular mechanism remains obscure (Kim and Marques, 2012).

Since BMP signaling has profound effects on NMJ structure and function, it is not surprising that its activity is tightly controlled to prevent uncoordinated growth of the synapses. Multiple molecular mechanisms have been implicated in regulating BMP signaling at the NMJ. In muscles, Gbb release is inhibited by Drosophila Cdc42-interacting protein 4 (dCIP4) acting downstream of Cdc42 and activating the Wsp (Drosophila orthologue of mammalian Wiskott-Aldrich syndrome protein, Wasp) pathway (Nahm et al., 2010). The Cdc42-Wsp pathway is, in turn, inhibited by Drosophila Rich (dRich), a Cdc42-selective GAP (Nahm et al., 2010). Therefore, a complex regulatory loop appears to be employed to control the release of Gbb. In the presynaptic motor neurons, hyper-activation of BMP signaling is prohibited by *highwire*, a ubiquitin ligase that presumably targets Medea for protein degradation (McCabe et al., 2004). The activated receptors are also subject to negative regulation by internalization. Mutations in *nwk*, *spin* and *spict* whose products act in, or interact with, endocytic machinery result in overgrowth of the synapses (Oconnor-Giles et al., 2008; Sweeney and Davis, 2002; Tan et al., 2007). Finally, retrograde signaling of Gbb also occurs in the central motor circuit, which is necessary to strengthen the synaptic activity. Therefore, it appears that the retrograde signaling is a general theme by which Gbb regulates synaptic development and function (Baines, 2004). On the other hand, release of Gbb from the presynaptic side is promoted by Crimpy, a

homolog of vertebrate Cysteine-rich transmembrane BMP regulator 1 (CRIM1), which binds Gbb and delivers it to a dense core vesicle (DCV) (James and Broihier, 2011). Interestingly, the ectodomain of Crimpy is also released together with Gbb from the DCV upon exocytosis. This has been proposed to help discriminate the presynaptic and postsynaptic pools of Gbb, thus setting the directionality of BMP signaling at the NMJ.

The retrograde Gbb signaling at the NMJ results in accumulation of pMad in the nuclei of motor neurons. In addition to the nuclear pMad, another pool of pMad has been identified. This pool of pMad is localized to the presynaptic side of the synapses at the NMJ and is regulated differently from the nuclear pMad (Sulkowski et al., 2014). Specifically, the level of synaptic pMad is independent of Gbb, but is positively regulated by the activity of postsynaptic iGluRs containing glutamate receptor IIA (type-A receptor). The synaptic pMad in turn stabilize the A-type glutamate receptors suggesting a positive feedback loop between the presynaptic and postsynaptic molecules. This has been proposed to be a mechanism to coordinate the maturation of synapses to the activity.

In contrast to BMP signaling, whose role in synaptic formation and function is well documented, relatively little is known about the role of the activin pathway in the regulation of NMJ development and activity, even though all three activin ligands are expressed in at least one cell-type of the neuromuscular system (Brummel et al., 1999; Gesualdi and Haerry, 2007; Lo and Frasch, 1999; Serpe and O'Connor, 2006; Zheng et al., 2003). Studies of *babo*, *dSmad2*, and

Actβ mutants indicate that *Actβ* is a motor neuron-derived anterograde signal that is necessary for achieving normal levels of GluRIIA and GluRIIB densities in muscle at the postsynaptic side of the NMJ (Figure 1-6), as well as proper resting membrane potential of the muscle (Kim et al., 2014). Actβ appears to control the synaptic GluRIIA density through a post-transcriptional mechanism while it regulates the GluRIIB density via dSmad2-dependent transcriptional activation.

1.7.11 Activin signaling stimulates neuroblast proliferation

In addition to its role at the NMJ, Activin signaling also has other roles in the nervous system including regulation of neuroblast proliferation, control of neurite outgrowth and target selection, as well as neuronal remodeling during metamorphosis. These activities are accomplished by deployment of the Activin-type ligands, i.e. Actβ, Daw and Myo, from different source cells in the nervous system acting on different target cells. In most cases, this signaling is canonical through Babo and dSmad2, but there is one example where non-canonical signaling appears to be employed.

One major function of Activin signaling in the nervous system is to stimulate production of neurons, which are generated from neuroblasts in the brain. Loss-of-function mutations in *babo* and *dSmad2* produce small brains due reduced proliferation of neuroblasts and their daughter cells, while expression of *babo* specifically in neuroblasts rescues brain size (Zhu et al., 2008). The ligands

Actβ and Daw have been implicated in this process. *Actβ* is expressed in numerous neurons within the central brain and ventral ganglia, while *daw* is expressed in subsets of glial cells. *Myo* may also be involved, since it, too, is expressed in many glial cells (Lo and Frasch, 1999). Mechanistically, activin signaling appears to control proliferation of neuroblasts by promoting S to M phase transition of the cell cycle (Zhu et al., 2008).

1.7.12 Activin signaling and axon guidance and target selection

In addition to generating neurons, activin signaling also regulates several aspects of axon targeting in different contexts. In the embryonic nervous system, activin signaling plays a role in guiding motor neuron axons to their target muscles. In *daw* mutant embryos, motor neurons leaving the CNS have pathfinding defects in both intersegmental nerve and segmental nerve roots (Parker et al., 2006; Serpe and O'Connor, 2006). These defects are also seen in *babo* and *dSmad2* mutant embryos (Parker et al., 2006; Serpe and O'Connor, 2006) indicating that canonical signaling is responsible. Because expressing dominant-negative forms of either Babo or Punt in the motor neurons also cause pathfinding defects, the target of Daw signaling appears to be the motor neuron itself and not the muscle (Parker et al., 2006). In addition, because *daw* expression in either the muscle or glia rescues pathfinding defects and excess *daw* expression is not detrimental, *daw* appears to provide a permissive cue for

motor neuron axon guidance (Parker et al., 2006). Interestingly, mutants in *tlr* also phenocopy the pathfinding defects of *daw* mutants (Serpe and O'Connor, 2006). Tlr was found to cleave the prodomain of Daw, as well as Actβ and Myo, and, in the case of Daw, cleavage enhances signaling in cell culture assays. These observations suggest that, as described above for Scw, prodomain processing of activin-like ligands at sites distinct from the normal furin maturation sites may be important for full signaling activity, perhaps by stimulating complete dissociation of the prodomain from the carboxy-terminal ligand domain (Serpe and O'Connor, 2006). Similar activating cleavages in prodomains of several vertebrate ligands have also been reported (Wolfman et al., 2003).

During the larval stage, photoreceptor axons must be targeted properly for light and color information to be processed correctly, and Actβ plays a role in regulating proper photoreceptor axon termination in the medulla. Clonal loss of *babo* or *dSmad2* in R7 photoreceptors causes their axons to target to the correct layer, but move laterally and enter the wrong column (Ting et al., 2007). *Actβ* is expressed in R7 photoreceptors, and Actβ RNAi in the photoreceptors also causes axon mis-targeting (Ting et al., 2007). These studies indicate that *Actβ* expression in R7 photoreceptors restricts their targeting to a single column in the medulla through an autocrine signaling mechanism (Ting et al., 2007).

Actβ also signals in a juxtacrine manner to negatively regulate dendritic branching and termination of medulla interneurons, which receive input from

photoreceptors. In this case, *Actβ* derived from R7 or R8 photoreceptors signals to Dm8 or Tm20 medulla neurons, respectively, to regulate their dendritic field size (Ting et al., 2014). Loss-of-function *babo* and *dSmad2* mutant clones in medulla interneurons produce expanded dendrites, whereas neurons with increased reception of activin signals have reduced dendrites. In loss-of-function mutants the expanded dendrites form ectopic membrane connections with presynaptic sites on multiple photoreceptors, potentially disrupting visual processing (Ting et al., 2014).

Activin signals also function to regulate MB neuron β-lobe axon growth. MB neurons are responsible for olfactory learning and memory. Expression of activated Babo causes axon truncation, whereas loss of *babo* results in overgrowth (Ng, 2008). This is independent of dSmad2 and requires the actin cytoskeleton regulators Limk1, Rho, and Rac. The identity of the responsible ligand has not been determined. This example is one of only two cases in Drosophila in which non-Smad signaling is responsible for mediating a response.

1.7.13 Activin signaling and neuronal remodeling

Apart from roles in axon guidance and target selection, activin signaling is also required during metamorphosis for MB remodeling. The MB undergoes stereotypic remodeling during the pupal phase to eliminate larval-specific

connections and to form new connections required for proper adult behaviors. The larval MB has two major branches of γ neurons: medial and dorsal. Both branches are pruned during metamorphosis, and only the medial lobe remains in the adult MB. Mutations in *babo* and *dSmad2* prevent pruning of dorsal and medial γ neurons of the MB, and these defects are rescued by expressing the proper wild-type gene in the MB neurons (Zheng et al., 2003). One major target of activin signaling in the remodeling MB neurons is the gene encoding the ecdysone receptor EcR-B1. Ectopic expression of EcR-B1 in the MB neurons partially rescues the pruning defect (Zheng et al., 2003). Although it was originally suggested that Actβ was the responsible ligand based on RNAi phenotypes, further studies using loss-of-function mutants demonstrate that glial-derived Myo provides the signal (Awasaki et al., 2011). In this example, Myo appears to signal primarily through the BaboA isoform (Awasaki et al., 2011) and can use either Punt or Wit as a type II receptor since only when both are eliminated is a MB remodeling defect observed (Zheng et al., 2003).

This signaling event is also noteworthy since efficient signaling requires a novel co-receptor in addition to the normal type I and type II receptors. Genetic screens for additional factors that regulate MB remodeling identified *plum*, a gene that codes for an immunoglobulin superfamily protein. Mutations in *plum* lead to loss of *EcR-B1* expression and defective MB remodeling (Yu et al., 2013). Since these phenotypes can be rescued by expressing activated Babo in MB neurons, but not by overexpressing *plum* in *babo* mutant MB clones, Plum appears to act

upstream of receptor activation (Yu et al., 2013). Limited structure-function studies demonstrate that the extracellular domain of Plum is required for rescue, but the cytoplasmic domain is dispensable (Yu et al., 2013). At present, the best guess is that Plum acts to either stabilize receptor complexes and/or to facilitate Myo binding to the receptor complex, although no biochemical interactions between any of these components have been reported.

1.7.14 Role of TGF-β family signaling in physiological and metabolic homeostasis

Roles of TGF-β family signaling in developmental processes are well established and extensively studied. Nevertheless, TGF-β family signaling components continue to be expressed throughout the lifespan of an animal and in various adult tissues, signifying potential roles of the TGF-β family signaling pathways in key physiological or homeostatic processes. Investigating the role of TGF-β family signaling in physiology is an active field of research, and the involvement of the TGF-β family in the regulation of physiological homeostasis in Drosophila larvae and adults has been demonstrated in a number of studies. In this section I highlight our understanding of how TGF-β family signaling in Drosophila regulates the following four key homeostatic and physiological processes: 1) metabolic homeostasis, 2) hormonal signaling, 3) innate immunity, and 4) tissue homeostasis.

1.7.15 TGF-β family signaling in metabolic homeostasis

TGF-β family signaling components are expressed in metabolically active tissues in both vertebrates and invertebrates, and their roles in regulating metabolism are gaining attention (Bertolino et al., 2008; Ghosh and O'Connor, 2014; Zamani and Brown, 2011). In Drosophila, both the TGF-β family ligand Dawdle (Daw) and the BMP family ligand Glass-bottom boat (Gbb) have been implicated in metabolic regulation.

The activin-like ligand Daw regulates insulin/insulin-like growth factor signaling (IIS) in feeding third instar larvae (Ghosh and O'Connor, 2014). Consistent with loss of IIS, daw mutant larvae show a significant increase in circulating sugar (glucose + trehalose) concentration, total triacylglycerol and glycogen content, and a significant reduction in Akt activation in the peripheral tissues (Ghosh and O'Connor, 2014). While these mutant animals did not show any change in expression of dilps in the insulin producing cells (IPCs), they were defective in the release of Dilps from the IPCs (Ghosh and O'Connor, 2014).

Independent of its role in regulating IIS, canonical Smad signaling downstream of Daw also regulates the internal pH balance, most likely by altering the output of acidic TCA cycle intermediates primarily in the fat body (FB) (Ghosh and O'Connor, 2014). FB-specific RNA sequencing of daw mutants and control flies revealed increased expression of multiple nuclear-encoded

mitochondrial genes, including enzymes of the TCA cycle, electron transport chain, β-oxidation and ketogenesis in the daw mutants (Ghosh and O'Connor, 2014). Additionally, metabolomics analysis revealed increased accumulation of multiple TCA cycle intermediates in these mutants. These results point towards a transcriptional role of Daw in mitochondrial biogenesis, energy metabolism, TCA cycle activity and pH balance. The involvement of Daw in expression of nuclear encoded mitochondrial genes may be reminiscent of the proposed role of Activin-A in mitochondrial biogenesis in vertebrates (Zamani and Brown, 2011).

Daw may regulate metabolic processes in a systemic dose-dependent manner. Expressing *daw* in any larval tissue could completely rescue larval lethality associated with mutations in *daw*, and had a graded effect in rescuing the metabolic phenotypes of *daw* mutants depending on the size of the tissue. Analyses of phospho-dSmad2 (pdSmad2) levels in the FB showed that Smad2 activation in the larval FB is primarily mediated by Daw and that the FB is poised to respond to a wide range of Daw signaling. Consistent with the endocrine nature of Daw signaling, expressing *daw* in a variety of larval tissues could rescue pdSmad2 levels in a daw mutant FB (Ghosh and O'Connor, 2014). These results indicate that Daw acts like a metabolic hormone capable of dose-dependently regulating cellular metabolism. Intriguingly, unlike most hormones, *daw* is expressed in multiple larval tissues, and it will be interesting to learn how each of these tissues uses this metabolic ligand for systemic communication. One possibility is that *daw* expression in each tissue is regulated by different

environmental stimuli and that Daw then acts on other tissues to bring about systemic changes to cope with the stimuli.

The involvement of the Drosophila TGF-β family ligand Daw in sugar homeostasis is further demonstrated by work showing that nutrient-sensitive expression of *daw* is required for inducing glucose repression (GR) in the Drosophila intestine (Chng et al., 2014). Glucose repression (GR) is a phenomenon whereby feeding of excessive dietary glucose leads to repression of amylase in the gut, presumably in an effort to protect the animal against deleterious effects of a high sugar diet (Benkel and Hickey, 1986; Hickey and Benkel, 1982; Musselman et al., 2011; Na et al., 2013). Smad signaling activated by Babo and dSmad2 mediates GR by negatively regulating the expression of digestive enzymes (amylases, hydrolases and lipases) in the gut in response to high sugar diet (Chng et al., 2014). This effect is mediated by the Babo isoform C in the gut, which is specific to Daw signaling (Chng et al., 2014; Jensen et al., 2009). Importantly, in response to high sugar diet, Daw is released from the adult fat body and signals to the gut to repress expression of digestive enzymes including amylase, further confirming the endocrine nature of Daw signaling. It is interesting to note that expression of oxido-reductase genes was also significantly suppressed in the gut when flies were kept on a high sugar diet. Since a high sugar diet increases Daw signaling in the gut, this finding is consistent with a role for Daw signaling in repressing the expression of

mitochondrial genes, including oxido-reductases, similar to what is seen in whole animal *daw* mutants (Ghosh and O'Connor, 2014).

Additional evidence suggests that Daw is one of the primary effectors of a conserved sugar sensing pathway mediated by the ChREBP/MondoA-Mlx complex (Mattila et al., 2015). The MondoA-Mlx transcription factors are activated by sugars and are essential for mediating multiple downstream processes essential for conversion of sugars to lipids and utilization of sugars. The *daw* promoter contains a carbohydrate response element that is occupied by Mlx in both S2 cells and in Drosophila larvae indicating that daw expression is directly regulated by Mondo-A/Mlx. Additionally, Daw is required and regulates the expression of a second key target of Mondo-A/Mlx called sugarbabe (sug) (Mattila et al., 2015). These findings put Daw firmly in a major sugar sensing and sugar metabolism pathway in Drosophila. Whether activin signaling in vertebrates is also a downstream target and effector of Mondo-A/Mlx complex remains to be determined.

Daw has also been implicated in lifespan extension in Drosophila. A screen for transcriptional targets of dFOXO identified *daw* as a potential target, and muscle-specific knockdown of daw leads to increased lifespan (Bai et al., 2013). Loss of *daw* in the muscle affects lifespan possibly by increasing macro-autophagy that helps remove age-related accumulation of protein aggregates in the muscle, thereby improving muscle function (Bai et al., 2013). Interestingly, they also found that *daw*-RNAi in the muscle can reduce Dilp2 levels in

circulation, whereas daw-RNAi in the FB leads to an increase in Dilp2 in the hemolymph (Bai et al., 2013). While these observations support a role of Daw in regulating IIS in the adult fly as well, it remains to be explained how tissue-specific knockdown of a ligand, which clearly works as an endocrinal systemic signal in the larva, can lead to opposing phenotypes in the adult. The relative contributions of the muscle and FB to circulating Daw levels and potential compensatory changes in daw expression when it is knocked down in any single tissue could explain some of these findings.

The BMP ligand Gbb has also been proposed to regulate metabolic processes, initially based on a striking morphological defect exhibited by gbb mutants in which the FB takes on a glassy appearance instead of its normal opaqueness (hence the name Glass bottom boat). Characterization of these mutant larvae revealed that the FB exhibits nutrient storage and morphological characteristics resembling a state of starvation (Ballard et al., 2010). Additionally, *gbb* mutants show alterations in the expression of multiple starvation response genes. Surprisingly, monitoring lipid uptake using a fluorescently labeled lipid derivative (Bo-C12) reveals that the *gbb* mutants show an increased rate of nutrient uptake, indicating defects in the ability to store nutrients. While Gbb produced by the FB regulates FB morphology and nutrient storage in a cell-autonomous manner, Gbb signaling in the FB may only be partially responsible for the increased nutrient uptake phenotype observed in *gbb* mutants (Ballard et

al., 2010). The mechanistic details of how Gbb affects utilization of absorbed nutrients remains unexplained.

1.7.16 TGF-β family signaling regulates hormonal control of Drosophila development.

Like other insects, Drosophila uses two primary hormonal signals, juvenile hormone (JH) and ecdysone (E), to coordinately regulate transitions in larval development (see section 1.5.3). TGF-β family signaling appears to work upstream of these hormonal signals by controlling the production of both these hormones, presumably in response to developmental or environmental cues (Gibbens et al., 2011; Huang et al., 2011). Both gain and loss-of-function studies show that activin signaling is required in the prothoracic gland (PG), the site of E production and release, to generate the large pulse of E necessary for entering metamorphosis (Gibbens et al., 2011). In the absence of canonical activin signaling in the PG, the larvae arrest at the third instar stage and do not undergo metamorphosis. This phenotype results from a requirement for activin signaling in the PG to make it competent to respond to two other hormonal signals, prothoracicotropic hormone (PTTH) and insulin. In the absence of activin signaling, expression of Torso, the PTTH receptor, and InR, the insulin receptor, and several other downstream components in the insulin signaling pathway, are all down-regulated in the PG (Gibbens et al., 2011). Since each of these two

signaling pathways is required for high-level expression of several key E biosynthetic enzymes, their simultaneous loss eliminates production of the E pulse that is required for initiating metamorphosis. A remaining question is the identity of the TGF-β ligand that signals in the PG since loss of any one ligand (*Actβ*, *daw* or *myo*) does not show larval developmental arrest phenotypes. This observation suggests redundancy among the ligands for providing competence to the PG for reception of PTTH and insulin signals.

In contrast to the involvement of activin signaling in the control of E production, JH synthesis is under the control of the BMP ligand Dpp (Huang et al., 2011). JH is critical for determining the nature of developmental transitions in insects. In the presence of JH, E induces a larval-larval molt, whereas, in the absence of JH, E induces a larval-pupal or pupal-adult molt. Using an elegant genetic screen, *tkv* and *Mad* were identified as positive regulators of JH signaling in the larva (Huang et al., 2011). JH is synthesized in the corpus allata (CA), and glutamatergic signals emanating from the brain induce *dpp* expression in the CA. Dpp then cell-autonomously induces production of the JH-synthesizing enzyme JH acid methytransferase to stimulate JH production in the developing larvae.

1.8 STATEMENT OF THESIS WORK

Inter-organ communication is vital for organisms. As discussed above, in *Drosophila* both branches of TGF-β suprefamily participate in regulating a wide variety physiological and developmental processes, often through inter-organ signaling. However, numerous outstanding questions that remain. Among them is the question of organ size coordination. The data presented in this dissertation aims to precisely define how TGF-β/Activin like ligands regulate overall animal growth as well as organ size. In chapter two, I discuss how Activin-β secreted by Motoneurons affect muscle and body size. In chapter three, I discuss how Myoglianin secreted by the muscles affect imaginal disc size. In chapter four, I conclude by bringing together the central finding from chapters three and four in an effort to explain how multiple axis of TGF-β signaling in *Drosophila* may be a mechanism of achieving proper organ to body size scaling. I speculate on how these findings relate to static allometry or organ size in *Drosophila melanogaster*.

CHAPTER I FIGURES

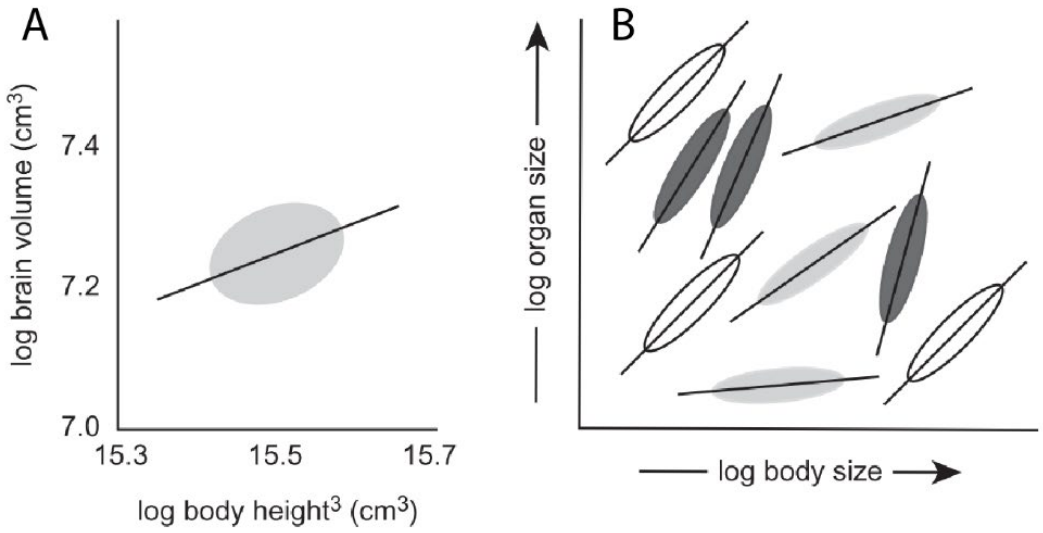

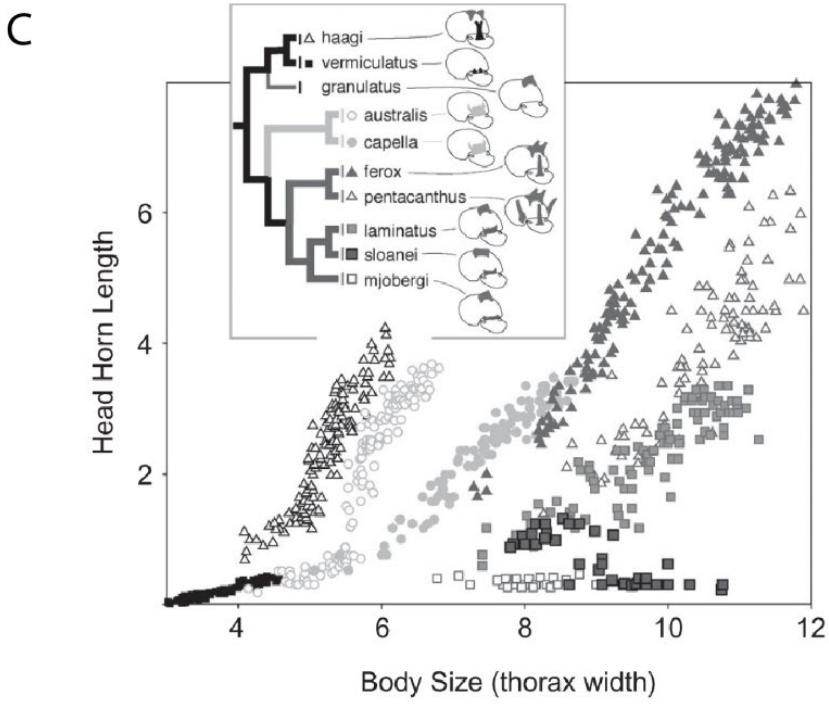

Figure 1-1. Static allometry of organ size within and among species.
(A) For a given group of individuals, size of any two traits can be mapped on a graph, represented by gray ellipse. Black line represents the scaling relationship between the sizes of those two traits. The slope of the linear regression is the allometric coefficient. (B) Comparison of the scaling relationships among different groups of individuals can reveal different allometric scaling coefficients. White ellipse represent isometric scaling, light gray ellipse represent hypoallometric scaling where organ size is less variable in the population, dark gray ellipse represent hyperallometric scaling where organ size is highly variable relative to body size. (C) Example of different scaling relationships in various closely related species of Onthophagus beetles. Plotting horn length vs body size demonstrates a tight scaling relationship within species. Comparing different species demonstrates that scaling relationships can vary dramatically. Figure adapted from (Frankino et al., 2009).

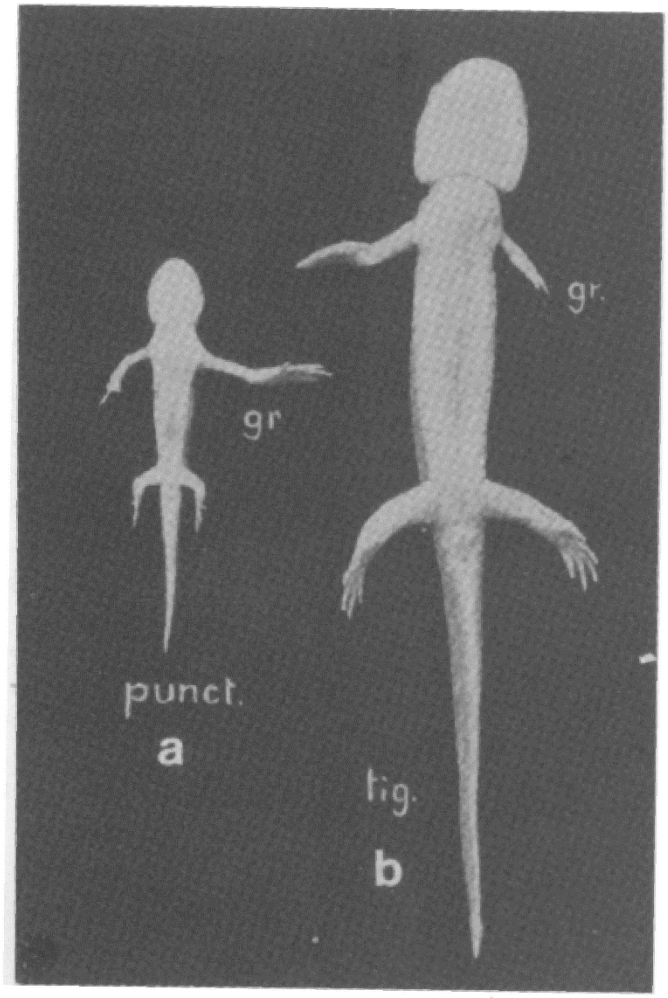

Figure 1-2. Limb xenograft experiments by Twitty and Schwind.
Anterior limb bud primordium from two closely related species of salamander, *Amblystoma punctatum* (smaller animal, left) and *Amblystoma trigrinum* (larger animal, right), were grafted (gr) onto the other's body. Both grafts grew to match the size of the donor animal, not the host. This indicates that tissue intrinsic factors regulate organ size. Image adapted from (Twitty and Schwind, 1931)

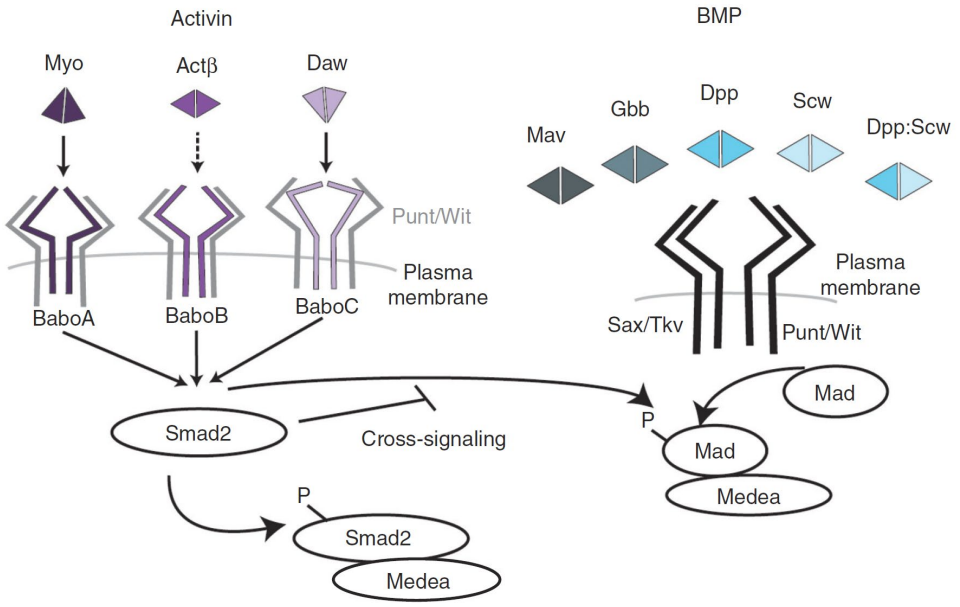

Figure 1-3. Core transforming growth factor β (TGF-β) family signaling components in Drosophila.

Activin branch: Three ligands signal through the activin-specific type I receptor Babo. Each ligand is thought to have a dedicated receptor isoform, although evidence for Actβ-BaboB is lacking. Ligand binding induces formation of a receptor complex of both Babo and either of the type II receptors, Punt or Wishful thinking (Wit). Constitutively active type II receptors phosphorylate Babo, which activates dSmad2. Phosphorylated dSmad2 binds to Medea and translocates to the nucleus to regulate the transcriptional response. Bone morphogenetic protein (BMP) branch: Four ligands signal through shared the BMP-specific type I receptors Tkv and Sax and either Punt or Wit. The ligands are thought to primarily form homodimers, but there is one example of a heterodimer: Dpp–Scw. Mav is a divergent ligand based on sequence, but signals to activate Mad. Activation of type II receptors causes phosphorylation of type I receptors and subsequent phosphorylation of Mad, which then complexes withMedea to regulate transcription. In the absence of dSmad2, Babo can phosphorylate Mad and can also activate theMad transcriptional response. Myo,Myoglianin; Actb,

Activin-b; Daw, Dawdle; Babo, Baboon; Mav, Maverick; Gbb, Glass-bottom boat; Dpp, Decapentaplegic; Scw, Screw; Sax, Saxophone; Tkv, Thickveins; Wit, Wishful thinking. Figure adapted from (Upadhyay et al., 2017)

Gene name	Symbol	Function	Interaction
armadillo	*arm*	Transcription factor	Complexes with Mad
crossveinless	*cv*	Lipoprotein	Modulates Dpp movement
crossveinless 2	*cv-2*	BMP binding protein	Binds extracellular BMPs
dally-like protein	*dlp*	Heparan sulfate proteoglycan	Controls Dpp gradient by binding Dpp
division abnormally delayed	*dally*	Heparan sulfate proteoglycan	Controls Dpp gradient by binding Dpp
follistatin	*fs*	Secreted factor	Modulates ligand activity
pentagone	*pent*	Secreted factor	Interacts with heparan sulfate proteoglycans to control Dpp gradient
Plum	*plum*	Immunoglobulin protein	Genetic interaction with Myo
Schnurri	*shn*	Transcription factor	Complexes with Mad and Medea
Shrew	*srw*	Secreted factor	Role unknown
short gastrulation	*sog*	Secreted factor	Binds extracellular BMPs
Tolloid	*tld*	Protease	Binds extracellular BMPs, cleaves Sog
tolkin (also called *tolloid-related*)	*tok, tlr*	Protease	Cleaves extracellular BMP and activin ligands
twisted gastrulation	*tsg*	Secreted factor	Binds extracellular BMPs
Yorkie	*yki*	Transcription factor	Complexes with Mad

Figure 1-4. TGFβ family accessory factors in *Drosophila*

List of known proteins that interact with core members of the TGFβ signaling pathway. Figure adapted from (Upadhyay et al., 2017)

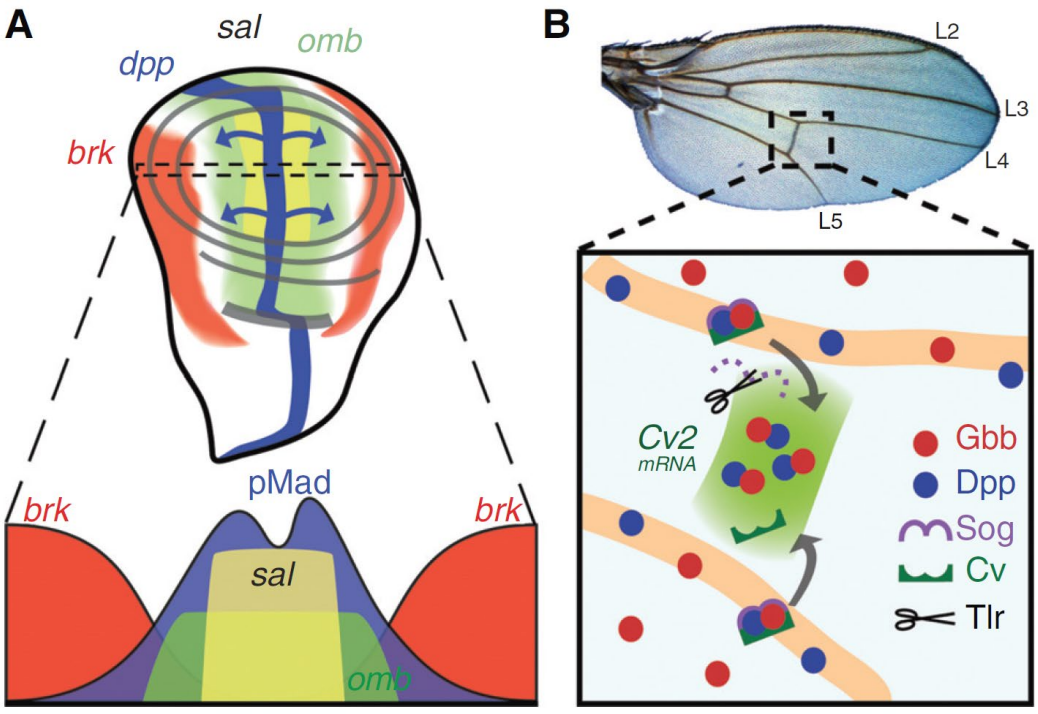

Figure 1-5. Dpp signaling in *Drosophila* wing development.

(A) During larval development, dpp (blue, top) is expressed along the A/P border and its gene product spreads to both compartments (blue arrows). High Dpp signaling in the middle of the disc results in activation of Mad (blue, below), which silences brk (red). The inverse gradients of pMad and Brk form the nested expression pattern of sal and omb. pMad is slightly lower in cells abutting the A/P axis due to local tkv down-regulation (Funakoshi et al. 2001). (B) Posterior crossvein (PCV) forms between the L4 and L5 veins (top), which begins during pupal development. Dpp–Gbb heterodimers bound by Sog (purple) and crossvein (dark green) allow for facilitated diffusion of ligands into the presumptive PCV space. Tolloid-related (Tlr) cleaves Sog and allows for signaling to occur. The initial broad signaling induces expression of CV-2, which further sharpens the signaling, resulting in PCV formation. Figure adapted from (Upadhyay et al., 2017)

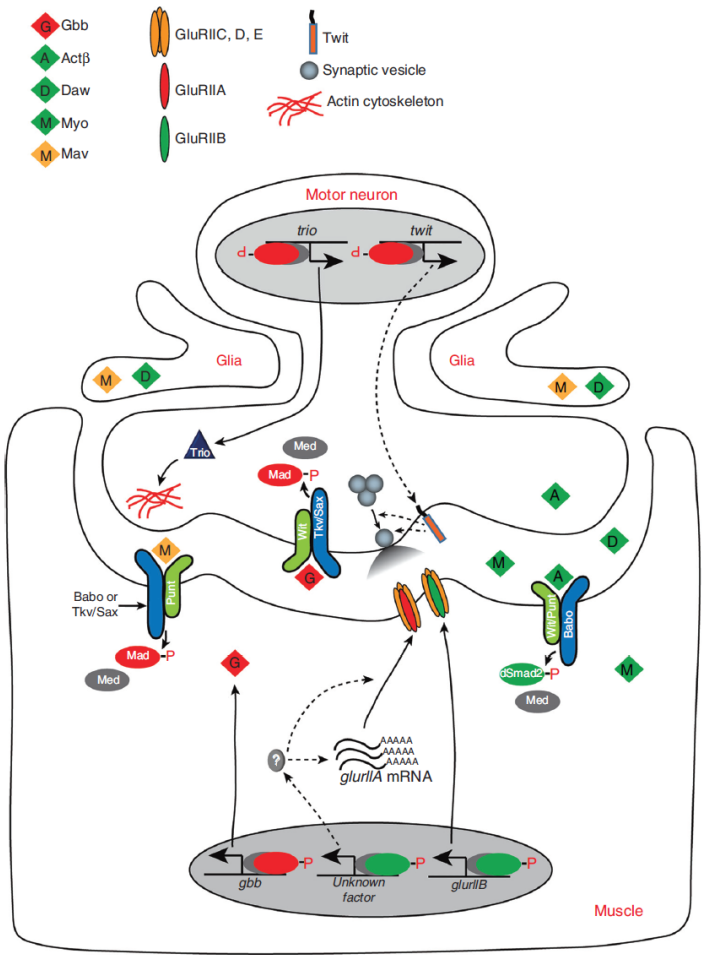

Figure 1-6. BMP and Activin signaling at the neuromuscular junction

Activin-like ligands from motoneurons activate dSmad2 in the muscle. Signaling induces transcription of glurIIB and an unknown factor(s) that controls posttranscriptional processing or mRNA stability of glurIIA. Muscle released Gbb binds to Wit-Tkv/Sax complex in the motor neuron and stimulates Mad phosphorylation. The resultant pMad–Medea complex activates the transcription of trio and twit whose products promote synaptic growth and control spontaneous vesicle release, respectively. The expression of Gbb in the muscle is fine-tuned by glia derived Mav. Figure adapted from (Upadhyay et al., 2017).

Chapter II

Motoneuron-derived Activinβ regulates Drosophila body size and tissue-scaling during larval growth and adult development

Others that contributed to this chapter:
Lindsay Moss-Taylor conducted experiments for figures: 2-1, 2-4 G, 2-5, 2-7, 2-8 (A-E), 2-9, and 2-12. Xueyang Pan conducted experiments for figures: 2-4 (A, C-E, H). Myung-Jun Kim conducted experiment for figures: 2-8 (F-H). Michael B. O'Connor conducted experiments for figures: 2-6, 2-11, 2-13, 2-14, and 2-15 A-C. All other experiments were done by me.

SUMMARY

Correct scaling of body and organ size is crucial for proper development and survival of all organisms. Perturbations in circulating hormones, including insulins and steroids, are largely responsible for changing body size in response to both genetic and environmental factors. Such perturbations typically produce adults whose organs and appendages scale proportionately with final size. The identity of additional factors that might contribute to scaling of organs and appendages with body size is unknown. Here we report that loss-of-function mutations in Drosophila *Activinβ (Actβ)*, a member of the TGF-β superfamily, lead to production of small larvae/pupae and undersized rare adult escapers. Morphometric measurements of escaper adult appendage size (wings, legs), as well as heads, thoraxes, and abdomens, reveal a disproportional reduction in abdominal size compared to other tissues. Similar size measurements of selected *Actβ* mutant larval tissues demonstrate that somatic muscle size is disproportionately smaller when compared to fat body, salivary glands, prothoracic glands, imaginal discs and brain. We also show that Actβ control of body size is dependent on canonical signaling through the transcription-factor dSmad2 and that it modulates the growth rate, but not feeding behavior, during the third instar period. Tissue and cell-specific knockdown and overexpression studies reveal that motoneuron derived Actβ is essential for regulating proper body size and tissue scaling. These studies suggest that, unlike in vertebrates where Myostatin, and certain other Activin-like factors act as systemic negative

regulators of muscle mass, in Drosophila Actβ is a positive regulator of muscle mass that is directly delivered to muscles by motoneurons. We discuss the importance of these findings in coordinating proportional scaling of insect muscle mass to appendage size.

INTRODUCTION

Some members of the animal kingdom, including most species of fish, amphibians, lizards, turtles, and salamanders, undergo indeterminate growth and increase their biomass throughout their lifespan. In contrast, birds, mammals and many insect species exhibit determinate growth whereby ideal body length and weight is fixed upon reaching sexual maturity. This process produces a more limited range of sizes that are characteristic for the species (Hariharan et al., 2015). In these animals, growth rate can vary during development and is influenced by both intrinsic and extrinsic factors. For example, in humans, at the conclusion of the high pubertal growth period, the long bone growth plates are ossified thereby preventing additional increase in overall skeletal size (Kronenberg, 2003; Shim, 2015). Similar to mammals, holometabolous insects also exhibit determinate growth. In Drosophila, a larva increases its mass 200-fold (70% of which occurs in the last larval instar) before terminating growth at pupariation (Church and Robertson, 1966). During the non-feeding pupal stage, the adult structures differentiate from larval imaginal tissue and there is no net

increase in body mass. Thus, the final body size is set by the rate of larval growth and the timing of its termination...

In recent years, numerous studies have centered on elucidating the molecular mechanisms that regulate hormonal activity during larval development in holometabolous insects to better understand how growth rate and duration are controlled (reviewed in (Boulan et al., 2015; Rewitz et al., 2013). In Drosophila, growth is largely regulated by the Insulin/IGF Signaling (IIS) and Target of Rapamycin (TOR) pathways, which are themselves regulated by different nutritional inputs. IIS is regulated by systemic sugar concentrations and TOR by circulating amino acid levels. Mutations that attenuate either pathway lead to slower growth rates resulting in diminutive animals with smaller and fewer cells (Böhni et al., 1999; Chen et al., 1996; Oldham et al., 2000; Rulifson et al., 2002). Conversely, activation of either pathway can lead to larger organs and cells if there are adequate nutrients (Goberdhan et al., 1999; Leevers et al., 1996; Stocker et al., 2003). Interestingly, systemic manipulation of IIS/TOR pathways typically leads to smaller or larger animals, with proportional effects on organ and appendage size (allometric growth) (Shingleton and Frankino, 2013; Shingleton et al., 2007).

While IIS/TOR are central regulators of growth rate in holometabolous insects, the major regulator of growth duration is the steroid hormone 20-hydroxyecdysone (20E) (reviewed in (Yamanaka et al., 2013a). During the final larval stage, a pulse of 20E extinguishes feeding, terminates growth and initiates

pupariation. The timing of the 20E pupariation pulse is triggered, in part, by the neuropeptide prothoracicotropic hormone (PTTH) which in Drosophila is produced by the two pairs of neurons in each brain hemisphere that innervate the prothoracic gland (PG) (McBrayer et al., 2007; Shimell et al., 2018). PTTH binds to its receptor Torso and stimulates synthesis and secretion of ecdysone from the PG (Rewitz et al., 2009; Yamanaka et al., 2013a). PTTH production/release responds to a variety of environmental signals including nutritional status, light, and tissue damage as well as internal signals such as juvenile hormone (JH) to further tune the timing of pupariation (De Loof et al., 2015; Shimell et al., 2018; Yamanaka et al., 2013b).

In addition to IIS/TOR signaling and steroid hormones, other signaling pathways have also been identified that affect final body mass and proportion scaling in both vertebrates and invertebrates. In particular, the TGFβ signaling pathway has known roles in controlling cell, tissue, and body size. TGFβ super-family ligands signal by binding to a heterotetrameric complex of type I and type II serine-threonine receptor kinases (Heldin and Moustakas, 2016). Ligand binding triggers type II receptors to phosphorylate type I receptors, thereby activating its kinase. In canonical signaling, the activated type I receptor phosphorylates its major substrates, the R-Smads (reviewed in (Hata and Chen, 2016). Once phosphorylated, R-Smads oligomerize with a co-Smads and translocate to the nucleus where together with other cofactors they regulate gene transcription (review in (Hill, 2016). The ligand super-family is broadly divided into

two major sub-divisions based on phylogenetic and signaling analysis (Kahlem and Newfeld, 2009). These include the TGFβ/Activins, which in vertebrates signal through R-Smads 2/3, while the BMP/GDF-type factors signal through R-Smads 1/5/8 (Macias et al., 2015).

TGFβ family members contribute to tissue and body size growth by a variety of mechanisms. For instance, in mammalian mammary cells, TGFβ cell-autonomously regulates cell size via mTOR during epithelial-mesenchymal transition (EMT) (Lamouille and Derynck, 2007). In addition, BMPs have been shown to control cell proliferation at the long bone growth plate and have been identified by genome-wide association studies as regulating human height (Hirschhorn and Lettre, 2009; Wood et al., 2014). Another particularly stunning example is Myostatin, a circulating Activin-type ligand, whose loss causes skeletal and muscle hypertrophy in vertebrates (McPherron and Lee, 1997; McPherron et al., 1997). TGFβ-type factors also affect the body size of invertebrates. For example, in *C. elegans*, a BMP-type ligand *DBL-1*, is secreted from neurons and signals via *small* (*sma*), a worm Smad, in the hypodermis to regulate expression of cuticle genes (Madaan et al., 2018; Tuck, 2014).

To further explore how TGFβ ligands influence body size, we investigated the role of Drosophila Actβ in regulating these traits using both loss and gain-of-function studies. In Drosophila, genetic studies as well as phylogenetic analysis suggests that Actβ signals via Baboon (Babo) and Punt, type I and type II receptors respectively, to phosphorylate dSmad2 (reviewed in (Upadhyay et al.,

2017). We find that canonical Actβ signaling through dSmad2 regulates adult viability, body size, and tissue scaling. *Actβ* mutants produce small larvae and pupae along with rare adult escapers. Compared to controls, these rare mutant adults exhibit small abdomens while other structures such as the head, thorax, leg, and wing are of relatively normal size. In larvae, muscle size is most profoundly affected while imaginal discs and the larval brain are of normal size. Furthermore, *Actβ* mutants have a slower overall growth rate, but show no defects in food intake. Using tissue specific gain and loss-of-function, we demonstrate that motoneuron derived Actβ is required for proper muscle growth and adult viability. Conversely, hyperactivation of Activin signaling in muscles by overexpression of activated Babo produces a much larger animal with bigger muscles, but smaller imaginal discs. These observations demonstrate that muscle size can be perturbed without having proportional effects on the size of the imaginal tissues. Therefore, we suggest that either muscles and appendages do not typically coordinate their growth or that such coordination requires *Actβ* signaling.

RESULTS

Actβ is required for adult viability, normal body size, and correct tissue scaling

Drosophila *Actβ* has been shown to be involved in a diverse group of developmental processes, including neuroblast proliferation, photoreceptor tiling, regulation of Akh signaling, inter-organ regulation of mitochondrial and hemocyte function (Makhijani et al., 2017; Song et al., 2017a; Song et al., 2017b; Ting et al., 2007; Zhu et al., 2008). However, in none of these studies was the lethal stage or the gross morphological phenotype carefully documented. To examine this issue, we initially characterized mutant phenotypes using the previously reported putative $Act\beta^{ed80}$ null allele (nonsense mutation) (Zhu et al., 2008). However, since the *Actβ* locus is on the fourth chromosome, additional recessive background mutations on the $Act\beta^{ed80}$ chromosome cannot be removed by recombination and therefore could complicate the phenotypic analysis of homozygous $Act\beta^{ed80}$ mutants. To resolve this issue, we generated several independent deletion alleles ($Act\beta^{4E}$, $Act\beta^{10E}$ and $Act\beta^{4dd}$) in the w^{1118} background using the CRISPR/Cas9 system (Ren et al., 2013; Sebo et al., 2014). All phenotypes initially described using Act^{ed80} homozygotes were confirmed using different combinations of transheterozygous alleles to rule out 4th chromosome background effects.

All examined *Actβ* mutant alleles are predominantly late pupal (pharate) stage lethal (Fig. 2-1 A and B). Many of the pharates show limited movement inside the pupal case, but most never eclose. Manual cracking of the operculum allowed a small percentage (~1%) to escape and produce viable adults that exhibit severe locomotive defects, and held out immobile wings rendering them flightless (Movie available upon request). Despite these behavioral/physical defects, females could mate and produce offspring from wildtype males. *Actβ* mutant males were unable to produce progeny with either mutant females or wildtype females. Whether this is a behavioral issue (i.e. unable to initiate courtship behavior) or a fertility defect was not determined.

In addition to pharate lethality, *Actβ* mutants exhibit a small body size at all stages of development. $Act\beta^{ed80}$ homozygous pupae (mixed male and female populations) are 21% smaller by volume relative to w^{1118} or heterozygous pupae (Fig. 2-1C). Similar to the $Act\beta^{ed80}$ homozygous phenotype, all trans-heterozygous combinations ($Act\beta^{ed80/4E}$, $Act\beta^{10E/ed80}$, $Act\beta^{10E/4E}$) are also significantly smaller (21%, 22%, and 26%, respectively) compared to w^{1118} control (Fig 2-1D) indicating that the small pupal size is not caused by secondary mutations on the mutant chromosome. Taken together, these data indicate that *Actβ* is required to produce normal pupal volume and adult viability.

Appendage size is proportionally scaled with body mass in Drosophila (Mirth and Shingleton, 2012). To examine if the adult body components of *Actβ* mutants are proportionally reduced, we collected 1 day old escaper males and

females and measured various traits. We found that the *Actβ*^{ed80} homozygous male weights are reduced on average 28% compared to the control (Fig. 2-2 A, female 20% not shown). We next measured the abdomen, thorax, and prothoracic leg lengths, along with head projection area and wing surface area of *Actβ* mutant males and controls. Interestingly, the size of some adult structures of *Actβ* mutants are more severely affected than others (Fig. 2-2 B-L). The abdomen length in *Actβ* mutants is reduced by a much greater proportion, -24% (Fig. 2-2 D, F) than any other measured component: head projection area, -8% (Fig. 2-2 B, C), thorax length, -4% (Fig. 2-2 D, E), prothoracic leg length, -2% (Fig. 2-2 G, J), wing area -4% (Fig. 2-2 H, K). Using the wing trichome density as a proxy, we found no difference in cell size between *Actβ* mutants and the *w*^{1118} control (Fig. 2-2 K, I, L), indicating that the minor reduction in wing size is likely caused by a subtle defect in cell proliferation at some time during development.

Actβ disproportionately affects larval muscle and certain polyploid tissue sizes

To understand the size discrepancy of adult structures in *Actβ*^{ed80} mutants, we examined directly the size of various larval tissues including brain, wing and leg discs, and body-wall muscles, and indirectly the sizes of several polypoid tissues including the fat-body, proventriculus, salivary and prothoracic gland cells using the size of the nucleus as a proxy for cell size.

The most pronounced defect of *Actβ*^{ed80}mutant larvae is exhibited by the body wall muscles which in males are reduced by 37% (Fig. 2-3 A-C), and muscle nuclear size by 53% (Fig. 2-3 D-F). The muscle size reduction is not caused by an earlier myoblast fusion defect since mutant muscles contain the same number of nuclei as wildtype (Fig. 2-9). In contrast, neither the brain volume (Fig. 2-3 J, K) nor the 2-D projected surface area of the wing, leg, and haltere disc (Fig. 2-3 K-P) were significantly affected. Interestingly, we note that the nucleus size of several other polyploid tissues including the fat body and the prothoracic glands are also significantly reduced, but to a lesser degree than the muscle nuclei (22% for fat body, Fig. 2-3 G-I, 37% prothoracic gland vs 53% muscle Fig 2-10 G-I). Curiously, the nuclear sizes of the cells within the proventriculus remained unchanged (Fig. 2-10 A-C) and the average salivary gland cell nuclear size actually increased. (Fig. 2-10 D-F). We conclude that the small pupal volume and reduced escaper weights are primarily due to the disproportionate reduction in muscle size rather than alterations in mitotic tissue growth such as the brain and imaginal discs.

Actβ mutants feed normally but grow slowly

Body size is largely determined by two factors, the duration of growth and the growth rate, or some combination of the two parameters. In addition, a slower growth rate may reflect reduced food intake, diminished absorption of nutrients,

or an alteration in metabolic flux. We examined several of these parameters to determine if they were altered in *Actβ* mutants. First, we measured the larval growth rate during the L3 period, when most of the larval growth occurs. At the start of the L3 stage, there is no difference in mass of the mutants versus the controls; however, over the course of 36 hours, a slower rate of mass accumulation becomes apparent such that, at the time when larvae begin to wander, the $Act\beta^{ed80}$ mutants weigh 18% less than w^{1118} controls (Fig. 2-4 A). This difference in growth rate likely accounts for a large portion of the reduced body size phenotype. To examine whether the diminished growth rate might reflect reduced food intake, we measured feeding rates of foraging early L3 larvae by the mouth-hook contraction assay (Wu et al., 2003a; Wu et al., 2005). Surprisingly, we found no difference in the head contraction rates of the *Actβ* mutants (Fig. 2-4 B) suggesting that the slow growth rate of these mutants is not likely caused by reduced food intake, but instead may reflect an alteration in nutrient absorbance or dysfunctional metabolic flux.

Next, to determine whether the small body size might also involve a reduced growth period, we measured the time to pupariation as well as the critical weight (CW), which is a nutritional checkpoint that ensures larvae have enough nutrient stores to produce viable adults (Nijhout and Callier, 2015). In both the control and $Act\beta^{ed80}$ mutant, starvation after just 2 hours into the L3 stage blocks pupariation (Fig. 2-4 C). In the $Act\beta^{ed80}$ mutant, starvation beginning 4 hours after L2/L3 ecdysis results in delayed pupariation, while starvation 12

hours after L3 ecdysis results in no developmental delay, indicating attainment of CW. The w^{1118} control achieves CW 8 hours after L2/L3 ecdysis (Fig. 2-4 D,E). Given the four hour difference between the time the $Act\beta^{ed80}$ mutant and the w^{1118} control reach CW, and considering that *Actβ* mutants grow slower, we calculated that the weight at the time when CW is reached for *Actβ* mutants is similar to that of controls (0.88 mg for w^{1118} vs 0.84 mg for $Act\beta^{ed80}$, Fig. 2-4 F). Therefore, we conclude that $Act\beta^{ed80}$ does not affect the CW checkpoint.

Although the CW represents the lower threshold of mass necessary for pupariation without delay, body size can be altered by either a shorter or longer terminal growth period which occurs after CW has been reached (Nijhout and Callier, 2015). Therefore, we also measured the total time to pupariation. We find that, although $Act\beta^{ed80}$ homozygous mutants grow slowly, they pupariate on average 4 hours earlier when compared to w^{1118} at 25°C. (Fig. 2-4 G). However, the $Act\beta^{ed80}$/+ heterozygotes also pupariate earlier than w^{1118} (Fig 2-4 G) suggesting either a haplo-insufficient effect of $Act\beta^{ed80}$ or that this phenotype is attributable to the genetic background differences between $Act\beta^{ed80}$ and w^{1118}. To examine this issue, we repeated the experiment with two CRISPR alleles. In this case, we find no difference in pupariation timing during the third instar stage between trans-heterozygous $Act\beta^{4dd}/Act\beta^{10E}$ mutants or $Act\beta^{4dd}$/*unc13* heterozygotes compared to w^{1118} controls (Fig. 2-4 H). However, we also observe that certain allelic combinations such as w^{1118}/*unc13* wild-type controls and $Act\beta^{4dd}/w^{1118}$ heterozygotes also pupariate 2 hours earlier than w^{1118} controls

(Fig. 2-4 H). Therefore, we conclude that the slight timing differences reflect either differences in genetic background, slight differences in the duration of first and second instar growth, or the limits of timing resolution in this experiment and that *Actβ* loss does not substantially affect developmental timing.

Overexpression of Actβ in its normal pattern produces larger and slower-growing larvae.

Since loss of *Actβ* results in small developmentally arrested pupae, we asked whether overexpression of *Actβ* in its endogenous pattern would have the opposite effect on pupal size, viability, and whether it might also affect developmental timing. For this purpose, we overexpressed *Actβ* using an *Actβ-Gal4* promoter enhancer line (Song et al., 2017a; Zhu et al., 2008). Relative to either the *UAS-Actβ-3B2* or the *Actβ-Gal4* controls, overexpression of *Actβ* (*Actβ > Actβ-3B2*) results in a significant increase in pupal volume and a delay in developmental timing (Fig. 2-5 A,B). Strikingly, pupariation is delayed over 20 hours compared to either w^{1118} or *Actβ* mutants however, there is no change in viability (Fig. 2-5 B,C). Together, these data show that *Actβ* regulates body size and perhaps developmental timing in a dose dependent manner.

Tissue and cell-type specific rescue experiments identify several potential sources of Actβ for controlling body size.

To investigate how Actβ affects body size, developmental timing and viability, we first sought to determine if one or more cell types serves as the source(s) of the ligand that controls different aspects of the mutant phenotype. Several features of endogenous *Actβ* transcription have been previously described including expression in motoneurons, mushroom body neurons, peripheral neurons including multi-dendritic and chordotonal neurons, developing photoreceptors in the eye disc, and in midgut enterocytes (Gesualdi and Haerry, 2007; Kim et al., 2014; Makhijani et al., 2017; Song et al., 2017a; Ting et al., 2007; Ting et al., 2014; Zhu et al., 2008). We examined the *Actβ* expression pattern in the larvae by crossing an *Actβ-Gal4* to *UAS-cd8GFP* or *UAS-GFP*. We also confirmed expression in particular cell types using RNA *in situ* hybridization (Fig. 2-11). As previously described, *Actβ* is almost exclusively expressed in the central and peripheral nervous systems (Fig. 2-6 E). More detailed examination reveals that in the central brain lobes, *Actβ-Gal4>UAS-GFP* is expressed strongly in mushroom body neurons and in a 14-cell cluster in the anterior medial region of each brain lobe (Fig. 2-6 A-A''). A subset of 7 cells within this 14 cell cluster also stain with α-Dilp5 (Fig. 2-6 A'), which marks the ~7 insulin producing cells (IPCs) (Brogiolo et al., 2001). In the ventral nerve cord, *Actβ* >Gal4 is expressed strongly in the motoneurons, marked by α-p-Mad (Fig. 2-6 G-G'')

(Marqués et al., 2002). We also see strong staining in all α-Dimm-marked neuroendocrine cells (Fig. 2-6 H-H") (Park et al., 2008).

Because of the possible developmental timing defects, we were particularly interested in whether *Actβ* is expressed in the neurons that innervate the ring gland (RG), the major endocrine organ of larvae, or in any of the RG cells themselves. We found strong expression in the corpus cardiacum (CC) cells that produce the hormone Akh which is involved in regulating sugar metabolism (Fig. 2-6 C-C'', Fig 2-11 D). While we observed no expression in the cells of the prothoracic gland (PG), which produces the steroid hormone ecdysone (Yamanaka et al., 2013a), or in the corpus allatum (CA) which produces juvenile hormone (Riddiford et al., 2010), we did see signal in axons tracts that innervate each of these tissues (Fig 2-6 F-F'). The PG neurons produce prothoracicotropic hormone (PTTH) and innervate the PG portion of the ring gland to regulate ecdysone production (McBrayer et al., 2007; Siegmund and Korge, 2001). Co-staining of *Actβ>cd8GFP* brains with α-PTTH reveals strong expression in the PG neurons (Fig. 2-6 B-B"). While we have no specific antibody that marks the CA neurons, the GFP positive innervations that we observe on the CA are highly suggestive that the CA neurons express Actβ (Fig. 2-6 F-F'). Actβ is also found in various other unidentified neurons within the central brain and ventral nerve cord. Outside the nervous system, we observe Actβ expression only in a limited number of enterocytes in the midgut (Fig. 2-6 D-D") and non neuronal tissue expression includes the enteroendocrine cells (Fig. 2-6 D-D", Fig 2-11 H) as

previously reported (Song et al., 2017a), and the ovariole follicle and border cells (Fig. 2-6 I-J, Fig. 2-11 G) and some tracheal cells. (Fig. 2-6 K, Fig. 2-11 F). Our observation that the rare escaper females are fertile suggests that Activin signaling in the follicle cells is either not required for full fertility or that its expression might be redundant with another activin like ligand such as Dawdle or Myoglianin.

Motoneuron-derived Actβ regulates body size and viability

To determine which *Actβ*-expressing cell types influence size and viability, we attempted rescue experiments using different tissue specific Gal4 drivers to overexpress the *Actβ* transgene in the $Act\beta^{ed80}$ mutant background. $Act\beta^{ed80}$ mutants with one copy of either the *UAS-Actβ* or the various *Gal4* transgenes served as negative controls. Since overexpression of *Actβ-GAL4* driving *UAS-Actβ* is sufficient to increase body size (Fig. 2-5 A), here we asked whether it is able to rescue the small body size (pupal volume) and pupal lethality of *Actβ* mutants. Indeed, *Actβ>Actβ* in the mutant background is not only sufficient to rescue body size, but actually produces larger animals (47% bigger Fig. 2-7 A) similar to what we see upon overexpression in a wild type background (Fig. 2-5 A). Overexpression of Actβ in its normal pattern also resulted in strong rescue of lethality (Fig. 2-7 B, 42.7% viability vs 1-4% viability of mutant controls; the test cross viability rate for w^{1118} is 73.8%, Fig. 2-7 B).

To narrow down the relevant source of ligand that regulates each phenotype, we used increasingly restrictive (tissue specific) Gal4 lines to overexpress *Actβ* and then measured body size and viability. Overexpression of *Actβ* using the pan-neuronal driver, *nrv2-Gal4*, rescues both body size and adult viability (Fig. 2-7 C-D). Surprisingly, overexpression of *Actβ* from the motoneurons, *OK371>GAL4,* alone rescues both body size and viability (Fig. 2-7 E-F). Interestingly, *Actβ* overexpression in Dimm^{+} neuroendocrine cells (*C929>Gal4*), also rescues both body size and viability (Fig. 2-7 G-H). Just like overexpression of *Actβ* from its endogenous sources, we also found that overexpression of *Actβ* in either motoneurons or neuroendocrine cells in wildtype animals also produces large adults (Fig. 2-12). Lastly, overexpression of *Actβ* in only the IPCs (*dilp2>Gal4*), which makes up a much smaller subset of all neuroendocrine cells, does not rescue either phenotype (Fig. 2-7 I-J).

The finding that expression in only the motoneurons rescues body size suggests that Actβ may be supplied directly to the muscles via the neuromuscular junctions. However, we also find that overexpression in neuroendocrine cells is sufficient to rescue body size, which suggests that Actβ may be able to function as a systemic endocrine signal and need not be directly delivered to the muscle via the neuromuscular junction synapse. Therefore, we asked if expression of *Actβ* from non-neuronal, but highly secretory tissues, was able to rescue various aspects of the null phenotype. Interestingly, expression of *Actβ* using the *ppl-Gal4* (fat body and muscle) driver increases pupal volume

beyond wild-type levels and partially rescues adult viability (Fig. 2-7 K and L). Overexpression in only the body wall muscles (*MHC-Gal4*) also increases body size beyond wild type levels, but does not rescue adult viability (Fig. 2-7 M-N). However, we note that overexpression of *Actβ* using either *MHC-Gal4* or *ppl-Gal4* in a wild type background results in most animals dying as large oversized and curved pupae (Fig. 2-13). These phenotypes are likely due to hyperactivation of TGFβ signaling in the muscles because we observe a similar phenotype when a constitutively activated version of Babo is overexpressed in the muscles (Fig. 2-13). Taken together, these results suggest that, although Actβ signaling in muscles is required for proper body size, too much signaling in muscles can be deleterious. We were not able to specifically test the ability of enteroendocrine-derived Actβ to rescue mutant phenotypes, because overexpression of *Actβ* using the midgut enteroendocrine cell driver (*EE-Gal4*) (Song et al., 2017a) is lethal in both wild type and *Actβ* mutant backgrounds, likely due to overexpression in many cells besides enteroendocrine cells, including fat body, CNS and PNS (data not shown). In summary, we conclude that since overexpression of Actβ from motoneurons or neuroendocrine cells rescues both body size and viability and can increase body size when overexpressed from these sources in wild type animals, they are likely the most important endogenous sources of ligand for viability and body size control.

Motoneuron derived Actβ signals through the canonical Babo/dSmad2 pathway to control muscle and body size.

The rescue experiments described above suggest that either motoneurons or Dimm^{+} neuroendocrine cells, or both can produce enough Actβ to regulate body size. Since data from overexpression alone does not reflect the *in vivo* importance of various endogenous ligand sources, we sought a complementary set of loss-of-function data using tissue specific RNAi knockdown. First, we tested all publicly available (TRiP, VDRC, and NIG) *Actβ* RNAi lines to phenocopy the *Actβ* mutant. Using the ubiquitous driver *da-GAL4* to overexpress *dicer2* along with the various *Actβ* RNAi lines, we find that only the TRiP stock (BDSC#29597) can phenocopy the small, dead pharates similar to *Actβ* null alleles (data not shown). Most other lines produce viable flies of normal size suggesting that they are not very effective in knocking down endogenous *Actβ.* Both NIG lines (1162R-1 and 1162R-2) produce a more severe phenotype (early larval lethality) compared to the null suggesting it may have off-target effects.

Using the TRiP 29597 RNAi line, we tested whether knockdown of *Actβ* in either all neurons, motoneurons or neuroendocrine cells alone phenocopies any aspect of null alleles. We find that knockdown in Dimm^{+} neuroendocrine cells (*C929-Gal4*) produces viable normal-sized flies (data not shown). In contrast, knockdown in all neurons (Elav>Gal4 Fig. 8A) or motoneurons (*OK371-Gal4*, Fig. 2-8 A,B) completely phenocopies *Actβ* nulls giving rise to small, dead pharates with rare escapers that hold out their wings and have a slow gait (Movies

available upon request). The *OK371* driver is not expressed in the Dimm^{+} neuroendocrine cells (Fig. 2-14) leading us to conclude that the motoneurons are the major source of endogenous *Actβ* that regulates body size and viability.

We next determined if motoneuron-derived *Actβ* signals to the muscle via the canonical Smad2 pathway. Canonical TGFβ signaling is mediated by the Activin receptor, Babo, and the signal transducer, dSmad2. In muscles, overexpressed Babo is localized to the postsynaptic neuromuscular junction, perhaps sensitizing the muscles to receive motoneuron derived Actβ (Kim et al., 2014). Indeed, RNAi knockdown of *Babo* or *dSmad2* in the body wall muscle results in smaller pupal volume (Fig. 2-8 C-D). Furthermore, on Western blots, we detect lower levels of phosphorylated dSmad2 in *Actβ* mutant carcass extracts (containing somatic muscle, cuticle and associated cells) compared to the w^{1118} control (Fig. 2-8 E). Conversely, overexpression of *Actβ* in motoneurons both increases pupal/adult size (Fig. 2-12) and p-Smad2 levels in the carcass (Fig. 2-8 D-E), which is similar to overexpression of activated dSmad2 in the muscle, producing large larval muscles (Fig. 2-8 F-H) or overexpression of activated Babo or dSmad2 results in adult flies with extended abdomens (Fig. 2-15 A-C). Interestingly, the *MHC>dSmad2(SDVD)* animals with larger body size have slightly smaller wings, not larger wings as expected if organs are actively scaled to maintain size proportion between muscles and appendages (Fig. 2-15 D).

DISCUSSION

Identifying and characterizing how inter-organ signals regulate physiologic and metabolic homeostasis during development and adulthood is of central importance. Various types of inter-organ signals are also likely to be necessary for coordinating growth between organs during development to achieve proper body proportions (Droujinine and Perrimon, 2016). In this report, we demonstrate that Actβ is a key brain-derived factor that regulates somatic muscle size in *Drosophila* by signaling through the canonical Smad-dependent pathway. Furthermore, we find that disruption of Actβ signaling alters larval and adult organ allometry suggesting that Actβ might be a component of an inter-organ signaling pathway that helps coordinate muscle growth with appendage growth.

Localized versus systemic effects of Actβ

The question of whether Actβ acts locally or systemically via the hemolymph to target tissues is an important issue raised by our study and previous work (Song et al., 2017a; Song et al., 2017b). On the one hand, we find that *Actβ* is strongly expressed in most if not all neuroendocrine cells. We also find that overexpression of *Actβ* from these cells results in the rescue of mutant phenotypes and overgrowth of wild type animals indicating that direct tissue contact is not necessary for Actβ signaling to control muscle size. However, we also find that depleting *Actβ* expression in just the motoneurons phenocopies

Actβ mutants while depletion in neuroendocrine cells does not do so, at least with the *929>Gal4* driver. Therefore, we conclude that, while high systemic concentrations of Actβ produced by overexpression is capable of regulating muscle growth, the endogenous systemic level supplied by the combination of the neuroendocrine and the enteroendocrine cells is not sufficient to do so.

Whether local or systemic Actβ signaling is important in other contexts is less clear. Interestingly, Actβ has also been implicated in regulating hemocyte proliferation and adhesion within hematopoietic pockets localized on the larval body surrounding a number of peripheral neurons that express *Actβ* including da and chordotonal peripheral neurons (Makhijani et al., 2017). In contrast, enteroendocrine derived Actβ is able to affect AKH receptor levels in the fatbody to regulate glycemic index on a high sugar diet (Song et al., 2017a). In addition, it has been reported that upon mitochondrial perturbation, muscle-derived Actβ signals to the fat body to regulate triglyceride levels (Song et al., 2017b). In either case these observations raise the question: what dictates the requirement of a local versus a systemic signal for Actβ function? In the muscle motoneuron synapses and hematopoietic pocket paradigms, there may be physical barriers that help concentrate ligand from a local source to levels sufficient to produce a response. In the case of muscles, motoneuron synapses are embedded within the muscle fiber (Prokop, 2006; Prokop and Meinertzhagen, 2006) and therefore delivery of Actβ directly to the NMJ via the synapse likely provides a highly effective signal, especially since its receptor Babo is also highly concentrated at

the postsynaptic NMJ (Kim et al., 2014). This possibility might also account for the discrepancy between our findings (Fig. 2-11) that muscles do not express Actβ under normal conditions, while mitochondrial perturbations in muscle appears to release Actβ for signaling to the fat body (Song et al., 2017b). Perhaps disturbing mitochondrial function in muscle disrupt synaptic structure such that Actβ is liberated from defective NMJ synapses. Likewise, the hematopoietic pockets might provide a similar restricted niche-like signaling environment that is able to modulate hemocyte proliferation and adhesion. These types of physical constraints may limit the ability of endogenous circulating Actβ to produce sufficient levels of signaling at these locations, except under overexpressed conditions.

Another factor influencing the cellular response to Actβ levels is the composition of the surface receptors. The *babo* locus produces three receptor isoforms that only differ in the extracellular ligand binding domain, and each likely has a different affinity for the three Activin-like ligands (Jensen et al., 2009; Upadhyay et al., 2017). Therefore, the complement of receptor isoforms on a cell's surface is apt to determine the sensitivity of the cell or tissue to Actβ signals.

Mechanisms of Actβ control of tissue size

The molecular mechanism(s) by which Actβ affects tissue growth are unclear. The most well characterized factors that regulate insect body size are all systemic signals such as juvenile hormone, ecdysone and the IIS/TOR pathways (Boulan et al., 2015; Koyama and Mirth, 2018; Mirth and Shingleton, 2014; Rewitz et al., 2013). For example, *Ptth* mutants delay ecdysone accumulation allowing larvae to grow for an additional 24 hours ultimately leading to larger flies (Shimell et al., 2018). In this report, we demonstrate that Actβ, although it is expressed in the PTTH-producing neurons, does not appear to affect ecdysone signaling since *Actβ* loss affects neither critical weight nor developmental timing.

Interestingly, we also see Actβ positive innervation of the CA organ which produces juvenile hormone (JH), and lowering JH levels in Drosophila leads to production of smaller flies by slowing the overall growth rate (Mirth et al., 2014; Riddiford et al., 2010). Since we also observe a slower growth rate in *Actβ* mutants it is possible that Actβ might work to slow growth via reduction of JH signaling. However, given the strong expression of Actβ in all $Dimm^{+}$ neuroendocrine cells which secrete numerous peptides that regulate many aspects of behavior and metabolism including insulin, many other mechanisms must be considered for slowing growth. While food intake does not seem to be altered in Actβ mutants, it is possible that nutrient absorption or metabolic flux is disrupted. The latter possibility is particularly attractive since we see strong expression of *Actβ* in the CC organ, which produces the Drosophila glucagon-like

hormone (Akh), and in the insulin producing cells (IPCs) in the brain. As previously noted, Actβ has been implicated in regulating AkhR levels in the fat body (Song et al., 2017a) and perhaps it may also influence Akh synthesis or release. Furthermore, Dawdle, another Drosophila Activin-like ligand that also signals through dSmad2 has been previously shown to regulate metabolism and carbohydrate utilization (Chng et al., 2014; Ghosh and O'Connor, 2014). Therefore, Actβ signaling through dSamd2 may also regulate global carbohydrate synthesis or aspects of metabolism to adjust the larval growth rate.

Regardless of how overall growth defects occur, it is important to remember that not all larval tissues respond equally to Actβ. The brain and imaginal discs, for example, are of normal size while fat body and muscle are significantly smaller. In addition, the size and viability defects can be largely rescued by expression of Actβ solely in motoneurons. Therefore, it seems unlikely that a primary defect in systemic levels of insulin or Akh would account for the tissue specific responses. Rather, it is likely that alterations in muscle metabolism and perhaps factors secreted by muscles could account for the small muscle/body size.

Larval versus Adult requirements for Actβ

The requirement of Actβ for adult eclosion raises several issues. The first is whether the low eclosion rate is primarily a muscle defect or a neuronal

problem since both must be coordinated to produce the complex set of motor behaviors required for eclosion. Interestingly, ablation of Dimm+, Eclosion hormone (EH) producing neuroendocrine cells (Park et al., 2008), results in a defective eclosion motor program, which involves a series of coordinated head, thorax, and abdominal muscle contractions that ejects the animal through the operculum and out of the pupal case (McNabb et al., 1997). It may be that the small adult muscles lack the power to properly execute the eclosion motor program. In addition, the small muscle phenotype may also partially explain why the *Actβ* mutant adult escapers walk slowly and cannot move their wings. However, this must be reconciled with the observation that *Actβ* mutant larvae exhibit no obvious defect in locomotion, even though they have a similar proportional reduction in overall body and muscle size.

Improper synaptic development or NMJ function could also potentially account for adult locomotion defects. However, we have previously shown that, at least in larvae, the NMJ size and bouton number are not affected in *babo* and *dSmad2* mutant larvae when normalized to the smaller muscle size (Kim et al., 2014). Nevertheless, we did uncover a number of electrophysiological alterations including a decrease in the number and frequency of miniature excitatory potentials and a depolarized muscle membrane resting potential, both of which were primarily attributed to defective Actβ signaling in muscles (Kim et al., 2014). Despite these defects, the large action potentials in *babo* and *dSmad2* mutants are relatively normal and, as described, there are no obvious larval locomotion

defects (Kim et al., 2014). Since adult muscles are formed *de novo* during metamorphosis, it is possible that during this time more extreme defects in muscle or neuron physiology develop in *Actβ* mutants, perhaps leading to a more strongly depolarized muscle, for example, that would interfere with proper muscle function.

The motoneuron source of Actβ also raises questions concerning whether Actβ production/release is muscle/neuron activity dependent. We find that overexpression of Actβ in motoneurons can produce bigger muscles, but whether increased muscle activity also accompanies higher Actβ expression/secretion triggering increased muscle growth is an interesting issue to address. We note, however, that adult muscles, which develop during the immobile pupal stage, are also likely smaller than wild type in *Actβ* mutants suggesting that significant muscle activity is not likely required for Actβ release.

Body-appendage scaling

One of the more novel features of the *Actβ* null phenotype is the disproportionate effect it has on muscle size compared to other tissues. One might expect that evolutionary pressures fine tune mechanisms to coordinate muscle size with the size of the appendage that it moves. This is perhaps especially true in winged insects where flight muscle and wing size should be coordinated to produce efficient flight. Such coordination between wing and body

size in response to environmental perturbations has been best studied in *Manduca sexta* (Nijhout and Callier, 2015; Nijhout and Grunert, 2010). In this insect, nutritional restriction can result in as much as a 50% reduction in body size, with the wing scaling proportionally and containing half as many cells (Nijhout and Grunert, 2010). This scaling mechanism utilizes a shift in the amplitude and kinetics of steroid hormone production during the last instar stage. Since this mechanism involves systemic factors that adjust the growth rate of the whole body, presumably affecting muscles and discs simultaneously, it does not really address whether specifically perturbing muscle growth can directly or indirectly affect growth of the wing or other appendages.

In Drosophila, alteration in the growth properties of one imaginal disc perturbs growth of other wild type discs in a coordinated manner so that adults emerge with properly proportioned structures (Simpson and Schneiderman, 1975; Simpson et al., 1980; Stieper et al., 2008). Once again, the inter-organ signaling mechanism involves alteration in the levels of systemic hormones (Gokhale et al., 2016; Mirth and Shingleton, 2012; Parker and Shingleton, 2011). In these reports, is not clear whether muscle size was also altered to produce isometric scaling between it and the imaginal discs. However, it is interesting to note that growing Drosophila at low temperatures produces hyperallometric scaling where the wing size is disproportionally larger relative to body size (Shingleton et al., 2009). Since we observe similar phenotypes in *Actβ* mutants grown at normal temperatures, it is intriguing to speculate that Actβ signaling

might mediate hyperallometric scaling between wing and body in response to temperature.

The only other report that we are aware of where Drosophila larval muscle size was specifically manipulated, and the effect on growth of other tissues examined, involved genetic alteration of insulin signaling (Demontis and Perrimon, 2009). Similar to our analysis of *Actβ*, the level of insulin signaling in muscle is directly correlated with muscle, appendage, and overall animal size. Nevertheless, our findings for Actβ show several notable differences. First, insulin gain-of-function signaling in muscle lead to larger bodies and larger wings (Demontis and Perrimon, 2009), while we find that increased Actβ signaling in muscles results in larger bodies, but slightly smaller wings. In the insulin loss-of-function case, both muscles and wings were smaller, the latter due to a reduction in cell size not cell number. However, in the case of *Actβ* mutants, we see only a 4% decrease in wing size with no change in cell size. In both cases, the effect on muscle size appears to be much more dramatic than the effect on appendage size. Therefore, if a scaling mechanism exists, then either insulin or Actβ loss disrupts it, or it is not isometric as is found for the nutrient-dependent body-wing scaling response in *M. sexta*. The general similarity in phenotypes produced by insulin or Actβ signaling suggests that Actβ may exert its effect on muscle and body size, in part, through the insulin signaling pathway, a possibility that we are currently exploring.

TGFβ control of body size in other animals

TGFβ regulation of body or muscle size has been reported in both *C. elegans* and mammals. In *C. elegans*, BMP-type factors are also secreted from a specific set of neurons and appear to act systemically to regulate the size of the hypodermis through a canonical Smad dependent pathway (Tuck, 2014). In fact, the term Smad is a compound word derived from the *C. elegans* gene *sma* meaning small, and the Drosophila gene *mad* (mothers against dpp) which were the founding members of the Smad family of TGFβ signal transducers (Derynck et al., 1996). Recently, many transcriptional targets for the Sma factors in *C. elgans* have been identified, among which are several collagens that are major structural components of the hypodermal body-wall (Madaan et al., 2018). Hence, we speculate that one set of targets for both Actβ and insulin signaling in the *Drosophila* muscle could be structural proteins that build muscle. It is also possible that target gene expression is indirectly regulated by DNA copy number. In Drosophila, larval and adult muscle are polyploid tissues where DNA content is controlled by endocycling. Both Actβ (this report) and insulin signaling (Demontis and Perrimon, 2009) appear to regulate nuclear size in many polypoid tissues, possibly indicating that control of the endocycle maybe the primary mechanism regulating tissue size. However, at least in Actβ mutants not all polyploid tissues show regulation in the same direction, i.e. muscle, fatbody and the prothoracic gland all show smaller nuclei while the salivary gland has larger nuclei. Whether

systemic Actβ signaling is directly regulating size of polyploid tissues or acts indirectly through a muscle-derived myokine needs to be determined.

In mammals, the best characterized example of a TGFβ-type factor that regulates body and muscle size is provided by Myostatin (Mstn). Loss of Mstn was discovered to cause the muscle overgrowth phenotype of Belgian blue cattle and subsequent work in many other species including humans confirmed that Mstn is a negative regulator of muscle mass (McPherron and Lee, 1997; McPherron et al., 1997). *Mstn* mutant muscles have both an increase in myofiber number (Matsakas et al., 2010; Trendelenburg et al., 2009) as well as myofiber size (Elashry et al., 2009; McPherron and Lee, 1997). The molecular basis for the phenotype appears to be an alteration in protein homeostasis, where proteasome and autophagic degradative capacity is reduced relative to protein synthesis (Lee et al., 2011; Lokireddy et al., 2012). Mstn signals through Smads2/3 and is therefore considered to be within the TGFβ/Activin subgroup in the TGFβ superfamily. Additional studies of Activin ligands themselves suggest that that they also act as negative regulators of muscle mass similar to Mstn (Zhou et al., 2010). Furthermore, studies on the role of BMP signals in muscle size control suggest that they function as dominant positive regulators of muscle mass by promoting protein synthesis instead of breakdown (Sartori et al., 2013; Winbanks et al., 2013).

Our present work shows that in Drosophila, Actβ is a positive regulator of muscle mass, by affecting myofiber size not number. It is worth noting that

Drosophila has a close Myostatin homolog that is called *myoglianin* (*myo*) and recent studies suggest that loss of *myo* in muscle produces larger fibers similar to the vertebrate homolog (Augustin et al., 2017). How Actβ and Myo interact will be interesting to examine as will the role for BMPs in *Drosophila* muscle size determination. Lastly, the question of whether Mstn loss in vertebrates affects scaling of other tissues is largely unexplored although it does appear that bone density is increased in *myostatin* mutant animals (Elkasrawy and Hamrick, 2010). Additional studies of how local versus systemic roles of TGFβ ligands might affect growth and scaling between tissues and organs in vertebrates should be enlightening.

MATERIALS AND METHODS

Fly lines

For overexpression experiments single copies of Gal4 and UAS transgenes were used. *Actβ-Gal4* and *UAS-Actβ* (3B2) were previously described (Zhu et al., 2008). *C929-Gal4*, dilp2-*Gal4*, *Elav-Gal4*, *Mef2-Gal4*, *MHC-Gal4*, *Nrv2-Gal4*, *OK371-Gal4*, *ppl-Gal4*, *UAS-dicer2, UAS-cd8::GFP,* and *UAS-Actβ RNAi Ok6>Gal4* were all from the Bloomington stock center. *UAS-babo RNAi*, *UAS-dSmad2 RNAi*, were from O'Connor lab stocks. (details of construction available upon request). *UAS-dSmad2^{SDVD}* (constitutively activated dSmad2) was previously described (Gesualdi and Haerry, 2007).

The *Actβ*^{ed80} allele is an EMS-induced substitution leading to a premature stop codon and presumed to be a null mutation (Zhu et al., 2008). The chromosome carrying the *Actβ*^{ed80} allele (fourth) also contains a variegating w^+ transgene (P{hsp26-pt-T}39C-12, FlyBaseID= FBti0016154) inserted between *Hcf* and *PMCA* (John Locke, personal communication). This w^+ transgene causes red speckles with dominant inheritance in an otherwise w^- background.

Actβ^{4E} and *Actβ*^{10E} and *Actβ*^{4dd} were all generated using the CRISPR/Cas9 system. Two guide RNAs were cloned into the BbsI site of pU6-BbsI-chiRNA plasmid (obtained from Addgene) and injected by Best Gene into *w*^{1118}*; PBac{y[+mDint2]=vas-Cas9}VK00027* on chromosome 3 (Bloomington Stock Center #51324). The following guides were used to target the genomic locus, guide 1: 5'-GGGTTGTGGAAATGACTTCC-3', guide 2: 5'-GCGATTGCACGGGCTCTTTT-3'. G0 male flies were backcrossed to a balancer stock (*CiD/unc13-GFP*) to isolate *w*^{1118}*;;;Actβ*$^{?}$*/unc-13-GFP* stocks. To identify new *Actβ* alleles, DNA from homozygous (non-GFP) larvae was used to PCR amplify the genomic region flanking the CRISPR target sites using the following primers (FWD: 5-CTGCTGCAACAGCCTTGGCTCCC-3; REV: 5-GGGGCGCAACACGGTCGCATTCC-3).

Line 4E and 4dd are independent ~3 kb deletions that remove that remove exons 2 and 3. Line 10E is a ~1.3 kb deletion that removes exon 4 and 5. Exact deletion junction sites are available upon request.

Rearing Conditions

Eggs were collected over a 2-3 hour time period on apple juice plates inoculated with yeast paste and aged until hatching into first instar larvae. Larvae of the desired type were then transferred to vials containing standard cornmeal food (Bloomington recipe) and incubated at 25°C in a 12 hour light/dark cycle until scoring. Animals were transferred to vials at a low density (30 or 40 per vial) to prevent crowding affects.

Size measurements of larval tissues and nuclei

To measure size of larval organs, tissues were prepared using standard protocols for immunohistochemistry (see below). To measure size of larval body wall muscles, larval fillets of late wandering L3 larvae were prepared, and the surface area of muscle #6 of the A2 segment was measured in FIJI by outlining the muscle segment using the free-hand selection tool. Larval brains were stained with DAPI and rhodamine-phalloidin and placed onto a glass microscope slide between two #2 coverslips that acted as a bridge to prevent deforming the shape of the brain lobes. Confocal Z-stacks of the entire lobe were captured, and manual 3D segmentation using ITK-SNAP (PMID: 16545965) was used to measure lobe volume. Imaginal discs were stained with DAPI, imaged using confocal microscopy, and then maximum intensity projections were generated and processed in FIJI using the threshold and measure functions to obtain a 2D area of each disc. For fat body, proventriculus, muscle salivary and the

prothoracic glands, tissue was stained with DAPI and rhodamine-phalloidin and then Z stacks obtained. Nuclear size was measured using FIJI (Schindelin et al., 2012) at the sections where nuclei were largest.

Pupal Volume determination

Pupal volume was calculated from the length and width of individual pupae assuming a prolate spheroid shape [V = (4/3) π (width/2)2 (length/2)] (Demontis and Perrimon, 2009). Pupal length was measured from the anterior tip midway between spiracles to the base of the posterior spiracles**.** Pupal width was measured at the mid-length of the pupae.

Measurement of Adult appendage sizes

Adult specimens were fixed in 95% Ethanol. Structures were dissected and mounted in Canadian Balsam (Sigma, C1795) and Wintergreen oil (Sigma, M2047) solution (50:50). To measure size (length or area) of adult body parts images were processed in FIJI using either the free-hand or polygon tool (illustrated by red lines in Fig. 2-2).

Developmental Timing and Growth Assay

To measure developmental timing, flies were transferred to a constant light environment for at least 2 days prior to egg lay and all subsequent assays were carried out under constant light conditions to avoid circadian rhythms. Eggs were collected on apple juice plates with yeast paste for two hours. The next day, early L1 larvae were transferred to standard cornmeal food with yeast paste.

For *Actβ*^{ed80}/*Actβ*^{ed80} mutants the time to midpoint of pupariation was measured. For the CRISPR alleles, an additional synchronization step was employed. After ~48 hours of growth, 20-30 synchronized L2-L3 ecdysing larvae were transferred to cornmeal food without yeast paste to measure time to pupariation. Pupariation was scored every 2 hours by monitoring for anterior spiracles eversion and larval movement. The half point is the time it takes for half of the population to pupariate, which is calculated using a simple linear regression.

To measure growth rate, L3 larvae were cultured for appropriate times after L2-L3 ecdysis, washed in water and weighed individually on a Mettler Toledo XP26 microbalance. For adult mass, groups of 8-10 animals were weighed on the microbalance.

Statistics

Data were analyzed using either Graph Pad – Prism or R-studio. A single test variable was compared to a single control using a Welch Two Sample t-test. Multiple test variables were compared to controls using a one way ANOVA followed by Tukey's multiple comparison test. For rescue experiments with two controls and one test cross, the test cross must be significantly different in the same direction (e.g. larger) to be considered a significant result. Where the test cross was reported to be *x* units different than the controls, the different was in reference to the control with smaller variation. P values designation: ns= not significant, * $p<0.05$, ** $p<0.01$, *** $p<0.001$, **** $p<0.0001$.

Immunohistochemistry

Wandering third instar larvae were rinsed, dissected, fixed in 3.7% formaldehyde in PBS for 25 minutes, and then washed three times in PBS-(0.1%) TritonX-100. Samples were incubated with primary antibody overnight at 4°C followed by secondary antibodies for 2 hours at 25°C. Tissues were mounted in 80% Glycerol. The following stains and antibodies were used: Rhodamine-phalloidin (Molecular Probes R415), α-Dachshund (DSHB, mAbdac2-3), α-PTTH (guinea pig) a gift from P. Leopold, α-p-Mad (Eptitomics), α-DIMM a gift from P. Taggert.

Microscopy

Confocal images were generated using a Zeiss Axiovert microscope with a CARV attachment or Zeiss LSM710. Pupae, adult heads, and body were imaged live with Zeiss Stemi stereo microscope using a 1X objective. Adult wings and legs were imaged using Nikon Optiphot light microscope with a 4X objective. Trichomes were imaged using a 40X objective.

Western Blots

L3 larvae were dissected and all organs were removed from the carcass samples. Carcass samples were lysed with reducing gel loading buffer. Bands were resolved on 4-12% gradient gels (Invitrogen), and transferred to PVDF membrane (Biorad). Membrane blocking and antibody incubation were performed using standard protocols for ECL detection. α-pSmad2 (CST, 138D4)

and α-tubulin (Sigma, T9026) were used at 1/1000 dilutions. Bands were visualized using Pierce ECL Western Blotting Substrate (#32209).

CHAPTER II FIGURES

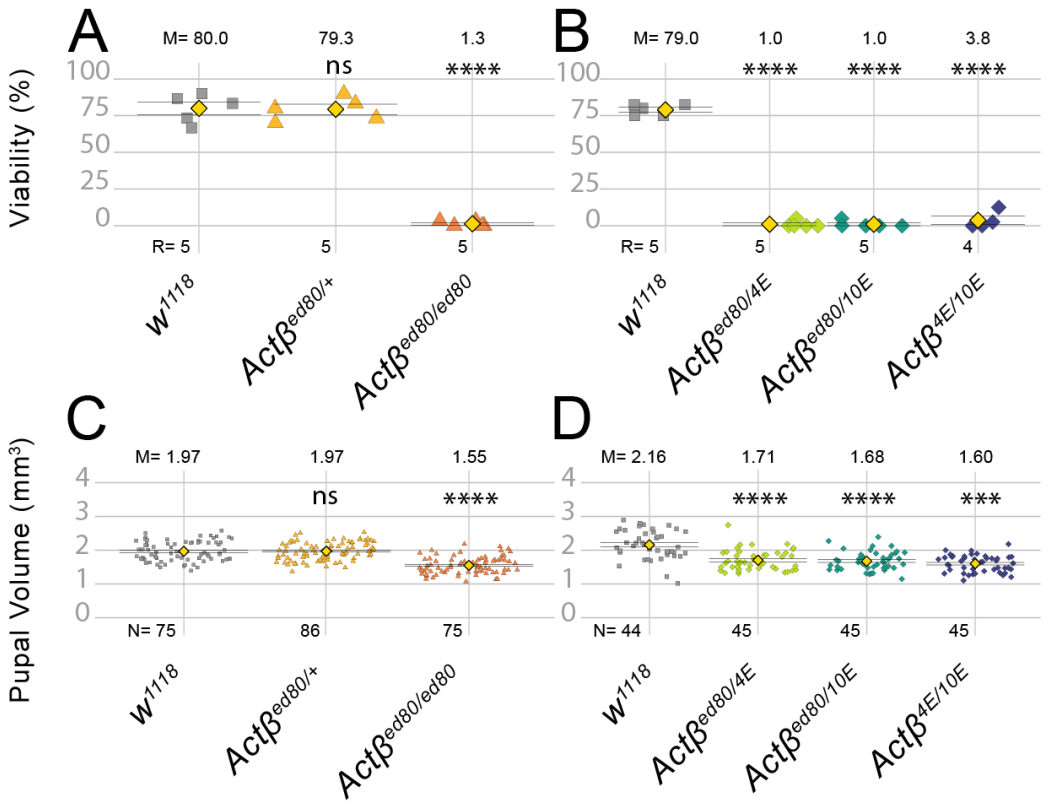

Figure 2-1. *Actβ* null mutants exhibit a small body size and late pupal lethality.

(A,B) Most *Actβ* mutants die as late pharates in the pupal case with between a 1-4% escaper rate. Heterozygotes and w^{1118} controls exhibit ~80% viability. (C) Pupal volume of $Actβ^{ed80}$ (mixed male and female pupa) null mutants (orange triangles, 1.55 mm^3) are ~20% smaller than heterozygous individuals (yellow triangle, 1.97 mm^3) and w^{1118} controls (grey squares, 1.97mm^3) (D) Pupal volumes of other A*ctβ* trans-heterozygous mutant combinations show similar decreases in pupal volume. M is the sample mean shown above each data set, N is sample size for pupal volume and R is number of replicates for each genotype (A,B), each replicate consists of 30 - 40 larvae. Means indicated by yellow diamond, ± SEM.

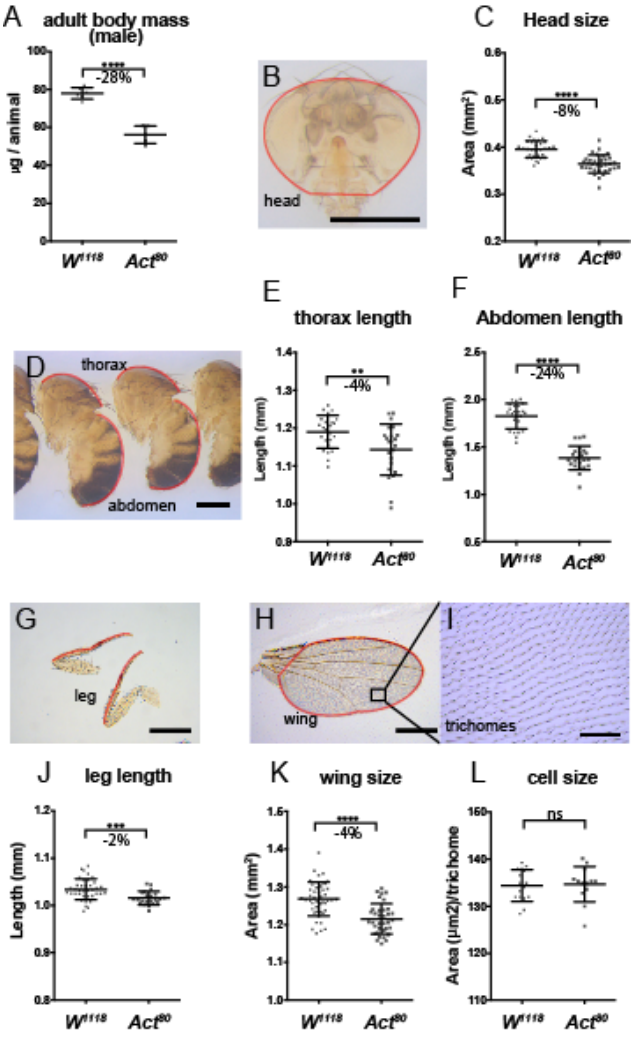

Figure 2-2. *Actβ* mutant adult escapers have a disproportionately smaller abdomen compared to head, thorax, leg, or wing.

(A) *Actβ*^{ed80} mutants that eclose as adults weight ~ 28% less than vs *w*^{1118} controls (n = 3-4 groups containing 9-10 individuals). (B-C) Heads of mutant males are ~8% smaller, (scale 500µm, n>30). (D) Thorax and abdomen (F) are ~4% and ~24% smaller respectively, (scale 500µm, n = 23). (G,J) Legs and wings (J,K) of mutants are ~2% and ~4% smaller respectively (scale 500µm, n = 22 – 46). (I, L) trichome density in the adult wing shows no difference in cell size (scale 50µm, n = 13 – 16). Means ± S.D. are shown.

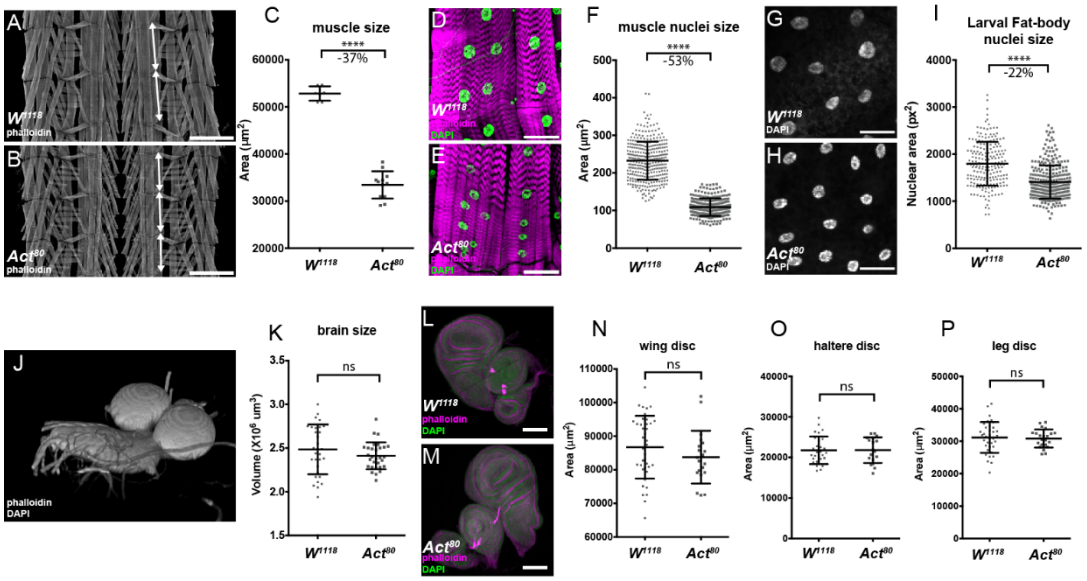

Figure 2-3. Actβ disproportionately affects the size of larval body wall muscles and fat body nuclei size.

Late wandering L3 larvae were dissected and the size various tissues determined. (A,B) Larval fillets were stained with rhodamine-phalloidin and imaged in the muscle plane. Double headed arrows mark the extents of a larval segment photographed at the same magnification (scale bar = 500µm). Note that approximately 3 segments of *Actβ* mutant muscles occupy the same area as 2 wildtype segments. (C) Loss of *Actβ* results in a 37% decrease in the surface area of muscle #6 from the A2 segment compared to control (n = 7 – 12). (D - F) Muscle nuclei (DAPI, green) of *Actβ* mutants are 53% smaller (scale bar =50µm, n > 250) than controls. (G – I) Fat body nuclei (DAPI, gray) of *Actβ* mutants are 22% smaller than control (scale bar = 50µm, n > 200). (J – K) 3D reconstruction of larval brains stained with DAPI and rhodamine-phalloidin, the volume of each brain lobe was measured separately and *Actβ* mutants showed no significant difference of brain size compared to control (n > 30). (L-P) Wing, leg, and haltere imaginal discs (DAPI green, phalloidin magenta) of *Actβ* mutants are the same size as controls, scale 100µm, (n > 20 in each group). Means ± S.D. are shown.

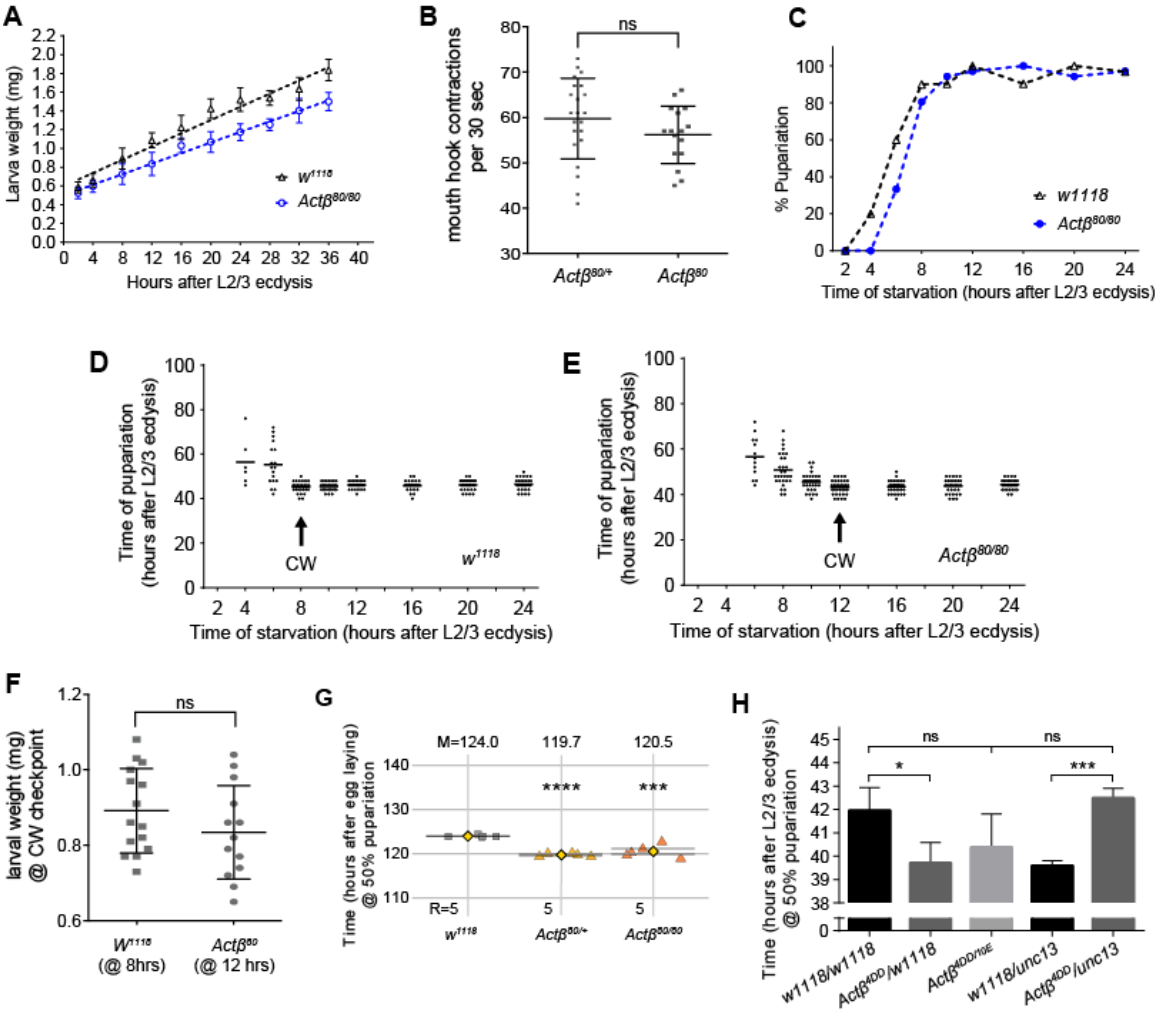

Figure 2-4. *Actβ* mutant larvae grow slowly but do not exhibit differences in Critical Weight or Developmental timing.

(A) wet weight of L2/L3 synchronized larvae were measured. No difference in weight of *Actβ* mutants (blue circles/line) and w^{1118} controls (black triangles/line) early but after 36 hours weigh ~18% less than controls, (n = 8 – 10 per group). (B) *Actβ* (squares) mutants feed at the same rate as controls (circles) (n = 16 – 22). (C) *Actβ* mutants are more sensitive to starvation in the early L3 stage than controls (D, E) The critical weight checkpoint was determined by identifying the time at which starvation does not delay pupariation. *Actβ* mutants reach the CW checkpoint 4 hours after controls. (F) Comparing the larval mass when larvae

reach their respective CW checkpoints shows that Actβ (at 12 hrs AL2/3) weight the same as controls (at 8 hrs AL2/3). (G) Developmental timing analysis of when 50% of the population have pupariated of $Actβ^{80}$ mutants and heterozygotes vs controls, shows that both mutants and hets pupariate ~5 hrs earlier mean ± SEM). (H) Developmental timing analysis of CRISPR alleles and various heterozygous controls. $Actβ^{4dd/10E}$ mutants do not develop faster than the w^{1118} control, however both $Actβ^{4dd}/w^{1118}$ and $unc13GFP/w^{1118}$ hets develop ~3 hrs faster mean ± SEM than either w^{1118} or the $Actβ^{4dd/10E}$ mutant combination. Unless indicated mean ± SD is shown.

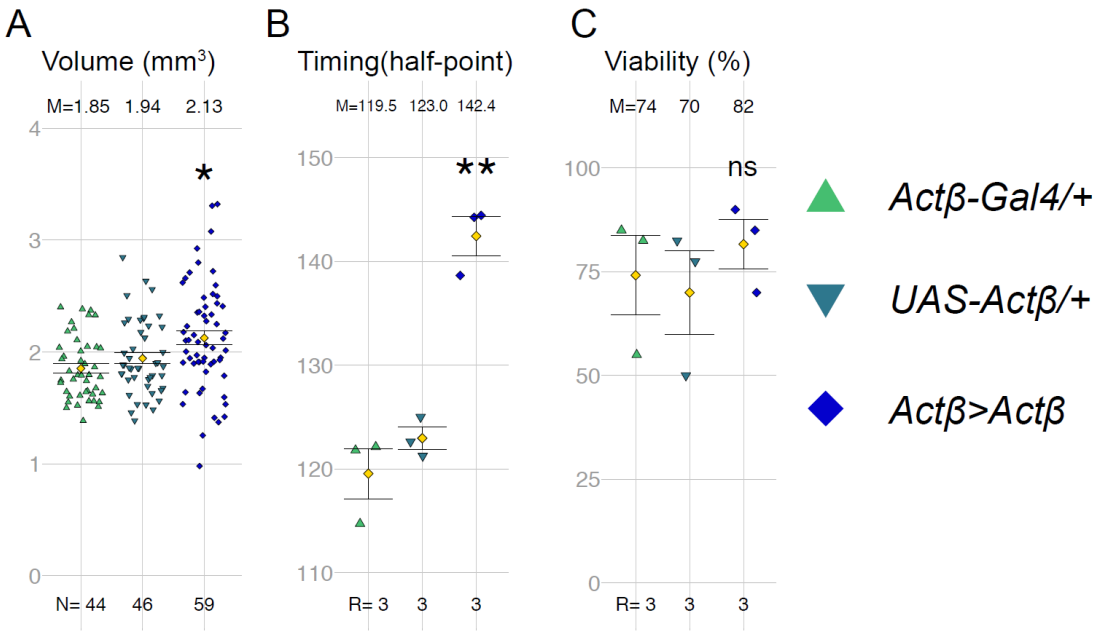

Figure 2-5. Actβ overexpression increases body size and delays developmental timing.

(A) Expression of *UAS-Actβ* using *Actβ-Gal4* significantly increases pupal volume. (B) *Actβ>Actβ* animals pupariate about ~20 hours later than controls. (C) Adult viability is not significantly impacted in *Actβ>Actβ* animals. M=mean, N=number of individuals, R= number of groups containing 10-30 larva).

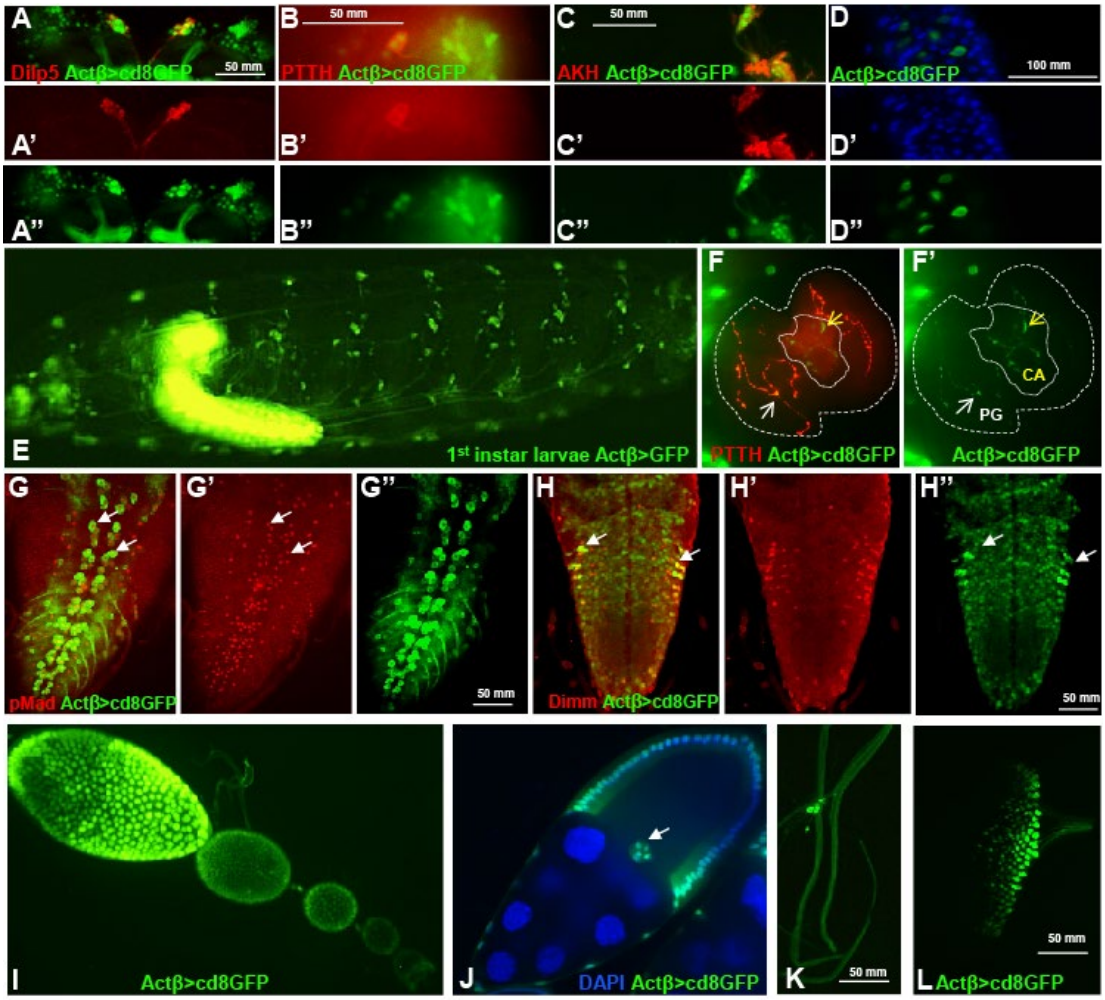

Figure 2-6. Analysis of *Actβ-GAL4* driver expression pattern (green) in L3 larvae.

(A-A'') Actβ-GAL4 is expressed in the Insulin Producing Cells in the central brain, marked with α-Dilp5 (red). (B-B'') Actβ reporter is expressed in the cell bodies of PTTH neurons (α-PTTH, red) in the central brain. (C-C'') Actβ reporter is expressed in AKH producing (α-AKH, red) neurons. (D-D'') *Actβ-Gal4*-driven GFP is expressed in midgut enteroendocrine cells (Blue DAPI) (E) An intact L1 larvae, *Actβ-Gal4*-driven GFP is expressed in both the central and peripheral nervous systems. (F,F') *Actβ-Gal4*-driven GFP is found in PTTH synaptic boutons (red) on the PG (thicker dotted line, white arrows) as well as unique boutons in the CA (finer dotted line, yellow arrows). PG= prothoracic gland, CA=

corpus allatum. (G-G") *Actβ* reporter drives expression in the motor neurons (marked with α-pMad red) in the ventral nerve cord (white arrows highlight two individual motor neurons. (H-H") Actβ reporter is expressed in neuroendocrine cells (α-DIMM, red) in the ventral nerve cord (I) *Actβ-Gal4*-driven GFP is found in follicle cells and the border cells during egg development. (K) *Actβ-Gal4*-driven GFP is found in certain tracheal associated cells and (L) in differentiating photoreceptor cells in the eye disc.

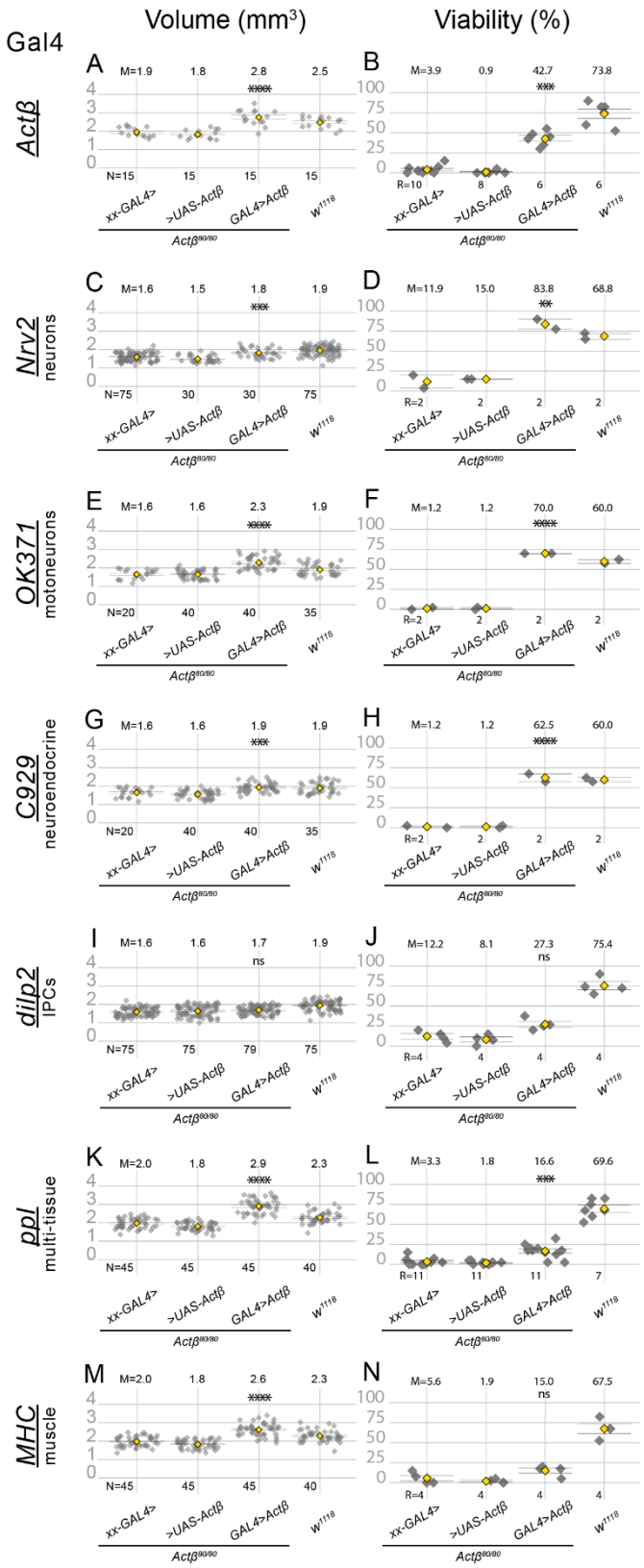
Gal4
Volume (mm3)
Viability (%)
Actβ
Nrv2
neurons
OK371
motoneurons
C929
neuroendocrine
dilp2
IPCs
ppl
multi-tissue
MHC
muscle
A
B
C
D
E
F
G
H
I
J
K
L
M
N
M=1.9 1.8 2.8 2.5
M=3.9 0.9 42.7 73.8
M=1.6 1.5 1.8 1.9
M=11.9 15.0 83.8 68.8
M=1.6 1.6 2.3 1.9
M=1.2 1.2 70.0 60.0
M=1.6 1.6 1.9 1.9
M=1.2 1.2 62.5 60.0
M=1.6 1.6 1.7 1.9
M=12.2 8.1 27.3 75.4
M=2.0 1.8 2.9 2.3
M=3.3 1.8 16.6 69.6
M=2.0 1.8 2.6 2.3
M=5.6 1.9 15.0 67.5
N=15 15 15 15
R=10 8 6 6
N=75 30 30 75
R=2 2 2 2
N=20 40 40 35
R=2 2 2 2
N=20 40 40 35
R=2 2 2 2
N=75 75 79 75
R=4 4 4 4
N=45 45 45 40
R=11 11 11 7
N=45 45 45 40
R=4 4 4 4
xx-GAL4>
>UAS-Actβ
GAL4>Actβ
w1118
Actβ80/80

Figure 2-7. Expression of Actβ from specific cell types differentially rescues Actβ mutant phenotypes.

The first two groups in each panel are controls in which *Actβ* mutants contain one copy of either the GAL4 driver (indicated on the left side of each panel row) or the UAS Actβ transgene. The third group in each panel is the testcross, and the last group in each panel is the w^{1118} control. All GAL4 drivers (except *dilp2-GAL4)* used to overexpress *Actβ* rescue body size phenotype (A, C, E, G, K, M). Overexpressing *Actβ* in neuronal tissues (D, F, H) completely rescues adult viability phenotype, and partially rescue when overexpressed in body wall muscles using MHC-GAL4 (L). ANOVA was used to determine statistical significances between genotypes with one copy of either Gal4 or UAS transgenes in an $Actβ^{ed80}$ homozygous background compared to animals with both Gal4 and UAS transgenes in an $Actβ^{ed80}$ homozygous background. w^{1118} is the wild-type control and was reared side-by-side in each case. M=mean, N=number animals, R= repetition number (10- 30 animals per rep).

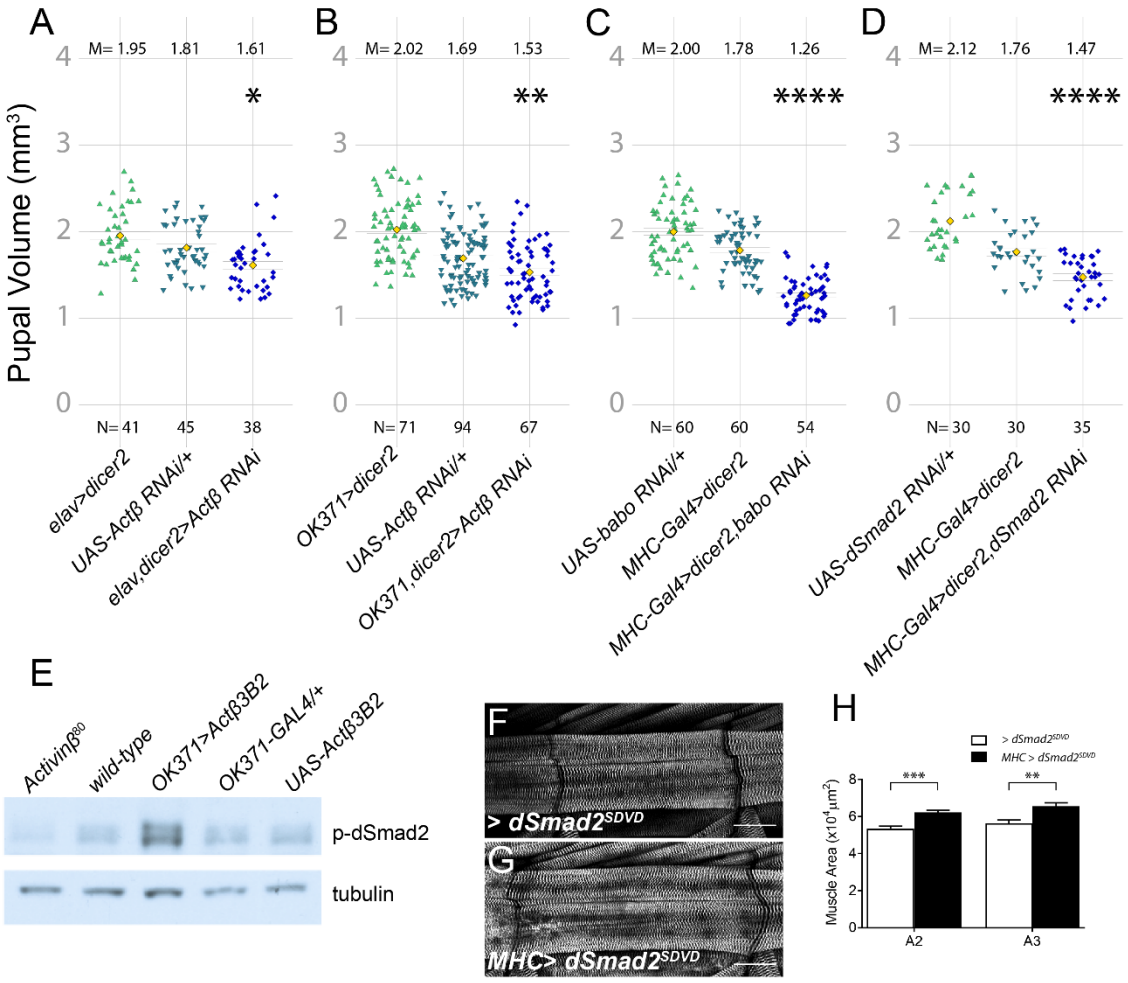

Figure 2-8. Motor neuron derived Actβ signaling through Babo and dSmad2 controls body size.

(A). Knockdown of *Actβ* using a pan-neuronal driver (*elav-Gal4*) with *UAS-dicer2* reduces pupal volume (B) Motor neuron knockdown of *Actβ* using *OK371-Gal4* to also reduces pupal volume. (C) Knocking down the Actβ receptor *baboon* or the signal transducer *dSmad2* (D) in muscles using *MHC-GAL4* with UAS-*dicer2* reduces pupal volume. M=mean, N=number (E) *Actβ* mutants have lower levels of p-dSmad2 (E, lane 1 vs 2) in carcass tissue lysates (cuticle, skeletal muscle). While overexpressing Actβ in motor neurons leads to increased level of dSmad2 compared to controls (E, lanes 3-5) Anti-tubulin staining serves as a loading

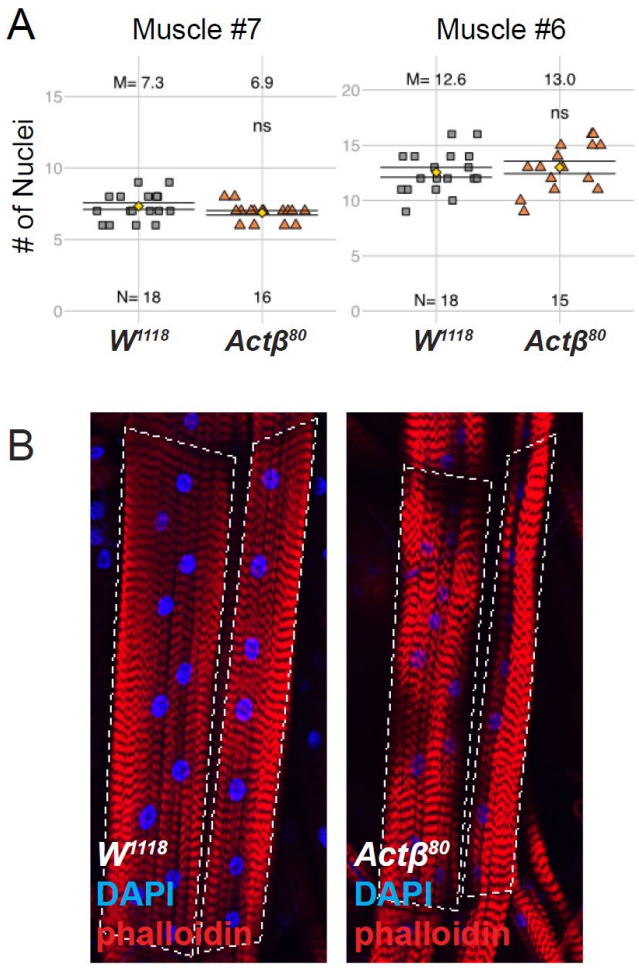

control. (F – H) Overexpressing activated dSmad2 (dSmad2^{CA}) in the muscles using *MHC-GAL4* increases muscle size by ~20%.

Figure 2-9 *Actβ* does not affect muscle nuclei number

3rd instar larvae were filleted and stained with DAPI (blue) and phalloidin (red). (A) Quantification of the number of nuclei in muscle #6 and #7 for w^{1118} controls and *Actβ*^{ed80}mutants shows no significant difference. (B) Representative image of muscle fiber (red) with stained nuclei (blue) for w^{1118} controls and *Actβ*^{ed80}mutant. Each image has muscle #6 (left) and muscle #7 (right) outlined with dashed line. N is shown for each group in A, ns = not significant

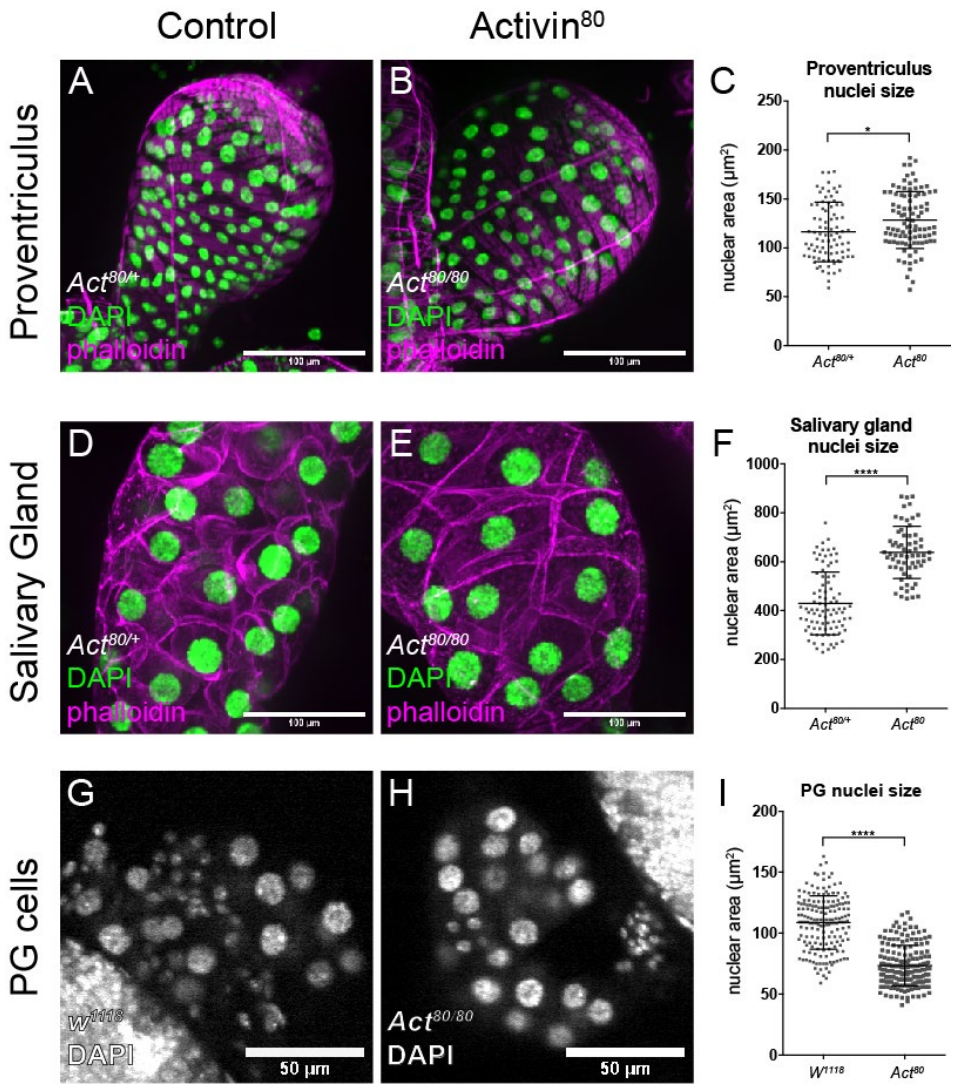

Figure 2-10 Size of various polyploid nuclei in *Actβ* mutants.

Proventriculus, salivary gland, and the prothoracic gland of 3rd instar wandering larvae were dissected, stained with DAPI (green, A, B, D, E; grey, G, H) and phalloidin (magenta, A, B, D, E) to quantify nuclei size. (A-C) The nuclei of the cells of the proventriculus in *Actβ*^{ed80}mutants are 10% larger. (D-F) The nuclei of the salivary gland cells in *Actβ*^{ed80}mutants are 48% larger. (G-I) The nuclei of the prothoracic gland cells are -32% smaller. Size of scale bar indicated on the image. For each group n = 60-170.

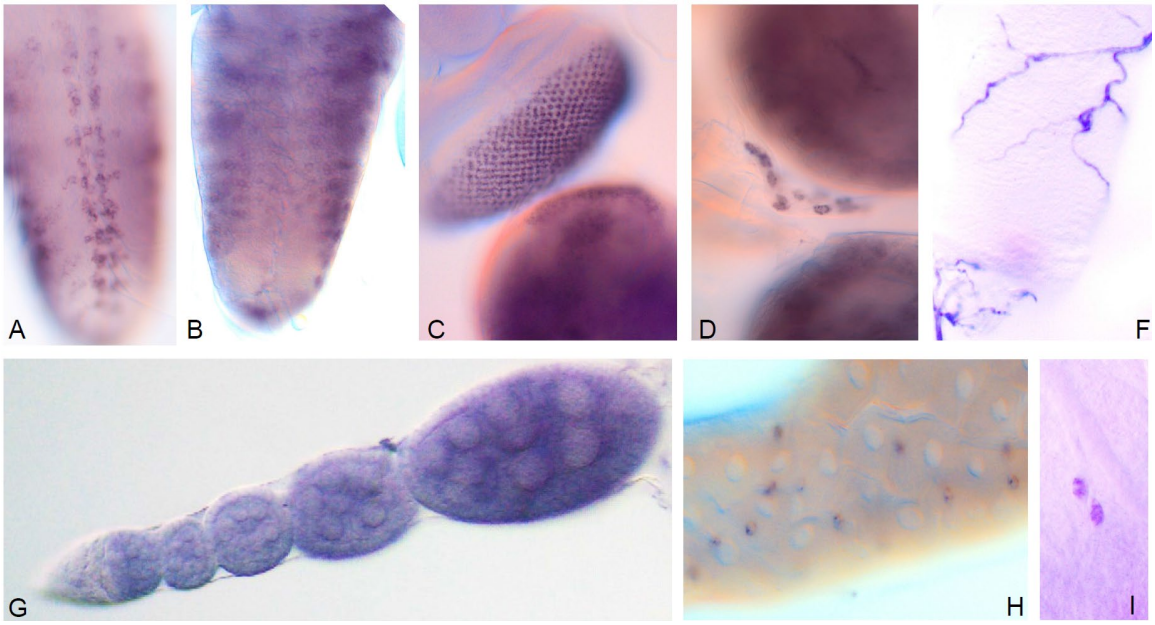

Figure 2-11 RNA *in situ* hybridization of *Actβ* shows expression in various tissues

(A-I) *Actβ* is expressed in cell body of motoneurons (A) and neuroendocrine cells (B) in the ventral ganglion of 3rd instar larval CNS, (C) eye disc, (D) CC cells, (F) trachea, (G) maturing follicle cells, (H) enteroendocrine cells in the midgut, (I) two PNS neurons.

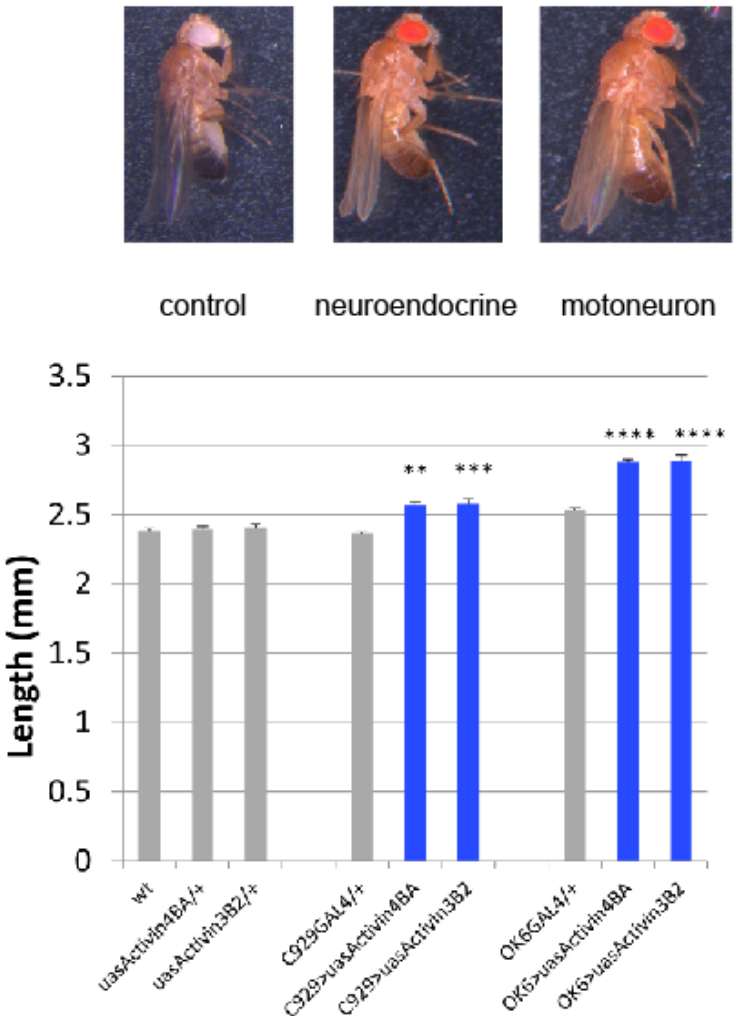

Figure 2-12 Overexpression of *Actβ* in motoneurons or neuroendocrine cells increases adult body size.

Relative to controls (UAS-*Actβ*, left) overexpression of *Actβ* (line 3B2 or 4BA) in motoneurons (OK6-Gal4, right) or neuroendocrine cell (C929-Gal4, middle) results in larger animals. The body length for the indicated genotype shown (bottom panel) with representative images of adult flies (top panel). n = 20-30 individuals, bars indicate mean ± SEM.

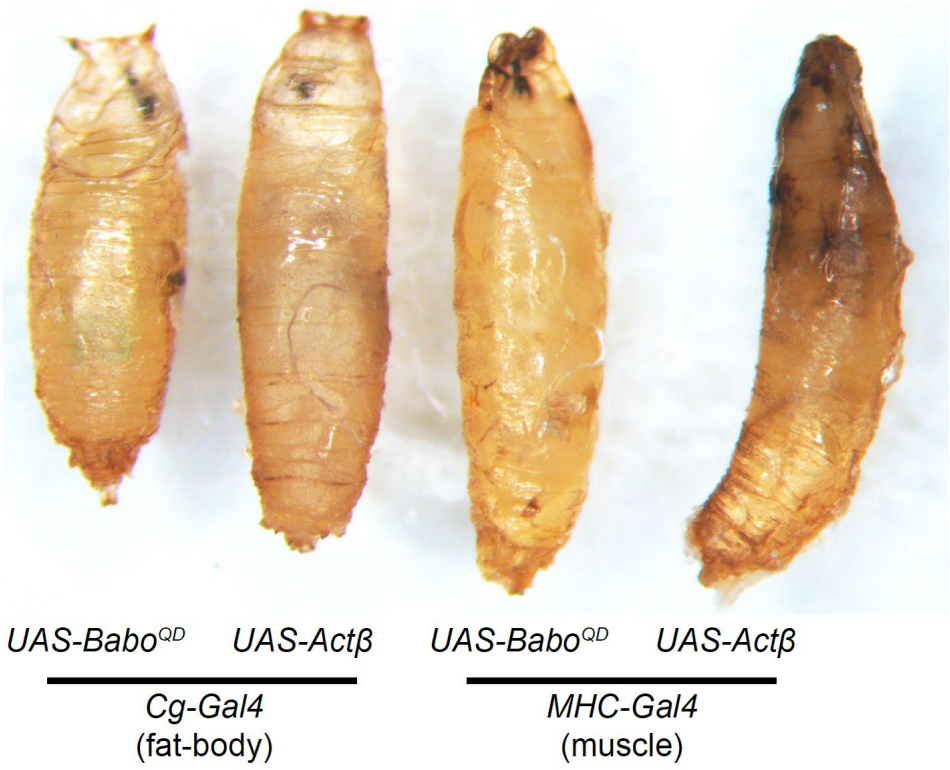

Figure 2-13 Hyperactivation of Activin signaling in muscles but not fatbody is larval lethal

Images of pupae resulting from overexpression of constitutively activated Babo (Babo^{QD}) or *Actβ* in the fat-body (*Cg-Gal4,* left) or muscles (*MHC-Gal4*, right). Note that the left most pupa in which activated Babo was expressed in the fatbody produces a normal pupa that gives rise to a viable adult. However expression of the ligand (Actβ) in the fatbody produces a larval lethal phenotype similar to that produced by either overexpression of Actβ or activated receptor in muscle. We conclude that overexpression of the ligand in the fatbody produces a lethal phenotype by non-autonomous activity in the muscles.

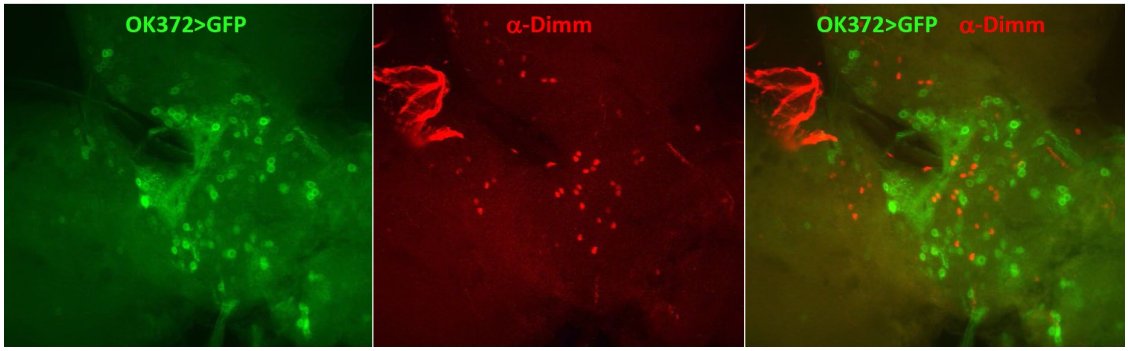

Figure 2-14 OK372-Gal4 is not expressed in Dimm+ neuroendocrine cells

Third instar larvae brains of *OK371-Gal4>UAS-GFP* (green) were dissected and stained with α-Dimm (red). We find no overlap in signals demonstrating that OK371-Gal4 is not expressed in Dimm+ cells (merge panel, right).

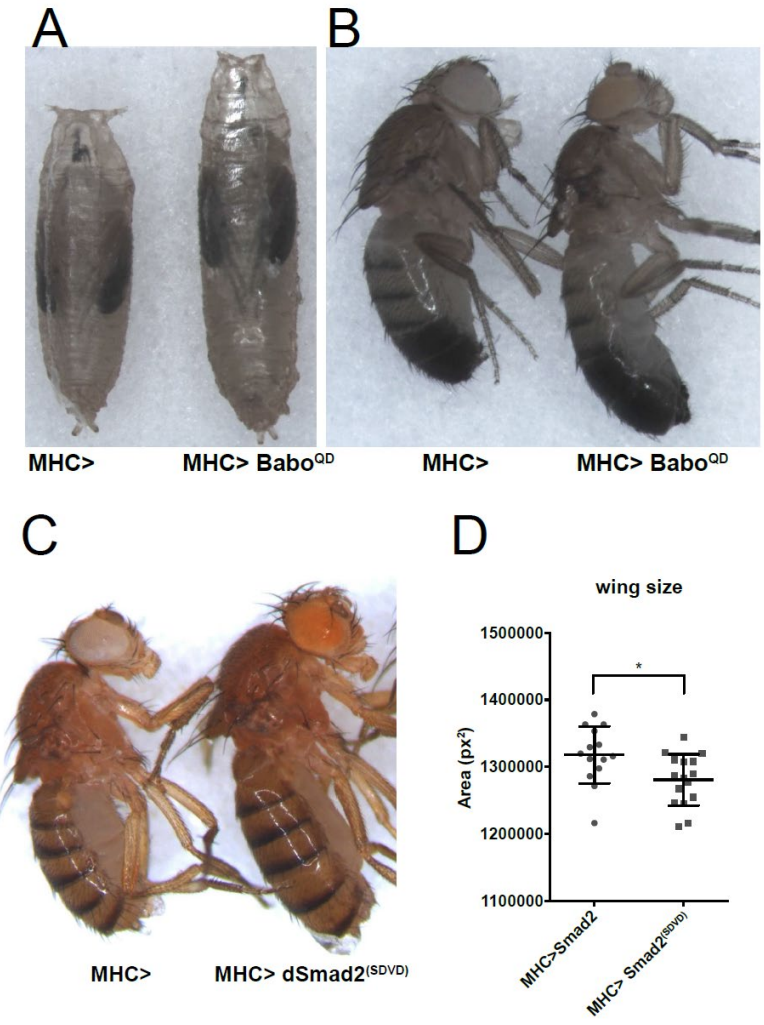

Figure 2-15 Muscle specific activation of Activin signaling increases body size but not wing size

(A-B) Overexpression of activated Babo (Babo^{QD}) in muscles results in larger pupae (A) and adult larger adult flies (B). (C-D) Overexpression of activated dSmad2 (dSmad2^{SDVD}) in muscles also results in larger adult flies. (D) adult wings of *MHC>dSmad2*^{SDVD} are smaller than *MHC-Gal4* control.

Chapter III

Muscle-derived Myoglianin regulates imaginal disc growth

Others that contributed to this chapter:

Aidan J. Peterson conducted experiments for figure 3-4 (C-E).

All other experiments were done by me.

SUMMARY

Organ growth and size is finely tuned by intrinsic and extrinsic signaling molecules. In *Drosophila,* the BMP family member Dpp is produced in limited set of imaginal disc cells and functions as a classic morphogen that regulates pattern and growth by diffusion through the tissue. The role of Activin-like ligands in disc growth control however, remain ill-defined. Here we demonstrate that among the three Drosophila Activin-like ligand, only *myoglianin* (*myo*) controls wing imaginal disc growth and it does so as an extrinsic signal that is produced by body-wall muscle. In the wing disc, muscle derived Myo stimulates phosphorylation of the downstream signal transducer and transcription factor dSmad2, and requires type I receptor isoform Babo-A, type II receptor Punt, and the co-receptor immunoglobin like protein Plum. Loss and gain-of-function studies demonstrate that Myo signaling, or lack thereof, can alter the final wing size from -40% to +20% of its total surface area, by controlling cell proliferation. We propose that this mechanism provides a means of coordinating muscle size with appendage size which is likely important for overall fitness and survival of the species.

INTRODUCTION

How organ growth is regulated to achieve proper scaling with final body size has been a long standing question in developmental biology. Organ growth is a dynamic process that is finely tuned by highly conserved molecules that are produced within the tissue (intrinsic) as well as in other distant organs (extrinsic) that act in an endocrine manner (Boulan et al., 2015; Hariharan, 2015; Johnston and Gallant, 2002; Mirth and Shingleton, 2012). These growth signals regulate final organ size through three distinct processes, cell division (proliferation) mass accumulation (cell growth) and cell death (apoptosis). The *Drosophila* wing imaginal disc, the larval precursor to adult wings and thorax, has been widely used as a model to study the molecular mechanisms that control organ growth and size control (Martin et al., 2009). Genetic analysis has identified numerous wing disc intrinsic factors, such as Wnt, Hedgehog, Bone Morphogenetic Protein (BMP) homologs, that are required for proper patterning and proliferation (Hariharan, 2015). In contrast, examples of extrinsic factors that regulate imaginal disc growth are not as common. The Insulin-like signaling pathway is one clear exception. Insulin-like peptides are produced in the brain and fatbody and are well known to promote both growth and proliferation in many tissues including imaginal disc cells (Boulan et al., 2015; Grewal, 2012; Nijhout, 2003; Shingleton et al., 2007; Sopko and Perrimon, 2013). Insulin-like factors act in a physiological capacity to coordinate overall organismal growth with nutrition. Identification of other extrinsic signals that might provide additional means of

coordinating growth specifically between tissues could provide new insights into mechanisms governing coordinated organ scaling.

The largest and most diverse group of signaling molecules belong to the Transforming Growth Factor β (TGF-β) superfamily of growth and differentiation factors. The superfamily is subdivided into the BMP and the TGF-β/Activin-like subfamilies based on sequence and signaling relationships. In higher vertebrates, these growth factors play a myriad of roles during development from cell fate specification and stem cell maintenance to control of cellular growth and proliferation (Morikawa et al., 2016). Both branches of TGF-β are conserved in *Drosophila*, where limited functional redundancy and a powerful genetic toolkit provide an attractive system for study. The *Drosophila* BMP ligand Decapentaplegic (Dpp) functions as a classic intrinsic morphogen, secreted from a single source and diffusing throughout the tissue, to regulate proliferation and patterning based on its concentration gradient (Campbell and Tomlinson, 1999; Lecuit et al., 1996; Restrepo et al., 2014). Conversely, the Activin-like branch also plays a significant role in disc growth, however it is much less well characterized (Brummel et al., 1999; Hevia and de Celis, 2013; Peterson and O'Connor, 2013).

In *Drosophila* Activin-like signaling is initiated by three ligands, which include Myoglianin (Myo), Activinβ (Actβ), and Dawdle (Daw). These ligands bind to and activate a hetero-tetrameric receptor complex on the cell membrane consisting of two type-I receptor subunits encoded by *baboon (babo)* and two

type-II receptor subunits encoded by either the *punt* or *wishful-thinking (wit)* genes or perhaps a combination of the two. (Upadhyay et al., 2017). Activated Babo phosphorylates cytosolic dSmad2 which then accumulates in the nucleus and, along with a co-Smad, regulates expression of target genes (Brummel et al., 1999; Hevia et al., 2017). Notably, there are three splice isoforms of *babo* with different ligand binding domains, which presumably provide ligand binding specificity (Jensen et al., 2009). *Babo* null mutant die at the larval-pupal transition and have significantly smaller wing imaginal discs, and escapers produced by hypomorphic alleles also have smaller adult wings (Brummel et al., 1999). Furthermore, expression of constitutively activated Babo in wing imaginal discs leads to larger adult wings without significantly altering cells size, suggesting that Activin-like signaling has a role in regulating proliferation (Brummel et al., 1999; Hevia and de Celis, 2013). Additionally, Babo can signal non-canonically through Mad (the BMP Smad) to stimulate wing disc overgrowth, but only in the background of a protein null allele ($dSmad2^{f4}$) and not with a genetic null missense allele ($dSmad2^{MB388}$) that produces a non-functional product (Peterson and O'Connor, 2013).

For both the canonical dSmad2 and the non-canonical Mad signaling pathways, it remains unclear which Babo isoform and which Activin-like ligands, or combination thereof, regulates disc growth. It is also not clear which tissue(s) provide the ligands that promote disc growth. Expression analysis by in-situ hybridization or transcriptome analysis suggests that all Activin-like ligands are

expressed in the imaginal wing disc, albeit at low levels, perhaps indicating collective contribution to stimulating tissue growth (Gramates et al., 2017; Hevia and de Celis, 2013). However it is important to recognize that mRNA expression does not necessarily correlate with functional ligand production, especially since TGFβ-type ligands undergo a series of post-translational modifications, including glycosylation, pro-domain cleavage, and dimerization, to generate an active molecule and these processes may vary within different tissues (Ballard et al., 2010; Upadhyay et al., 2017).

Here we report our analysis of how Activin-like ligands and Baboon isoforms regulate imaginal disc growth. Through a series of genetic experiments, we demonstrate that among the three Drosophila Activin-like ligands, only Myo is required for proper growth of imaginal discs. We also identify the receptors Babo-A, and Punt along with the co-factor Plum as being necessary for Myo dependent phosphorylation of dSmad2 resulting in proper growth of imaginal discs. Surprisingly, we identify the tissue source of Myo that controls disc growth to be the larval muscle. We speculate that Myo acts a myokine, to help coordinate muscle with appendage growth.

RESULTS

Myoglianin is required for proper discs growth

All Drosophila Activin-like ligands (Myo, Actβ, and Daw) have tissue specific function yet signal via the sole Type-I receptor Babo. Hence, the *babo* mutant phenotype is likely a composite of all three individual ligand mutant phenotypes. The imaginal discs of *babo* mutants are approximately 30% smaller than wildtype but do not exhibit any obvious defects in tissue patterning (Brummel et al., 1999). We set out to identify which Activin-like ligand(s) are required for proper imaginal disc growth. The null mutants *myo*, *Actβ,* and *daw* are larval lethal (Awasaki et al., 2011; Ghosh and O'Connor, 2014; Zhu et al., 2008). Therefore, we analyzed the size of imaginal wing discs from late 3rd instar larvae of null mutant animals. For this initial analysis, we used a simple yeast/sugar diet (5Y5S) food, because *daw* mutants are sensitive to standard acidic cornmeal food (Ghosh and O'Connor, 2014). Interestingly, only *myo* mutants phenocopies *babo* small disc phenotype (Brummel et al., 1999). *Myo* discs are approximately 40% smaller than *yw* controls, but retain its normal shape and pattern (Fig. 3-1 B,E). *Actβ* mutant discs had no significant size defects, however *daw* mutant discs were slightly smaller, which could might be attributable to the reduction of insulin secretion in the *daw* mutants (Fig. 3-1 C-E) (Ghosh and O'Connor, 2014). Previous studies suggested that all Activin-like ligands are expressed in the wing disc (Hevia and de Celis, 2013). Despite this

observation, our result clearly suggests that only *myo* is functionally required for growth of the discs, and that other ligands may have other functions apart from disc growth. We next asked whether other imaginal tissues such as the haltere and leg discs are also affected by the loss of *myo*. Indeed, all three imaginal discs of *myo* mutants are approximately 50% smaller (Fig. 3-1F-H). Furthermore, by analyzing discs from the same animal, we determined that the size ratio of discs are not different in *myo* mutants vs *yw* controls (Fig. 3-1I). This suggests that Myo signaling regulates tissue growth in all three imaginal discs equally.

To explain the *myo* small discs phenotype, we measured cell size, proliferation, cell growth, and apoptosis. First, to assess cell size we measured the apical surface area of disc epithelial cells by phalloidin staining, which marks the apical actin belt, and found that wing disc cells of *myo* mutants are 22% smaller than controls (Fig. 3-1 J-L). Next, we measured proliferation rates by staining for phospho-Histone 3(ser10) which marks mitotic cells in discs, and found no significant difference between *myo* discs and controls (Fig. 3-1, M-O). Third, using apoptotic marker cleaved-caspase 3, we found no increase in apoptosis in *myo* mutants (Fig. 3-6 A, B). Another possible reason why *myo* mutant discs do not grow properly is a defective TOR signaling pathway. To address this, we stained growing early L3 imaginal discs for phospho-S6, which is a target of pS6k and is a readout of TOR pathway activation. We find no decrease in pS6 staining in *myo* mutant discs, indicating that TOR signaling is

not perturbed in these cells (Fig. 3-6 C, D). To briefly summarize *Myo* mutant imaginal discs are smaller in part due to smaller cells, but not increased apoptosis, defective proliferation or TOR activation. Important to note, that the 22% decrease in cell size is insufficient to completely account for 40-50% decrease in total tissue size. This could be due to the fact that our assays are snapshot experiments of fixed tissues. Therefore, we cannot completely rule out that there may be some proliferation, apoptosis, or cell growth defects during other stages of development. It has been reported that hyperactivation of Babo in the wing imaginal disc leads to approximately half of the cells undergoing one extra round of cell division (Brummel et al., 1999). Thus, it is possible that loss of *myo* results in smaller cells as well as slower/fewer rounds of cell proliferation accruing over the course of entire larval development resulting in overall smaller tissue. Such mild defects could gradually accumulate which could explain the phenotype.

Myo is homologous to vertebrate *Mstn*, which negatively regulates skeletal muscle size by inhibiting proliferation of muscle stem cells (Morikawa et al., 2016) and regulation of protein homeostasis (Lee et al., 2011; Rodriguez et al., 2014; Trendelenburg et al., 2009). Recent studies in *Drosophila* using RNAi tissue specific knockdown methods suggested that Myo also functions as a negative regulator of muscle size similarly to vertebrate *Mstn* (Augustin et al., 2017). We re-examined this issue using *myo* null alleles. Surprisingly, we found that the surface area of late L3 body wall muscles #6 and #7 (Segment A2) are

13% smaller than heterozygous controls but contain the same number of nuclei indicating no defect in myoblast fusion. (Fig. 3-1P-S). We conclude that respect to muscle size control, that Drosophila *myo* is not functionally conserved with vertebrate *Mstn*.

Myo signals canonically via dSmad2

Canonical TGFβ/Activin pathway activation in *Drosophila* is mediated by C-terminal phosphorylation of dSmad2 by the Type-I receptor Baboon (Brummel et al., 1999; Peterson and O'Connor, 2014). To determine if Myo acts through the canonical signaling pathway, we examined phosphorylated dSmad2 (p-dSmad2) levels in wing disc extracts of various mutants. Total wing disc cell extracts of late L3 larvae from *yw*, *myo* heterozygotes and null animals were western blotted for anti phospho-dSmad2. Indeed, we observe a dose dependent reduction in p-dSmad2 levels upon loss of *myo*, i.e. in heterozygous $myo^{+/-}$ the p-dSmad2 signal is reduced compared to wildtype whereas in homozygous mutants it is virtually absent (Fig. 3-1T). These findings strongly suggest that Myo signals canonically via dSmad2 in imaginal discs (Fig. 3-1U).

Myo signaling in imaginal discs requires a specific isoform of Baboon

Baboon, the sole TGFβ/Activin receptor in *Drosophila*, has three splice isoforms (Awasaki et al., 2011; Jensen et al., 2009). The three splice isoforms are a result of mutually exclusive alternative splicing of the fourth exon (4a, 4b, 4c) giving rise to three receptors (Babo-a, Babo-b, and Babo-c) that differ only in their extracellular-ligand binding domains (Brummel et al., 1999; Jensen et al., 2009). It has been suggested that different tissues express different isoforms, perhaps in order to tune tissue-specific responses to various ligands (Awasaki et al., 2011; Jensen et al., 2009; Peterson and O'Connor, 2014). Ectopic Myo signaling in the larval brain is lethal, however this can be rescued by simultaneously knocking down Babo-a but not Babo-b or Babo-c (Awasaki et al., 2011). This suggests that Myo signals specifically via Babo-a. Since only *myo* is required for proper growth of imaginal discs (Fig. 3-1B), we reasoned that Babo-a should be the major Babo isoform expressed in the discs, a conjecture confirmed by qPCR analysis of dissected late L3 wing discs (Fig. 3-2A). We confirmed that our primers for Babo-b and Babo-c are functional by testing other tissues such as carcass, brain, and fat body where we find different profiles for each isoform. (Fig. 3-7).

To confirm that the Babo-a isoform is indeed required for wing growth, we employed the GAL4/UAS system for tissue and isoform specific RNAi knockdown experiments. Using *escargot* (entire disc), *cubitus* (anterior), and *hedgehog* (posterior) GAL4 lines, we knocked down specific Babo isoforms and measured

overall tissue size and cell size/density. In support of the qPCR data, we find that knocking down *Babo-a* alone with *esg-GAL4* results in 40% smaller adult wings, whereas knocking down *Babo-b* or *Babo-c* resulted in no size difference (Fig. 3-2 B-E, J). *Ci>GAL4* driving *ibabo-a* reduces the anterior compartment by 50% (Fig. 3-2 F-I, L), likely due to Ci>Gal4 being a stronger driver than *esg>GAL4*. We next assessed cell size in these wings by measuring trichome density in adult wings. RNAi for *Babo-a* using *esg-GAL4* or *ci-GAL4* results in a fractional decrease (-6%) or increase (12%) in cell density respectively (Fig. 3-2 K, M) indicating that the *esg* driver results in slightly larger cells whereas *ci* driver results in somewhat smaller cells. Assuming the number of wing disc precursors at embryonic stage is the same in both conditions, we infer that the *esg* driver leads to smaller wing size (Fig. 3-2 C) due to defects in proliferation, whereas, in the case of the *ci* driver, the smaller compartment size (Fig. 3-2 G) is due to both smaller cells and fewer cell divisions. As a further test, we repeated the experiment with *hh-GAL4* which is expressed in the posterior compartment. Knockdown of *babo-a* using *hh* driver is pupal lethal, thus we analyzed the late L3 imaginal wing discs. At this stage, in addition to the predicted smaller posterior compartment (-35%, Fig. 3-2 P), we observe two additional phenotypes that are obscured in adult wings. Knockdown of *babo-a* results in an imperfect anterior/posterior boundary formation (Fig. 3-2 N-O) as well as a 40% decrease in epithelium thickness (Fig. 3-2 Q). The thin epithelium is a result of fewer disc cell stratified along the z axis, which suggests that there are far fewer cells in the compartment than estimated

simply based on the 2-dimensional area measurement (Fig. 3-2 P). Taken together, these set of experiments demonstrates that Babo-a is the only functional isoform in the wing imaginal disc, and loss of *babo-a* phenocopies *myo* mutants in regulating wing disc growth. Thus, similar to mushroom body neurons case (Awasaki et al., 2011), our data demonstrate that Myo signals solely through Babo-a in the wing imaginal disc.

Babo-a, Punt, and Plum mediate non-canonical signaling in wing imaginal discs

In addition to canonical signaling, Babo can also signal non-canonically by interacting with downstream components of the BMP/Dpp pathway(Peterson and O'Connor, 2013). Non-canonical Babo activity is noticeable only in a protein null mutant of dSmad2 or strong RNAi knockdown of dSmad2 (Peterson and O'Connor, 2013; Peterson et al., 2012; Sander et al., 2010). The current model suggests that Babo, in the absence of its preferred target dSmad2, promiscuously activates Mad, the BMP ortholog of dSmad2 (Peterson and O'Connor, 2013). This ectopic Babo/Mad activation occurs throughout the disc including at the lateral edges where it represses *brk* expression, which normally suppresses growth, and therefore results in overgrowth of the tissue along the anterior-posterior axis (Peterson and O'Connor, 2013). We hypothesized that the non-canonical signaling is mediated through Babo-a and not through other

isoforms ectopically signaling in the absence of *dSmad2*. Babo activation can be visualized in *dSmad2* loss-of-function clones using the *brk* (*b14-LacZ)* reporter (Müller et al., 2003; Peterson and O'Connor, 2013). We used this assay and first generated *dSmad2* RNAi clones and confirmed the ectopic *brk-LacZ* silencing (Fig. 3-3 A). Next, we performed genetic epistasis analysis by simultaneously knocking down *dSmad2* plus a specific Babo isoform in clones and then assayed for *brk-LacZ* rescue. Knocking down *dSmad2* and *Babo-a* rescued *brk* reporter expression (Fig. 3-3 A vs B), while the RNAi of dSmad2 and *Babo-b* or *Babo-c* did not (Fig. 3-3 A vs C-D). To further test if non-canonical activity of Babo-a occurs throughout the disc we knocked down *dSmad2* in the entire disc using *esg-GAL4*, which results in the overgrowth phenotype (Fig. 3-8 A-B) (Peterson and O'Connor, 2013; Sander et al., 2010). The overgrowth phenotype can be quantified by measuring the wing disc pouch height/width ratio. RNAi for *dSmad2* alone results in the H/W ratio dropping from 0.91 (ctrl, *esg>*) to 0.66 (*esg>idSmad2*) (Fig. 3-8 D-E). Similar epistasis analysis with specific babo isoforms demonstrates that only RNAi of *babo-a* and not *babo-b* or *babo-c*, suppresses the RNAi-*dSmad2* induced widening phenotype (Fig. 3-8). These two sets of experiments suggest that Babo-a is the sole signaling receptor in the wing imaginal disc mediating both canonical and non-canonical signaling.

TGFβ signaling requires ligands binding to hetero-tetrameric type-I and type-II receptor complexes. There are two type-II receptors in the *Drosophila* genome: *punt* and *wishful thinking* (*wit*), both of which can signal with Type-I

receptors from either branch of the TGFβ superfamily (Upadhyay et al., 2017). Punt is more commonly utilized during development, and facilitates Dpp signaling in the wing imaginal disc in combination with the BMP type I receptors Tkv and Sax (Brummel et al., 1994; Fuentes-Medel et al., 2012; Letsou et al., 1995; Parker et al., 2006). In cell culture models however, Punt can signal in combination with Babo and Activin-like ligands (Brummel et al., 1999; Jensen et al., 2009; Letsou et al., 1995). Wit on the other hand functions primarily in neuromuscular junction, with the BMP ligand Gbb (Marqués et al., 2002) although it has been shown to bind the Activin-like ligand Myo in combination with Babo (Lee-Hoeflich et al., 2005). Both *punt* and *wit* are expressed in the wing imaginal disc, however it is unclear whether one or both type II receptors are require for Myo-Babo signaling (Gramates et al., 2017). To address this issue we utilized the non-canonical *brk* silencing assay in RNAi clones. We find that ectopic silencing of *brk* by loss of Smad2 is completely suppressed by the simultaneous RNAi of *punt* (Fig. 3-3 E vs G). However, RNAi for *wit* does not suppress the *brk* silencing in the same context (Fig. 3-3 E vs F). Taken together, these experiments demonstrate that Babo-a requires Punt, but not Wit, for proper control of *brk* expression in this non canonical wing disc signaling assay. Thus, we conclude that Myo and Babo-a also signal with Punt to control normal wild-type wing disc.

In addition to Type-I and Type-II receptors, various sorts of additional co-receptors have been found to interact with TGFβ ligands and receptors to

facilitate signaling (Heldin and Moustakas, 2016). Drosophila *plum* encodes an immunoglobulin superfamily protein, and is required for Myo stimulated pruning of mushroom body neurons (Yu et al., 2013). Therefore, we examined whether *plum* also facilitates Babo activity in the context of wing imaginal disc growth. Indeed, we find that *plum-RNAi* in the wing disc completely suppresses the *dSmad2* mutant overgrowth phenotype, confirming that Plum is required for Myo/Babo signaling in the wing disc as well (Fig. 3-9). This observation together with the previous report (Yu et al., 2013) suggest that Plum may be a general requirement for Myo/Babo signaling in *Drosophila*.

Muscle derived myoglianin signals to the wing disc

Growth factors such as Wg and Dpp, are tissue intrinsic ligands which are produced by and act on the wing disc cells. We sought to determine the source of Myo that signals to the imaginal discs. The name *myoglianin* refers to the two tissues (muscles and glia) in which *myo* expression was initially discovered (Lo and Frasch, 1999). More recent RNA *in situ* hybridization experiments suggested that *myo might* also be expressed in the wing imaginal disc at low levels (Hevia and de Celis, 2013). To determine the source of Myo acting on the wing disc, we first, examined the expression pattern of *myo* in late L3 larvae using *myo-GAL4* reporter to drive *UAS-CD8-GFP* (Awasaki et al., 2011). We detect GFP expression in both the glial cells of the brain and ventral ganglia as well as the

larval body wall muscles (Fig. 3-4 A-B). Importantly, we do not observe any GFP signal in the wing imaginal disc (Fig. 3-4 A). Thus, we conclude that either *myo* is not expressed in the wing disc or that our *myo-Gal4* construct does not have all of the endogenous enhancers.

To determine the functional source of Myo that controls imaginal disc growth, we conducted loss-of-function studies in the *dSmad2* null mutant background, and tested for rescue of the disc overgrowth phenotype. First, using null mutant alleles, we confirmed that the *dSmad2;;;myo* double mutant discs suppress the *dSmad2* overgrowth and are small like *myo* mutants and have wild type height/width proportions (Fig. 3-4 C-E). Next, we knocked down *myo* using tissue specific GAL4 drivers. To confirm efficacy of the RNAi constructs, we used the da>Gal4 driver to ubiquitously knock down *myo* in the *dSmad2* background and confirmed that it leads to a complete suppression of the wing disc overgrowth (Fig. 3-4 F vs G). Second, knocking down *myo* using either *esg-GAL4* (wing disc) or *repo-GAL4* (glia) failed to suppress the *dSmad2* wide wing disc phenotype (Fig. 3-4 F vs H-I). This suggests that in these animals Myo is still able to signal to the discs and cause the overgrowth. In contrast, RNAi for *myo* in body wall muscles, using either *MHC-GAL4* or *mef2-GAL4* drivers, completely suppresses the *dSmad2* disc overgrowth phenotype phenocoping the *dSmad2;;;myo* double mutant (Fig. 3-4 F vs J-K). It is notable that when *myo* is knocked down in the muscles, expression in other tissues such as the glia and potentially the wing disc are unperturbed, but such signaling especially in the disc

itself is not sufficient to stimulate disc overgrowth in *dSmad2* mutants. Therefore, we conclude that muscle is likely the major source of Myo that stimulates imaginal disc growth.

Overexpression of Myo in muscle or fat body rescues myo mutant disc growth

While the suppression of disc overgrowth in a *dSmad2* mutant background strongly implicates muscle as the source of ligand, we also wished to examine if Myo expression in muscle, or other non-disc tissues, could rescue disc size in *myo* mutants. Surprisingly, overexpression in glia (*repo>Gal4*) provide some rescue (Fig. 3-5 C, F) while overexpression in muscle (*Mef2>Gal4,* Fig. 3-5 D,F) and fat body (*CG>Gal4,* Fig. 3-5 E, F) provided complete rescue and overexpression with a second muscle driver (MHC>Gal4) actually produced a large wing (Fig. 3-10). This resupply assay raises a couple of issues. The first is that Myo can act non-disc autonomously, most likely through the hemolymph, to drive disc growth. The second is that the growth response likely depends on the level and or activity of Myo being produced in the distal tissue. Thus, while loss of endogenous glial derived Myo is not sufficient to suppress disc overgrowth in the *dSmad2* knockdown epistasis assay, overexpression of Myo using *repo>Gal4* is expected to provide more Myo than the endogenous glial source and can therefore partially rescue the *myo* wing disc growth defect.

Likewise, expression from a large tissue such as muscle or fatbody produces more Myo than glia leading to normal disc growth or even overgrowth at high levels. It is also possible that Myo signaling activity is modified depending on the tissue source. As with most TGFβ family members, Myo probably needs to be cleaved by a furin protease at its maturation site to separate the C-terminal ligand from the prodomain (Akiyama et al., 2012; Fritsch et al., 2012; Künnapuu et al., 2009). However, Myo may require a second cleavage by a Tolloid protease family member to actually achieve full dissociation of the prodomain from the ligand (Serpe and O'Connor, 2006) and either of these cleavage reactions might be different depending on the tissue source. Considering all the data, the results of this study suggest that muscle-derived Myo reaches the discs in an endocrine-like manner through the hemolymph to activate a specific receptor complex containing Babo-A, Punt and Plum that signals to dSmad2 and associated factors to promote imaginal disc growth.

DISCUSSION

Understanding the roles of inter-organ signaling during development is an emerging and complex aspect of biology. In particular, how inter-organ signaling regulates organ/tissue growth remains an open question. In the present study, we demonstrate that the *Drosophila* Activin-like ligand Myoglianin, is a muscle derived myokine that acts systemically to fine tune imaginal disc growth. We

suggest that tuning of disc growth by Myo may play an important role in maintaining proper allometric scaling of appendage size with the size of the muscles that control their movements.

Only Myo regulates imaginal disc size

Although Babo/dSmad2 signaling has been implicated in imaginal disc growth control for some time (Brummel et al., 1999; Hevia and de Celis, 2013; Peterson and O'Connor, 2013) the ligand(s) responsible and their production sites(s) have not been identified. Previous *in situ* hybridization and RNAi knockdown experiments suggested that all three Activin-like ligands (Myoglianin, Activinβ, and Dawdle) affect wing size (Hevia and de Celis, 2013). However, our ligand reporter constructs show no expression in imaginal discs, with the one exception being Actβ which is expressed in differentiating photoreceptors of the eye imaginal disc (Moss-Taylor et al., 2019; Zhu et al., 2008). More importantly, using genetic nulls we show that only loss of *myo* affects imaginal disc size. A discrepancy between RNAi tissue-specific knockdown results and the genetic nulls with respect to phenotypes is often noted and not fully understood. Besides simple off-target effects within the wing disc itself, one possible explanation is that many GAL4 drivers are expressed in other tissues besides the target tissue of interest, potentially resulting in deleterious effects for the animal that indirectly affect size of the tissue. Another possible explanation is that perhaps in *Actβ* and

daw genetic null backgrounds a non-autonomous compensatory growth promoting signal is generated by some other tissue that does not occur in the case of tissue-specific knockdown. We think both these explanations are unlikely in this instance since we demonstrate that only the Babo-a receptor isoform is expressed in discs, and we have previously shown that Daw only signals through the Babo-c isoform (Jensen et al., 2009). Therefore, it is challenging to explain why knockdown of *daw* in the wing disc would result in a small wing phenotype (Hevia and de Celis, 2013). Similarly Actβ appears to primarily use the Babo-b isoform, which is not expressed in discs, for signaling (Moss-Taylor et al., 2019). We conclude that the small wing phenotypes caused by RNAi knockdown of *Actβ* and *daw* are probably the result of some unknown off-target effect and that Myo is the only Activin-type ligand that regulates imaginal disc growth.

Plum and Punt are required for efficient Babo-A signaling to dSmad2 in the wing disc

The signaling ability of TGFβ ligands is modulated by the specific combinations of receptors and co-receptors to which they bind (Heldin and Moustakas, 2016; Upadhyay et al., 2017). In Drosophila, the receptor requirements for effective signaling through dSmad2 are likely to be different for each ligand and tissue (Jensen et al., 2009). In this report, we find that Myo signaling in the wing disc requires Punt as the type II receptor, Babo-a as the

type I receptor and Plum as a co-receptor. Furthermore, we establish that Myo is predominant Activin-like ligand signaling to the discs since p-dSmad2 levels are practically absent in *myo* mutant discs. Since Babo-a is the only isoform expressed in wing discs we also conclude that Myo can function solely through this isoform in the absence of other isoforms. Whether Myo can also signal through Babo-b or c is not yet clear, although it should be noted that in the context of remodeling MB neurons Babo-a also appears to be the major receptor isoform required for efficient Myo signaling (Awasaki et al., 2011). Furthermore, similar to MB neurons where Plum is required for efficient Myo/Babo-a signaling, Plum is also required in the wing discs for growth (Yu et al., 2013). At present it is not clear whether Punt is the only type II receptor that can produce an efficient signaling complex with Myo. In the mushroom body case, indirect genetic evidence suggests that the two Type II receptors function redundantly (Zheng et al., 2003). However, in our wing disc example, only loss of Punt produces a phenotype in the *brk* reporter assay even though Wit is expressed in the wing disc (Marqués et al., 2002). The requirement of Punt and Plum for Myo signaling may also explain why a previous attempt to study Myo signaling in a heterotypic cell culture model failed (Lee-Hoeflich et al., 2005). In that study, Myo was found to form a complex with Wit and Babo-A in COS-1 cells but no phosphorylation of dSmad2 was reported. One explanation is that effective signaling by Myo requires Punt and Plum, as well as Babo-A, and neither of these is found in mammalian cells. Therefore, to our knowledge, the data reported here provides

the first *in vivo* functional evidence that identifies a complete signaling network for Myo.

Intrinsic (intra-organ) vs extrinsic (inter-organ) mode of Myo signaling

The most intriguing finding of this study is that muscle derived Myo acts non-autonomously to regulate disc growth. This is in stark contrast to the two BMP ligands Dpp and Gbb which are produced by disc cells and act autonomously with in the disc itself to regulate both growth and pattern (Haerry et al., 1998). The fact that a TGFβ ligand can act in an endocrine like manner is not particularly novel since many vertebrate members of the TGF beta family, including Myostatin, the closest homolog to Drosophila Myoglianin, are found in the blood (Rodgers and Eldridge, 2015). Even the disc intrinsic molecule Dpp has been recently shown to be secreted into the hemolymph where it circulates and signal to the prothoracic gland to regulate a larval nutritional checkpoint (Setiawan et al., 2018). Several reports indicate that ligands from the Activin-like subfamily circulate in the hemolymph to function in inter-organ signaling. For example, muscle derived Activinβ and Myoglianin signal to the fat-body to regulate mitochondrial function and ribosomal biogenesis respectively (Demontis et al., 2014; Song et al., 2017b). Subsequently, Dawdle derived from many tissue signals to the Insulin producing cells and the mid-gut to stimulate Insulin secretion and repress expression of sugar metabolizing genes respectively

(Chng et al., 2014; Ghosh and O'Connor, 2014). Whether circulating Myo can signal to other organs exposed to the hemolymph likely depends on the expression of specific type I and co-receptors in the target tissue. Nevertheless, it is likely the rule rather than the exception that most TGFβ ligands can act either locally or systemically.

Our study also points to another important question, how Myo is able to reach the disc cells? Whether it can signal from the basement membrane or the apical surface of the discs cells is unknown. TGFβ receptors are often restricted to the basolateral surface (Saitoh et al., 2013). Thus it is possible that Myo may be signaling through the basement membrane of the discs, however this must be experimentally tested. Furthermore, does Myo transport in and out of the disc using similar mechanisms as Dilps or Dpp? Certain Dilp ligands need to get inside the disc cells to regulate cell growth, whereas other, like Dilp 8 leave the tissue to regulate developmental timing (Colombani et al., 2012). Dpp can also exit the disc to regulate timing (Setiawan et al., 2018), and here our data suggests that systemic Myo must be getting inside. Whether these ligands navigate the same or different paths is an open question.

Significance of inter-organ communication

Endocrine signaling enable communication between two organs that need to function together (Droujinine and Perrimon, 2016). For example, Daw

mediates environmental and nutritional inputs into the fat-body (energy storage organ) and relays that information to other organs that regulates mechanisms for energy uptake and processing (Chng et al., 2014; Ghosh and O'Connor, 2014). Perhaps this allows the animal to synchronize different organs between feeding/growth phase and starvation/survival phase. The question our data raises is why have muscle signal to disc, and that to regulate organ size? One plausible explanation is that Myo signaling coordinates the size of appendages (the fly wing) to the size of the muscles (the indirect flight muscles). A large muscle powering a small wing would probably result in diminished fine motor control. Conversely, a small muscle would not be able to power a large wing to support flight (Mirth and Shingleton, 2012). These two organs, the muscle and wing, may need to be proportional to each other to achieve proper function (flight) and maximize fitness (Frankino et al., 2009). Why would coordination between the wing and the larval body-wall muscles take place given that the larval muscle undergoes histolysis during pupal development, and is replaced by a new set of myoblasts? Interestingly, whereas muscles from the abdominal segments do undergo complete histolysis, the ones in the thoracic segment do not (Dutta et al., 2004). The larval muscles in the thoracic segment are preserved as fibers that then act as scaffolds for the larval myoblasts to infiltrate and seed to become the adult indirect flight muscles (Dutta et al., 2004). As mentioned previously, *myo* mutants are late larval lethal however, if they were to survive to adulthood, they would likely have disproportionately larger flight muscles

powering tiny wings. Furthermore the final body size of flies are fixed at the end of larval stages, and so it is critical to coordinate the size of individual organs prior to metamorphosis. Thus, we propose that muscle-derived Myo may acts as a second messenger to synchronize the size of the imaginal discs to overall body size to ensure that the adult has large enough wings to fly.

MATERIALS AND METHODS

Fly strain:

TGFβ mutants: *myo*^{1}, *myo*^{4}, Act^{80}, daw^{11}, *dSmad2*^{F4} are described previously (Awasaki et al., 2011; Peterson and O'Connor, 2013; Serpe and O'Connor, 2006; Zhu et al., 2008). Babo isoform RNAi lines and *myo-GAL4* are described previously (Awasaki et al., 2011). RNAi lines for *dSmad2* and *tkv* and the strategy used to generate new RNAi lines are described previously (Peterson and O'Connor, 2013; Peterson et al., 2012). New RNAi lines for *wit* targeted (1103-1608 of NM_079953.3), and *punt* targeted (1069-1582 of NM_169591.1). RNAi lines for *myo* targeted (bp:2259-3503 of NM_166788.2) utilizing the "snapback" gDNA/cDNA hybrid method (Kalidas and Smith, 2002). Stocks and methods used for induction of GAL4 flp-out clones are described previously (Peterson and O'Connor, 2013)Briefly, clones were induced by incubation at 37°C for 30 minutes. Larvae were dissected 48 hours later at wandering L3 stage.

ci-GAL4 and *hh-GAL4* were kind gifts from H. Steller (Rockefeller University). A version of MHC we labeled *MHC^{f}-GAL4* was a kind gift from N. Perrimon (HHMI, Harvard). *UAS-plum-RNAi* was a gift from O. Schuldiner (Weizmann institute of sciences, Israel)

The following stocks are available from Bloomington *Drosophila* Stock Center: *da-GAL4* (#5460), *esg-GAL4* (#26816), *repo-GAL4* (#7415), *mef2-GAL4* (#27390), *MHC-GAL4* (#55133), cg-GAL4 (#7011), *UAS-mCD8::GFP*, *UAS-GFP.nls*,

Microscopy and Antibodies:

Cleaved Caspase-3 (Cell Signaling #9661), phospho-Histone3 (S10) (Sigma, H0412). For B14-LacZ reporter detection, wing discs were stained with anti-βgalactosidase (Promega, #Z378A). AlexaFluor 568 or 647 (Invitrogen) conjugated secondary antibodies were used when required. Larval muscle and wing disc epithelium actin-belt were stained with rhodamine-phalloidin. To measure wing disc size, tissues were stained with DAPI.

Tissues for fluorescence microscopy were mounted with 80% Glycerol in PBS (0.1% TritonX-100). Wide field images taken with a 20X objective on a Zeiss Axiovert microscope. CARV Confocal images were captured using a 20X objective on a Zeiss Axiovert. We also used the Zeiss LSM710 for confocal and “tile-scanning” imaging.

For adult wings, animals were dissected in 95% ethanol, and mounted with (50:50) Canadian balsam:wintergreen oil solution. Images were taken with a 4X objective (for whole wing) and 40X objective (for trichome density).

Images were processed in FIJI (imageJ). Wing disc size were calculated with the DAPI staining then using the threshold and measure functions. For larval muscle size and adult wing size, outlines were drawn using the polygon tool.

Western Blot:

Mid-late third instar larvae were dissected in cold PBS, and wing imaginal discs were collected and washed on ice. Total protein was extracted with RIPA buffer (Cell Signaling) with cOmplete protease inhibitor (Roche) and PhosSTOP phosphatase inhibitor (Roche). Lysates were mixed with reducing sample buffer, boiled, and 10 ∝l of sample were run on 4-12% graded precast gels (Invitrogen). Resolved protein samples were transferred to PVDF membrane. Membrane blocking and probing were performed using standard protocols for ECL. Antibodies used for western blot: phospho-Smad2 (Cell Signaling #3108), Tubulin (Sigma #T9026), goat anti-mouse HRP, and goat anti-rabbit HRP.

qPCR:

Late-third instar larvae were dissected in cold PBS, and tissues were pooled and washed in PBS on ice. Tissues were homogenized in Trizol (Invitrogen) and Total RNA purified using RNeasy Mini Kit (Qiagen). cDNA libraries were made using SuperScript-III (Invitrogen). qPCR was performed

using SYBR green reagent (Roche) on a LightCycler 480. *Rpl23* was used as a housekeeping gene for normalization. Following qPCR primers were used for *babo* isoforms:

babo-a: F 5’ GGCTTTTGTTTCACGTCCGTGGA 3’
babo-a: R 5’ CTGTTTCAAATATCCTCTTCATAATCTCAT 3’
babo-b: F 5’ GCAAGGACAGGGACTTCTG 3’
babo-b: R 5’ GGCACATAATCTTGGACGGAG 3’
babo-c: F 5’ GACCAGTTGCCACCTGAAGA 3’
babo-c: R 5’ TGGCACATAATCTGGTAGGACA 3’

CHAPTER III FIGURES

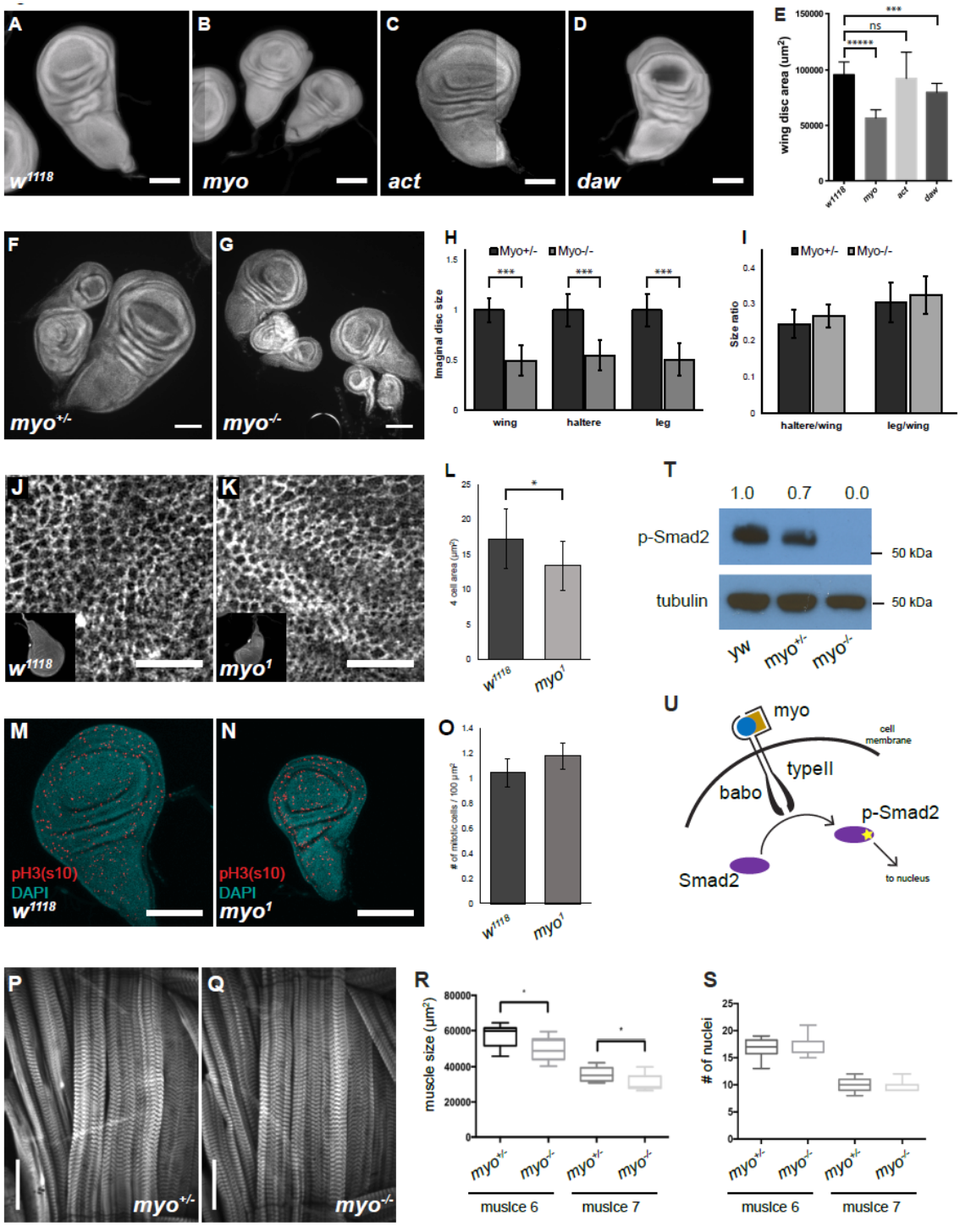

Figure 3-1. *Myoglianin* regulates size of imaginal discs by and activates dSmad2.

(A) DAPI staining of wing imaginal discs from late third instar larvae of w^{1118}, $myo^{1/4}$, act^{80}, $daw^{1/11}$. *myo* mutants are approximately 50% smaller vs controls w^{1118}, scale bar= 100μm, n= 20-40. B-D) Wing, Leg, and Halteer imaginal discs of $myo^{1/4}$ mutants are 50% smaller vs heterozygous controls $myo^{+/-}$. C) size of different imaginal disc, normalized to controls. D) Size ratio of haltere/wing disc (.25) or leg/wing disc (.3) is the same in *myo* mutants vs controls. E-F) Phalloidin staining showing the apical actin-belt of epithelial cells in wing discs, single confocal section is shown with the whole disc in insert. $Myo^{1/1}$ mutant discs cells are smaller vs control, circumference of 4 cells is plotted (F), scale bar= 10∝m, n>25. G-H) Phospho-Histone H3 (pSer10) (pH3) staining to mark mitotic cells in early third instar wing discs. No difference in number of mitotic cells in $myo^{1/1}$ mutants. Number of mitotic cells in 100μm^2 is plotted (H), scale bar= 100μm, n= 5. I-K) Phalloidin staining showing the late 3rd instar larvae skeletal muscle 6 and 7, muscle area (J) and number of nuclei (K) is plotted, scale bar= 100μm, n= 10. $Myo^{1/4}$ mutants have 13% smaller muscles however the number of nuclei does not change. L) Western blot analysis of phospho-dSmad2. $Myo^{1/1}$ mutants lack p-dSmad2 signal indicating loss of canonical signaling. M) Model for canonical TGFβ signaling in wing imaginal disc via Myo->Babo->dSmad2. Myo stimulation results in C-terminal activation of dSmad2 (yellow star) which regulates target gene expression.

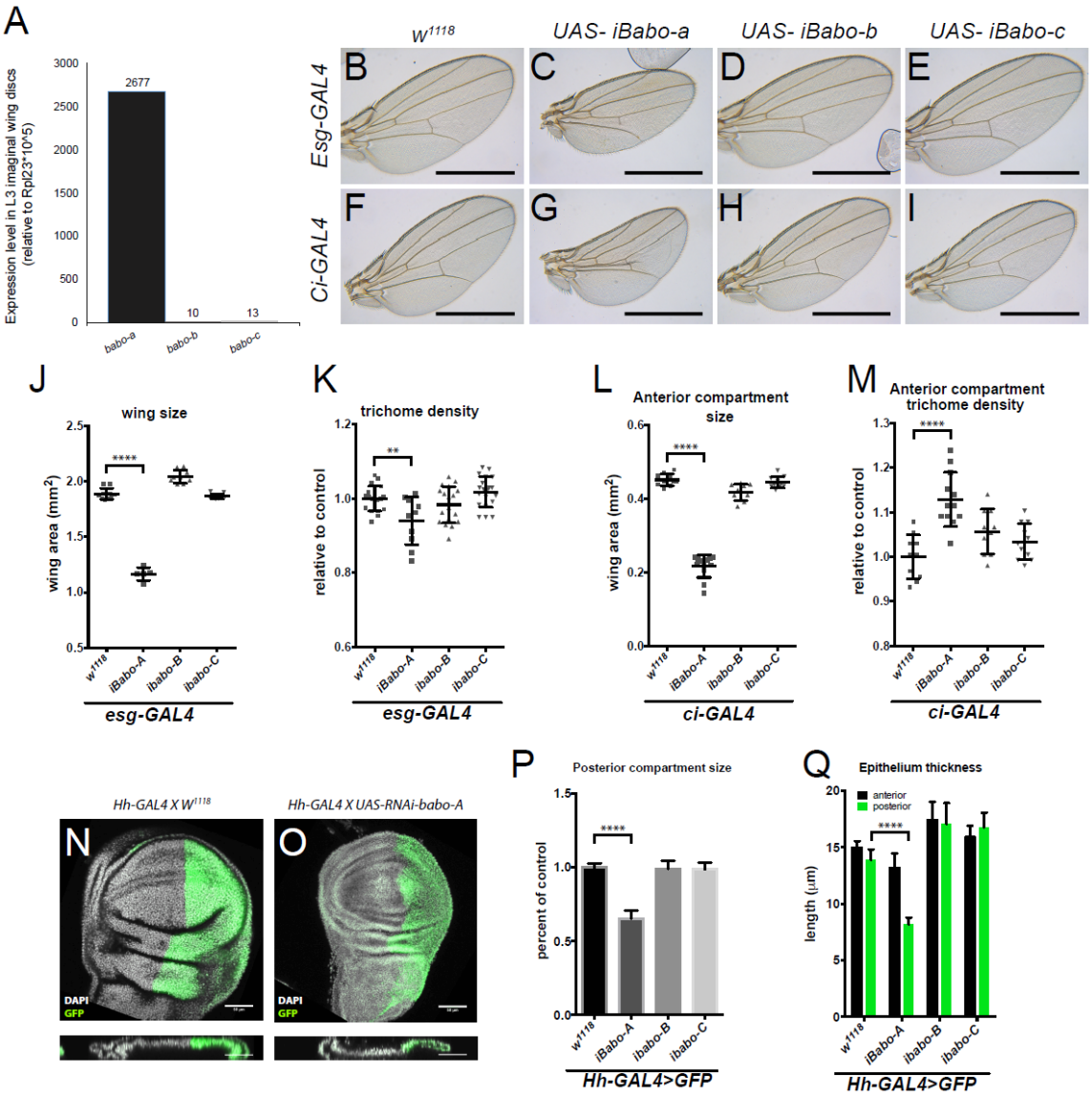
A
Expression level in L3 imaginal wing discs (relative to Rpl23*10^5)
3000
2500
2000
1500
1000
500
0
2677
10
13
babo-a
babo-b
babo-c
w1118
UAS- iBabo-a
UAS- iBabo-b
UAS- iBabo-c
Esg-GAL4
Ci-GAL4
B
C
D
E
F
G
H
I
J
wing size
wing area (mm2)
****
w1118
iBabo-A
ibabo-B
ibabo-C
esg-GAL4
K
trichome density
relative to control
**
esg-GAL4
L
Anterior compartment size
wing area (mm2)
****
ci-GAL4
M
Anterior compartment trichome density
relative to control
****
ci-GAL4
Hh-GAL4 X W1118
Hh-GAL4 X UAS-RNAi-babo-A
N
O
DAPI
GFP
P
Posterior compartment size
percent of control
****
Hh-GAL4>GFP
Q
Epithelium thickness
anterior
posterior
length (μm)
****
Hh-GAL4>GFP

Figure 3-2. Baboon-a regulates wing disc growth.

A) qPCR analysis of Babo isoform expression from late 3rd instar wing imaginal discs identifies only *babo-a* expression. *Rpl32* expression used as housekeeping gene control. B) RNAi for *Babo-a* throughout the wing imaginal disc (*esg-GAL4*) or just the anterior compartment (*ci-GAL4*) results in smaller adult wings and anterior compartment respectively (B, 2nd column), scale bar = 1mm. C) Quantification of wing size trichome density using *esg-GAL4* driver, babo-a RNAi wings are 40% smaller however the cells are larger. D) Quantification of anterior compartment area and trichome density using *ci-GAL4*, babo-a RNAi strictly in the anterior domain shrinks the size by 50% accompanied by smaller cells densely packed. E) RNAi for *Babo-a* using *Hh-GAL4* is pupal lethal. Representative image of late larval imaginal discs of control vs *Babo-A* RNAi, *UAS-GFP* used for indicating expression domain of *Hh-GAL4*, scale bar = 50μm. F) Quantification of posterior domain of larval imaginal discs from *Hh-GAL4* driven RNAi for Babo isoforms. Loss of *Babo-a* results in 35% smaller posterior domain as well as 29% decrease in epithelium thickness.

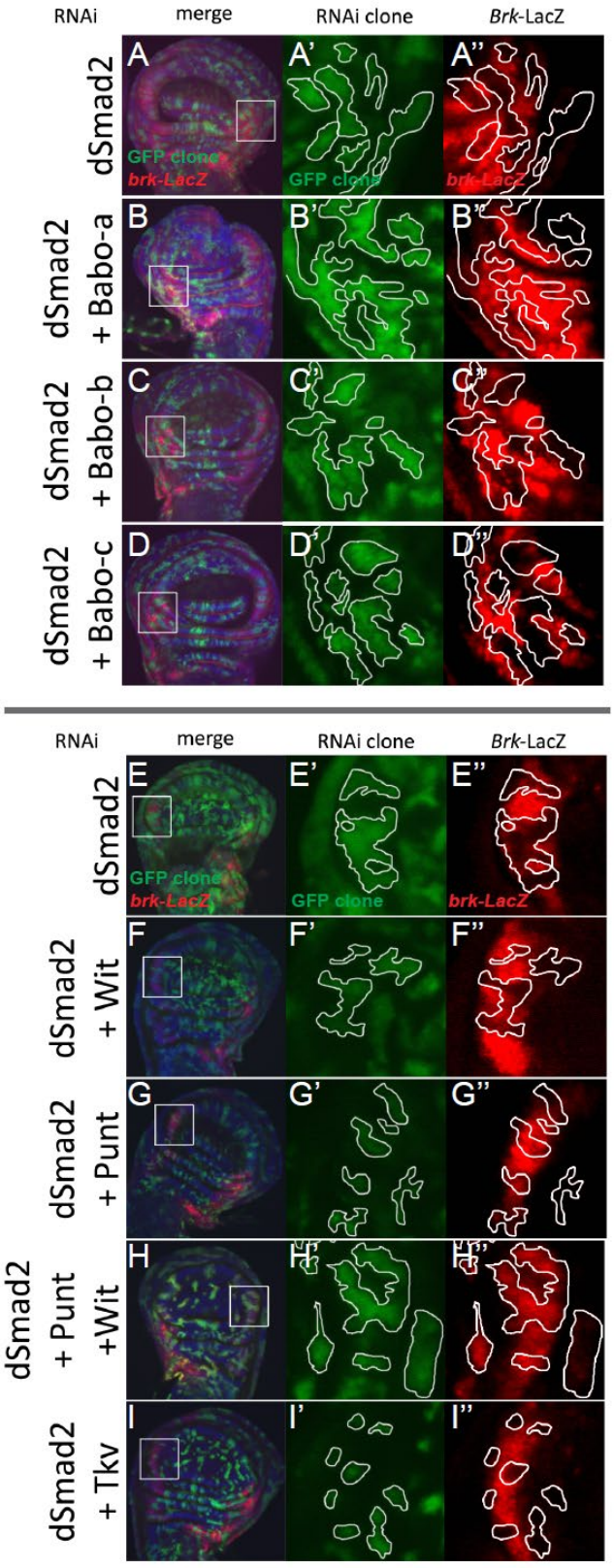
RNAi
merge
RNAi clone
Brk-LacZ
dSmad2
dSmad2 + Babo-a
dSmad2 + Babo-b
dSmad2 + Babo-c
dSmad2 + Wit
dSmad2 + Punt
dSmad2 + Punt +Wit
dSmad2 + Tkv
GFP clone
brk-LacZ

Figure 3-3. Babo-A and Punt are required for non-canonical silencing of *brk.*

In the background of *Brk-LacZ* reporter line random GFP+ (green) clones were induced by heat shock 48 hrs prior to analysis (see methods for details). GFP+ marked clones also express RNAi for the indicated genes to the left of respective panel. Clones at the lateral edges of the disc were analyzed to observe patterning defects of the *brk* reporter. (A-D) Analysis of Babo isoforms. (E-I) Analysis of Type-II receptor. (A-I) Max intensity projections of wing imaginal discs stained with DAPI (blue) and anti β-gal (red), and fluorescent clone marker (green). (A'-I') Single confocal section of higher magnification of insert in (A-I) showing GFP+ marked clone expressing RNAi for indicated genes. Clones are outlined with white line. (A''-I'') Same confocal section as in (A'-I') with outlined clones showing *brk-LacZ* reporter expression pattern. *Brk* reporter is ectopically silenced in dSmad2 RNAi clones (A and E). This ectopic silencing is rescued by the concomitant RNAi of Babo-a alone (A'' vs B'') but not Babo-b or Babo-c (A'' vs C'' or D''). Similarly the dSmad2 RNAi dependent *brk* reporter silencing (E'') can be rescued by the concomitant RNAi of Type-II receptor Punt (E'' vs G'') but not Wit (E'' vs F''). For a control RNAi for *punt,* plus *wit* appears different than in the *brk* reporter patterning compared to RNAi for *wit* alone (F'' vs H''). As a further control we ensured that the dSmad2 RNAi dependent silencing of the *brk* reporter is not mediated by Dpp-Tkv activation. RNAi for *Thickveins* (BMP Type-I receptor) does not rescue ectopic *brk* silencing (E'' vs I''), indicating that in these lateral clones where loss of dSmad2 leads to silencing of *brk*, it is due to signaling by TGFβ/Activin branch.

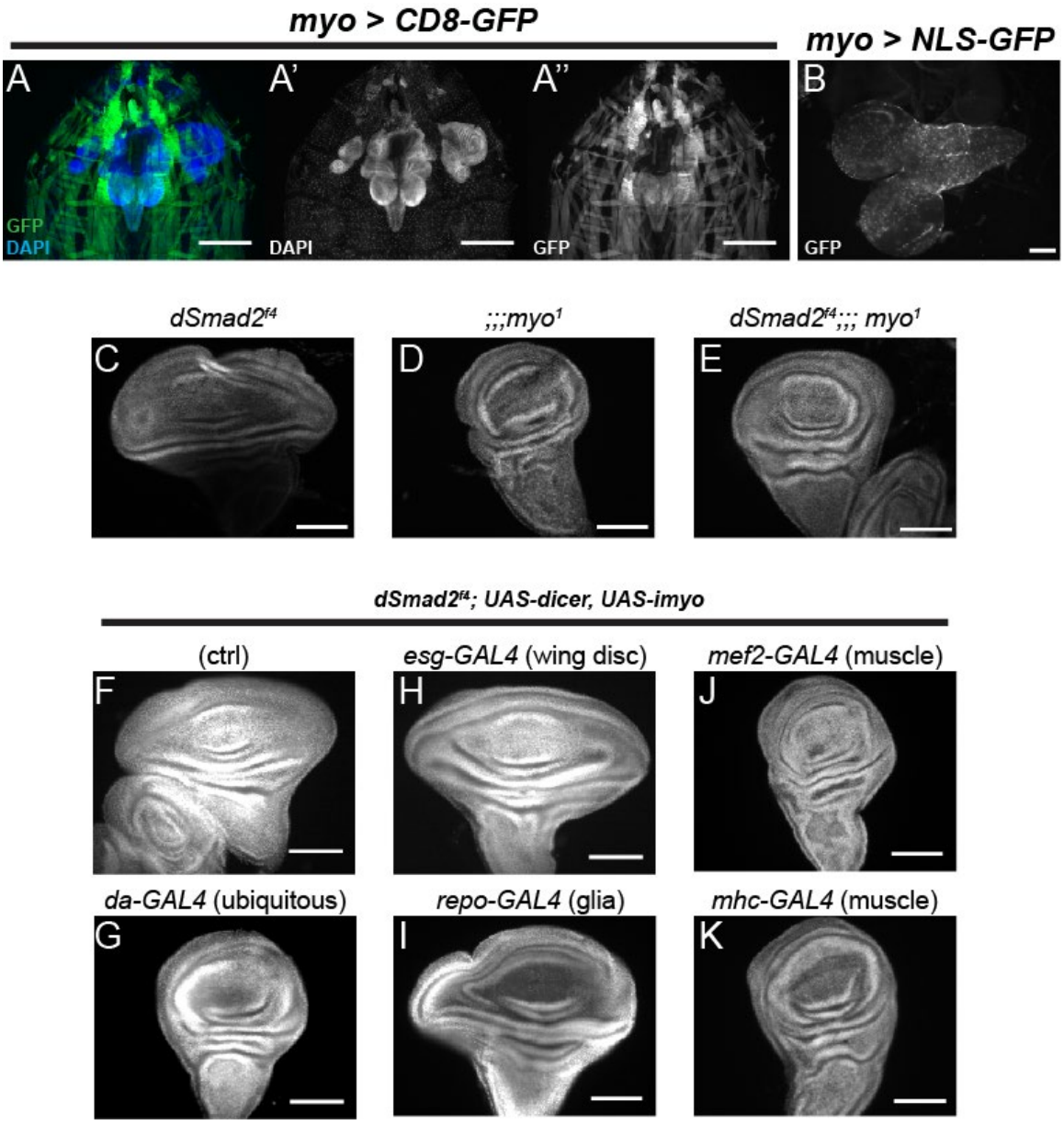
myo > CD8-GFP
myo > NLS-GFP
A
A'
A''
B
GFP
DAPI
DAPI
GFP
GFP
dSmad2f4
;;;myo1
dSmad2f4;;; myo1
C
D
E
dSmad2f4; UAS-dicer, UAS-imyo
(ctrl)
esg-GAL4 (wing disc)
mef2-GAL4 (muscle)
F
H
J
da-GAL4 (ubiquitous)
repo-GAL4 (glia)
mhc-GAL4 (muscle)
G
I
K

Figure 3-4. Muscle derived Myo is required for non-canonical Babo activation in imaginal discs.

(A) 3rd instar larval fillet showing *myo-GAL4* driving CD8-GFP (green), DAPI (blue) counterstain to image all tissues in the field of view. DAPI channel (A') shows muscle and cuticle associated cell nuclei, as well as the brain and several imaginal discs. GFP channel (A'') represents the expression pattern of the *myo-GAL4* reporter transgene. Note that the wing imaginal discs does not express GFP. (B) Higher magnification of 3rd instar larval brain from *myo>NLS-GFP* showing expression in glial cells. (C-E) *myo* is epistatic to *dSmad2*, and rescues the disc overgrowth phenotype. *dSmad2^{f4}* mutant discs (C) are overgrown, however *myo* mutant discs (D) retain the normal shape of the tissue. The *dSmad2^{f4};;;myo* double mutant discs (E) are similar to *myo* mutant discs, demonstrating rescue of the overgrowth phenotype, and that Myo can function in non-canonical Babo activation. (F-K) Muscle specific RNAi of *myo* is sufficient to rescue wing disc overgrowth phenotype of *dSmad2* mutants. RNAi of *myo* ubiquitously using *Da-GAL4* rescues the wing disc overgrowth (F vs G), phenocopying double *dSmad2;;;myo* double mutants (E vs G). RNAi of *myo* in either wing discs (*esg-GAL4*) or glia (*repo-GAL4*) is unable to rescue disc overgrowth (F vs H or I). RNAi of *myo* in larval muscles using *Mef2-GAL4* or *MHC-GAL4* rescues the disc overgrowth phenotype (F vs J or K), which phenocopies ubiquitous *myo* RNAi (G vs J or K).

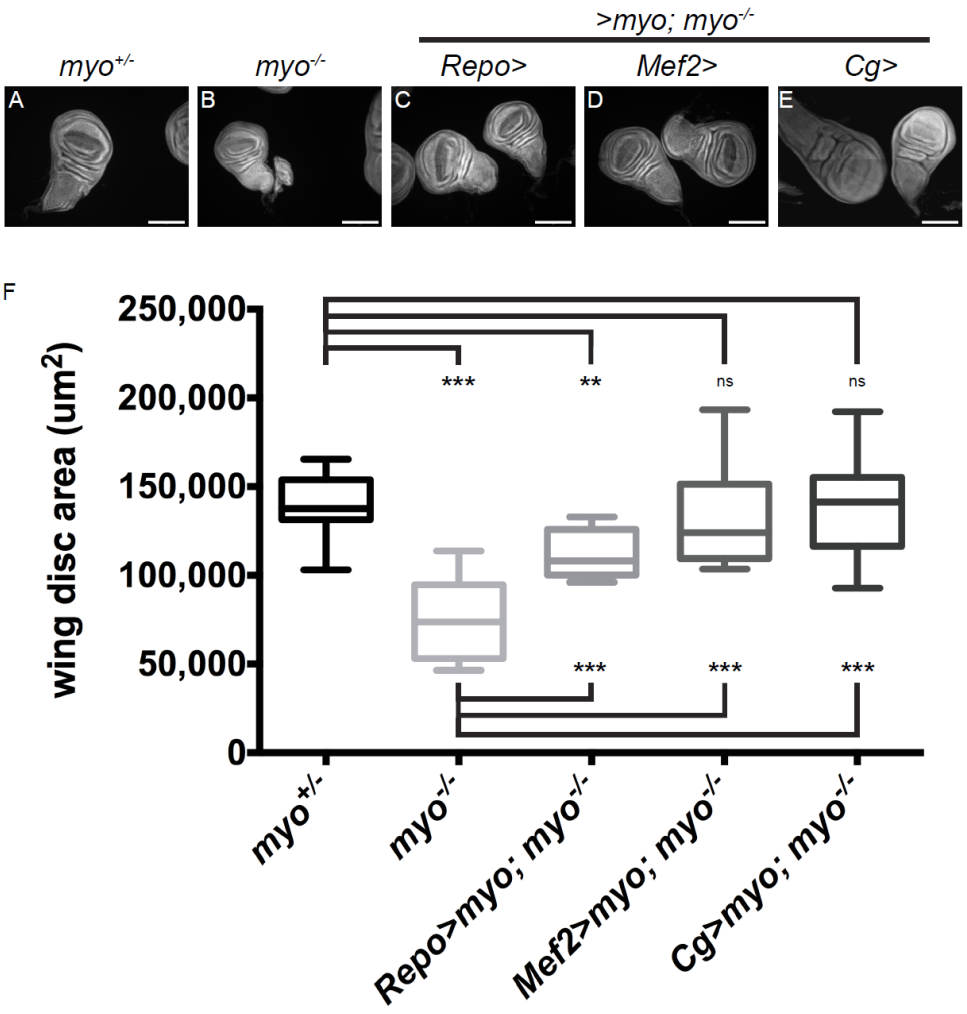

Figure 3-5. Overexpression of *myo* in muscles and fat-body rescues wing disc size of *myo* mutants.

(A-B) *myo*$^{1/4}$ mutant discs (B) are smaller than *myo*$^{+/1}$ heterozygous controls (A). (C-E) wing discs from *myo* overexpression rescue experiments. *Myo* overexpression in glial cells using *Repo-GAL4* partially rescues wing disc size (B vs C). This is due to ectopic expression of GAL4 transgenes in salivary glands. Overexpression in muscles completely rescues *myo* mutant discs back to wild type size (B vs D vs A). *Myo* is not normally expressed in the fat-body (Fig 4). However, ectopic overexpression in the fat-body is sufficient to rescue discs back to wild-type size (B vs E vs A). (F) Quantification of wing discs size from A-E.

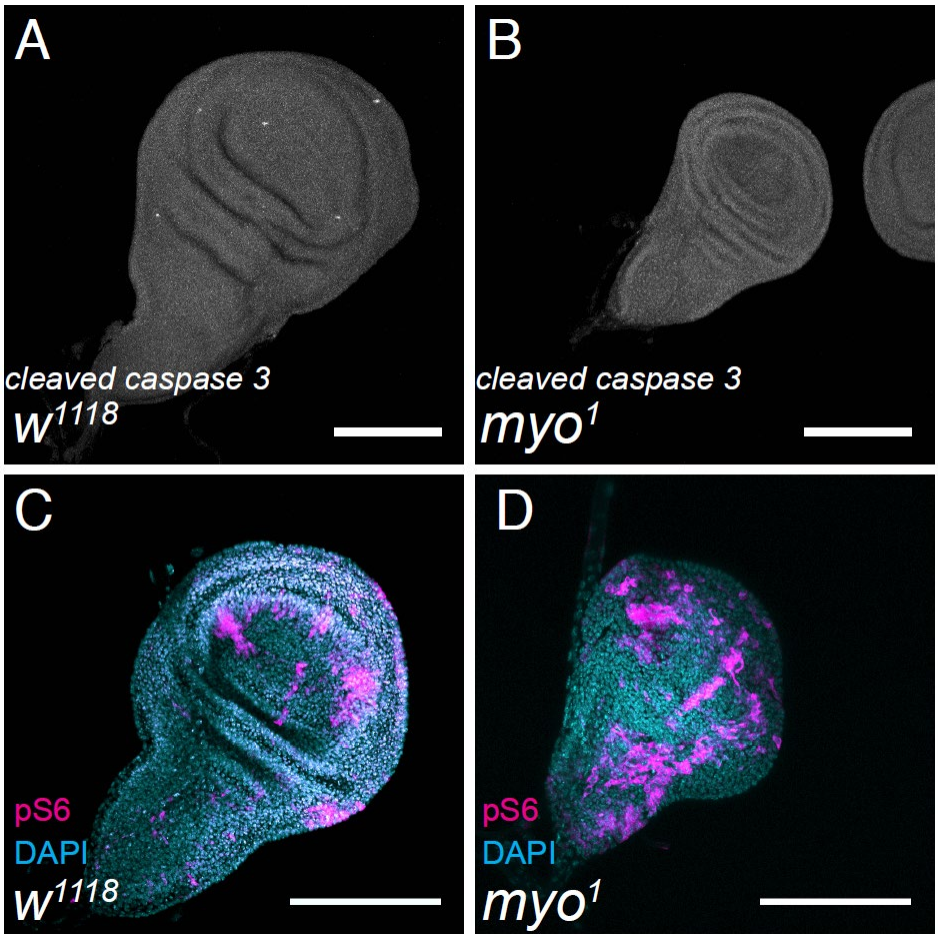

Figure 3-6. *myo* mutants show no defects in cell death or cell growth. A-B) Late 3rd instar larval wing discs stained for cleaved-caspase 3 shows no increase in cell death of *myo*$^{1/1}$ mutant discs. C-D) Early 3rd instar larval wing discs stained for phospho-S6, downstream of TOR signaling, shows no defects in cell growth. Scale bar= 100μm, n= 5-10.

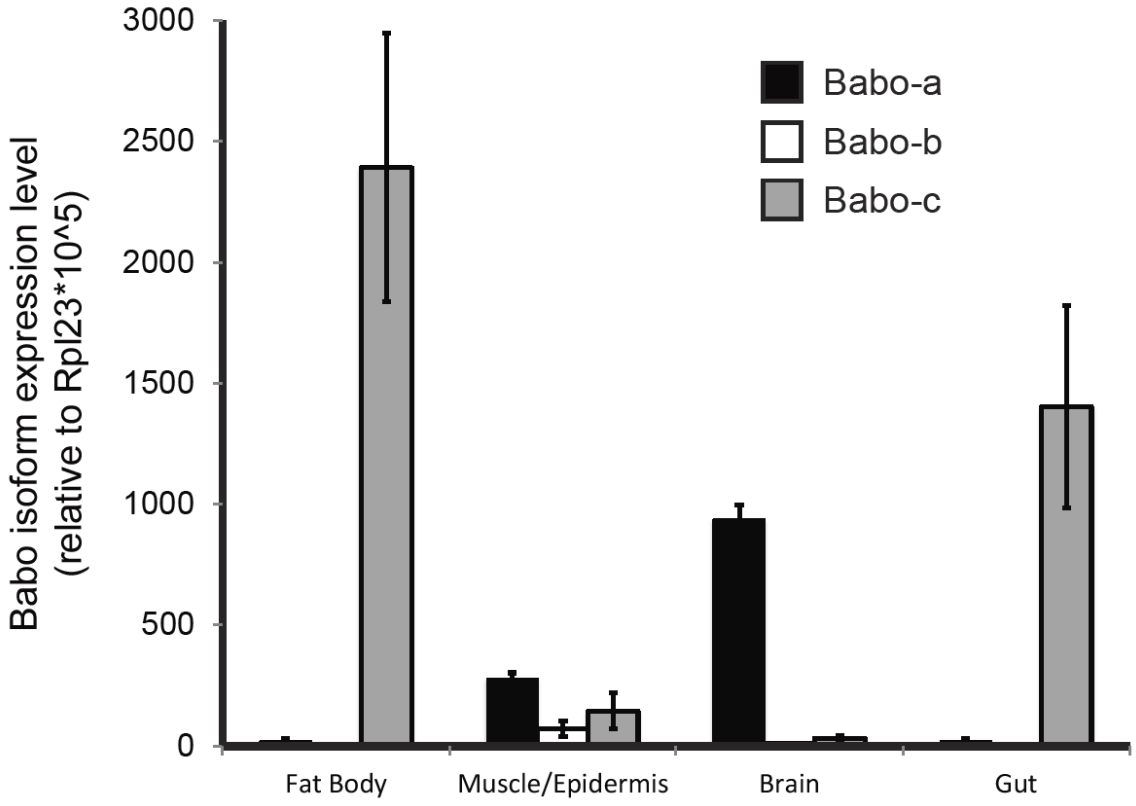

Figure 3-7 qPCR analysis of *babo* isoform expression in larval tissues
Tissues from late 3rd instar larvae express different isoforms of *babo*. Fat-body and Gut express only Babo-c, Brains samples predominantly express Babo-a. The carcass sample contains both Muscle and Cuticle associated cells. This sample is a mixture of various cell types and thus expresses all three isoforms. Expression levels are relative to *Rpl23*.

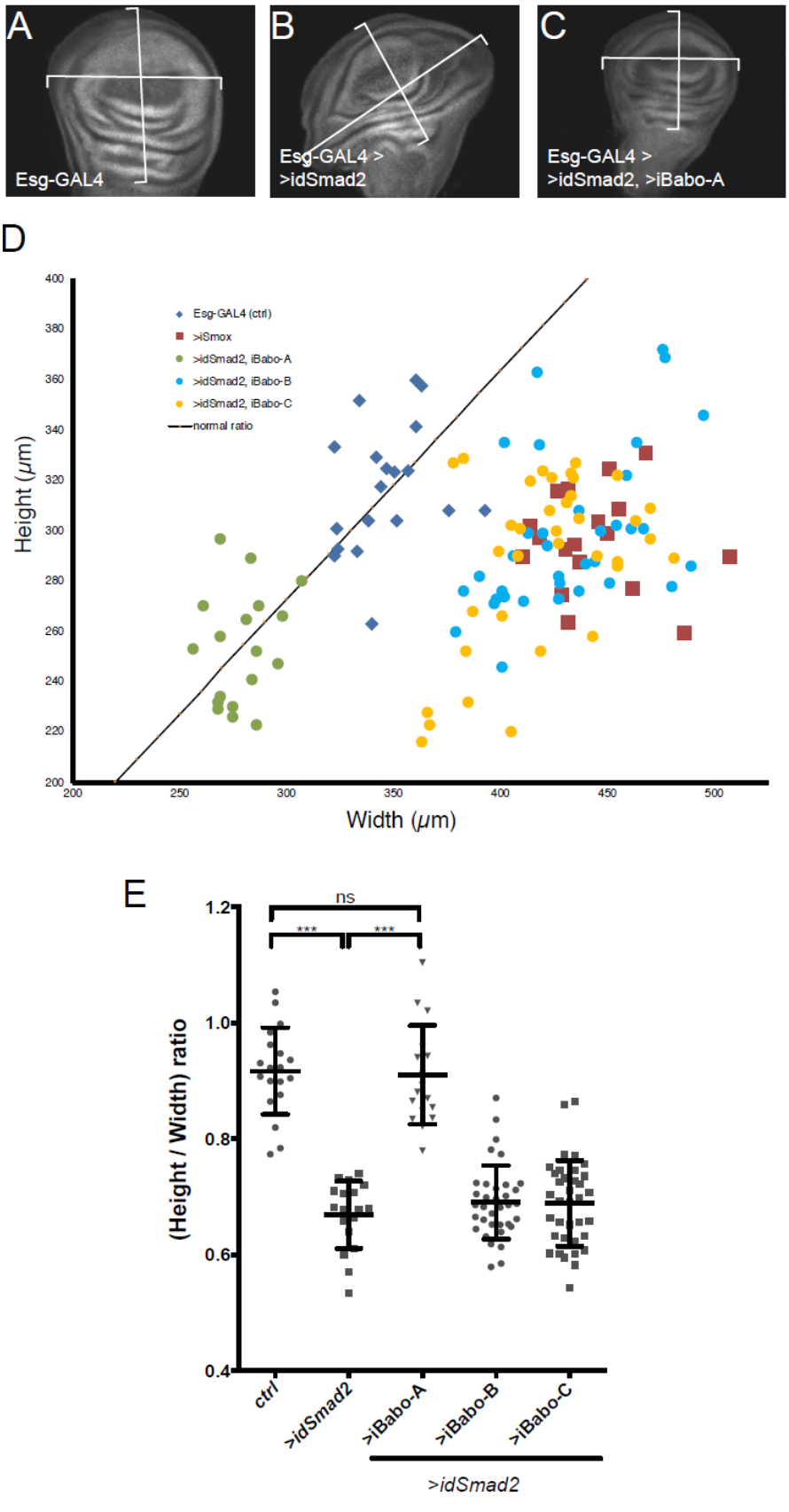
A
Esg-GAL4
B
Esg-GAL4 >
>idSmad2
C
Esg-GAL4 >
>idSmad2, >iBabo-A
D
Esg-GAL4 (ctrl)
>iSmox
>idSmad2, iBabo-A
>idSmad2, iBabo-B
>idSmad2, iBabo-C
normal ratio
Height (μm)
Width (μm)
E
ns
***
***
(Height / Width) ratio
ctrl
>idSmad2
>iBabo-A
>iBabo-B
>iBabo-C
>idSmad2

Figure 3-8. RNAi for *Babo-a* rescues wing disc overgrowth due to *dSmad2 RNAi.*

(A) Representative image of wild-type (control) imaginal disc. The height/width ratio is generally 0.9 (black line in D) for controls. (B) RNAi for *dSmad2* throughout the disc using *esg-GAL4* leads to ectopic *brk* silencing (Peterson and O'Connor, 2013) which results in overgrowth of the tissue along the anterior/posterior axis (widening) (red squares in D). (C) RNAi for *dSmad2* and *babo* (all isoforms) simultaneously rescues the widening phenotype where the H/W ratio is back to 0.9 (purple triangles in D). (D) Quantification of pouch size from Babo isoform specific rescue experiments. Control samples (Blue diamonds) have an average ratio of 0.9; RNAi for *dSmad2* (red squares) leads to widening with a ratio of 0.6; RNAi for *babo* (all isoforms, purple triangles) or *babo-a* (green circles) alone rescues the widening back to wild type ratios. These discs are smaller than wild type due to loss of canonical baboon activity (Fig.1 and Fig.2). There is no effect to widening by knocking down either *babo-b* or *babo-c* (blue and yellow circles vs red squares).

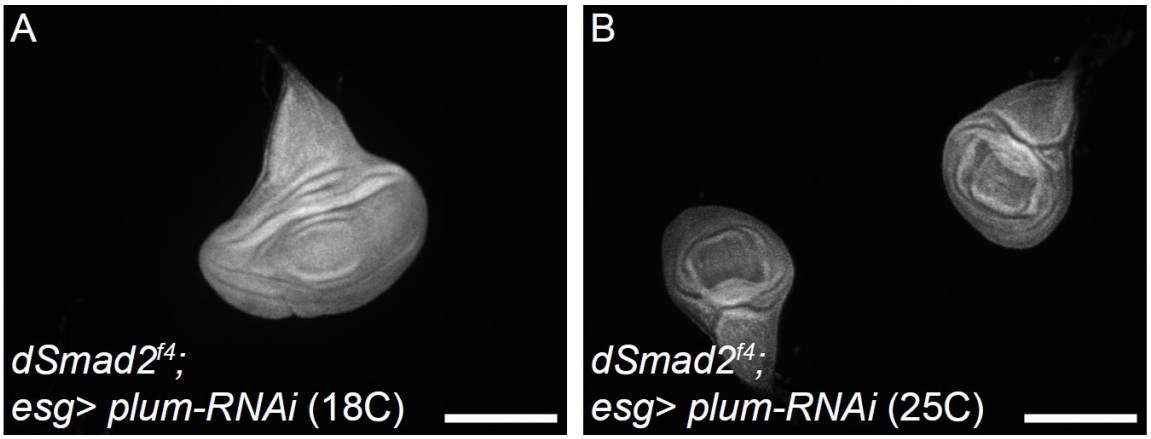

Figure 3-9. *Plum* is required for non-canonical babo activity.

dSmad2^{f4} null mutant wing discs are overgrown and show a widening phenotype. (B) *esg-GAL4* driving RNAi for *plum* at 25C in *dSmad2* mutant discs rescues the overgrowth phenotype. (A) Rearing the same animals at 18C reduces the expression of the RNAi transgene thus restoring *plum* expression which results in overgrowth of the imaginal discs.

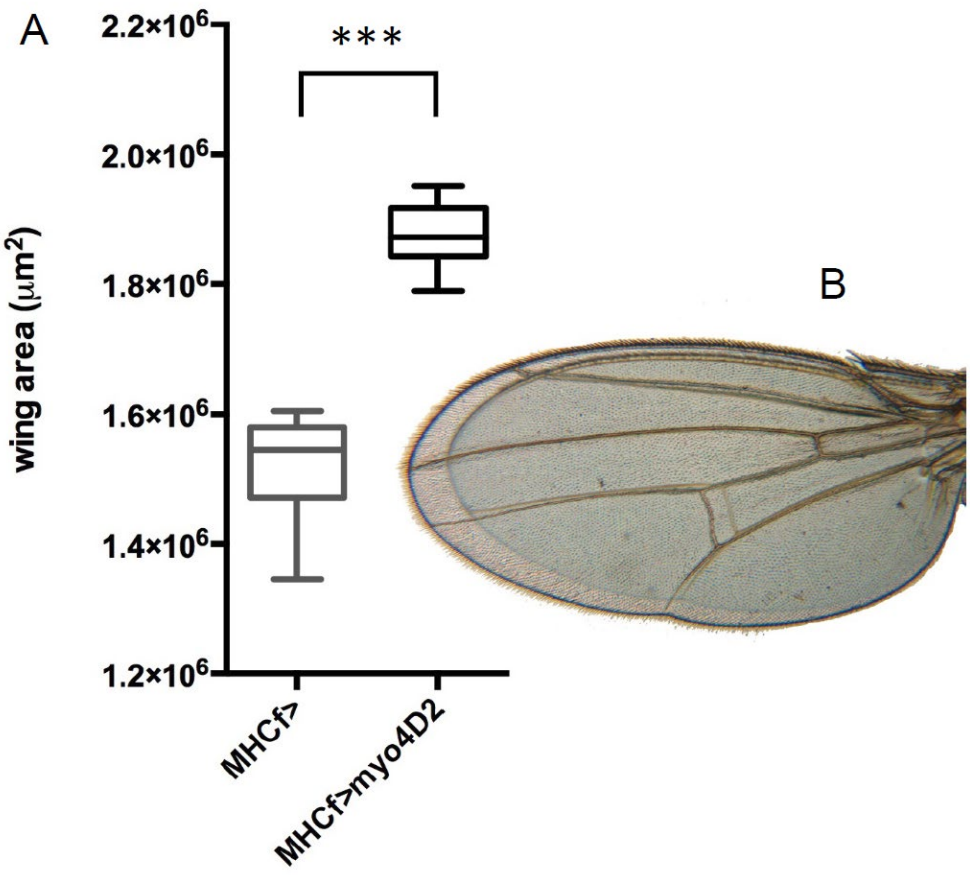

Figure 3-10. Muscle Overexpression of *myo* increases wing size

(A) Muscle specific *myo* overexpression in addition to endogenous levels increases final wing size of adults. (B) Representative wings from A of controls (smaller wing) vs *MHC>myo* (larger wing). Wings are superimposed on top of each other to show difference in size.

Chapter IV

Concluding remarks & future directions

Brief summary

How organs scale with overall body size remains an unsolved puzzle. Here, I tested the hypothesis that growth factors enable inter-organ signaling which regulate growth of the body and organs. Using *D. melanogaster* as a model, I investigated two uncharacterized growth factors which belong to the TGFβ superfamily. In chapter two, I show that motoneuron derived Activinβ signals to the larval body wall muscles to promote muscle growth and overall body size. In the absence of Activinβ, even though both the muscles and the animal are smaller, the wing imaginal discs maintain their proper wild type size, thus breaking the allometric scaling of wings. In chapter three, I show that muscle derived Myoglianin signals to the larval wing imaginal discs to promote disc growth. In the absence of Myoglianin, even though the larval muscle size is more or less similar to wild type, the imaginal discs are severely smaller (~40%), thus breaking the allometric scaling of wings, yet another way. In both muscle and imaginal discs, signal transduction via dSmad2 is necessary for proper growth of the tissue. These results suggests that either TGFβ signaling via dSmad2 is crucial for maintaining allometric scaling relationships or that it is an artifact of overall growth.

Significance of brain - muscle and muscle - wing communication

Evolutionary theory suggest that there is an advantage of scaling organs to body size (Brakefield, 2006). As far as insect wings are concerned, the

prevailing notion is that scaling of wings ensures proper flight for the animal (Dickinson et al., 1999; Frankino et al., 2009). Wild populations from higher latitudes on average have larger wing/body ratio compared to populations in warmer clines (Gilchrist and Huey, 2004). Rearing lab stocks in colder temperatures also result in larger wing/body ratio (Gilchrist et al., 2000). Interestingly, the genetic basis (wild populations) for allometry is due to changes in cell number, the plastic basis (temperature effects on lab stocks) for allometry is due to changes in cell size (Brakefield, 2006; Frankino et al., 2009). Furthermore, the fact that allometric relationships are highly variable across species yet invariable within, suggests that selection acts gradually on factors that tightly regulate growth of organs.

The fact that allometry within species is highly invariable suggest that there are robust mechanisms regulating organ growth. The mechanism by which Myoglianin regulates growth (i.e. the source of the growth factor) may provide the robustness necessary for proper allometry within species. As with any gene, it is possible that various environmental inputs such as temperature or nutrition may affect gene expression. Hence, it is possible that environmental cues regulate *myo* expression which then affects wing size. However, such mechanism alone could affect wing size even if *myo* was expressed in the wing tissue or broadly. On the other hand, the larval muscles serve as good estimate for overall body size. *Therefore, I propose that myo expression in larval body wall muscle provides the robustness for disc growth to match overall body size* (Fig. 4-1 A).

This model predicts that muscle/body size will determine the size of wings, which is consistent with observations of wild populations (McCabe and Partridge, 1997). Hence, our results of *Activinβ* mutants are quite surprising. The body size (and muscle size) of *Actβ* mutants are dramatically smaller, yet they have wild-type sized imaginal discs. There is no evidence of Actβ signaling in the imaginal discs, which partly explains why *Actβ* mutants have normal sized disc. However, why doesn't the smaller muscles in these mutants result in smaller imaginal discs? This remains an open question, but there are several possible explanations. First, the simplest explanation is that Actβ somehow interacts with Myo signaling, either by negatively regulating its transcription in the muscle or post translationally by negatively regulating its activity (Fig. 4-1 B). Another possibility is that loss of Actβ positively regulates other growth factors. These possibilities must be experimentally tested to completely understand the *Actβ* phenotype.

The primary role of Actβ to regulate muscle size should not be overlooked. It is intriguing that the nervous system regulates muscle/body size however, it is not the first time that such relationships have been documented. For example, nerves of a regenerating salamander limb secretes many growth factors, including BMPs, that are required for growth (Farkas and Monaghan, 2017). The question in *Drosophila* is, what is the significance of having motoneurons control size of the animal? With regard to why this might be important for organ scaling, I have no clear answer. However, I must note that regulating body size alone has

fitness advantages in insects, that is not due to muscle size or flight (Ewing, 1964). Essentially, what we observe as scaling defects might not be the primary function of Actβ. The primary role of Actβ is most likely regulating motoneuron function and coordination with muscle size.

In summary, a complex inter-organ signaling network regulates organ size and more importantly organ scaling. This network not only regulates animal growth by facilitating energy metabolism and homeostasis, but also directly coordinates growth of organs to pair with overall body size.

Future directions

Although the wing imaginal discs do not scale properly in *myo* and *Actβ* mutants, it is unknown whether other scaling relationships are lost as well. In other words, do imaginal discs in *myo* and *Actβ* mutants lose their ability to respond to nutritional or temperature changes? Determining the allometric coefficient for these mutants will be more informative on how this ligands control scaling.

Another important question is how cells respond to stimulation by different ligands? Both, Myo and Actβ signaling activate dSmad2, the signal transducer and transcription factor. Thus, the obvious question is whether pathway activation by Actβ in muscles have a different transcriptional output than Myo signaling in imaginal discs. This would help answer whether growth of these two organs controlled by similar or different mechanisms.

Lastly, the ability of a cell to respond to either Myo, Actβ, or Daw depends on the expression of a specific isoform of the ligand binding type-I receptor, Babo. Certain organs like the wing imaginal discs express a isoform Babo-a, whereas the fat-body expresses Babo-c. Thus, defects in isoform expression likely results in phenotypes similar to specific ligand mutants. Identifying splicing regulators that enable expression of specific isoform will shed light on how these systemic ligands yield tissue specific response.

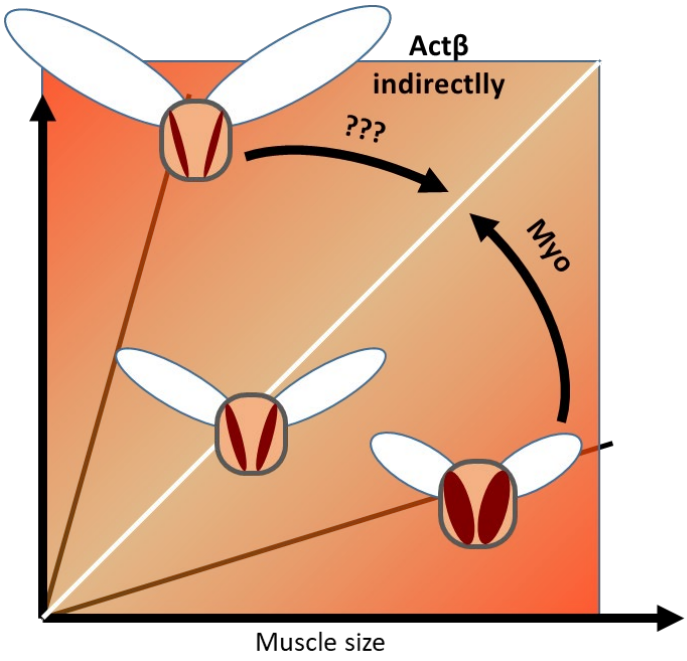

Figure 4-1. Model of wing/muscle scaling via Myo signaling

Wings scaling with respect to body size and muscles (depicted here as thorax cross section) is isometric (white line). Deviation from the white line leads to ectopically large muscles (lower line) or wings (top line). Myo signaling from the muscles restores the misbalance. Although, not directly, Actβ promotes body size and muscle growth and supporting the scaling of wings to body size.

REFRENCES

Aberle, H., Haghighi, A. P., Fetter, R. D., McCabe, B. D., Magalhães, T. R. and Goodman, C. S. (2002). wishful thinking encodes a BMP type II receptor that regulates synaptic growth in Drosophila. *Neuron* **33**, 545–558.

Affolter, M. and Basler, K. (2007). The Decapentaplegic morphogen gradient: from pattern formation to growth regulation. *Nat. Rev. Genet.* **8**, 663–74.

Akiyama, T. and Gibson, M. C. (2015). Decapentaplegic and growth control in the developing Drosophila wing. *Nature* **527**, 375–378.

Akiyama, T., Kamimura, K., Firkus, C., Takeo, S., Shimmi, O. and Nakato, H. (2008). Dally regulates Dpp morphogen gradient formation by stabilizing Dpp on the cell surface. *Dev. Biol.* **313**, 408–19.

Akiyama, T., Marqués, G. and Wharton, K. A. (2012). A large bioactive BMP ligand with distinct signaling properties is produced by alternative proconvertase processing. *Sci. Signal.* **5**, ra28.

Alarcón, C., Zaromytidou, A.-I., Xi, Q., Gao, S., Yu, J., Fujisawa, S., Barlas, A., Miller, A. N., Manova-Todorova, K., Macias, M. J., et al. (2009). Nuclear CDKs drive Smad transcriptional activation and turnover in BMP and TGF-beta pathways. *Cell* **139**, 757–69.

Aldaz, S. and Escudero, L. M. (2010). Imaginal discs. *Curr. Biol.* **20**, R429–R431.

Amore, G. and Casares, F. (2010). Size matters: the contribution of cell proliferation to the progression of the specification Drosophila eye gene regulatory network. *Dev. Biol.* **344**, 569–77.

Arbouzova, N. I. and Zeidler, M. P. (2006). JAK/STAT signalling in Drosophila: insights into conserved regulatory and cellular functions. *Development* **133**, 2605–16.

Augustin, H., McGourty, K., Steinert, J. R., Cochemé, H. M., Adcott, J., Cabecinha, M., Vincent, A., Halff, E. F., Kittler, J. T., Boucrot, E., et al. (2017). Myostatin-like proteins regulate synaptic function and neuronal morphology. *Development* **144**, 2445–2455.

Awasaki, T., Huang, Y., O'Connor, M. B. and Lee, T. (2011). Glia instruct developmental neuronal remodeling through TGF-β signaling. *Nat. Neurosci.* **14**, 821–3.

Baena-Lopez, L. A., Nojima, H. and Vincent, J.-P. (2012). Integration of morphogen signalling within the growth regulatory network. *Curr. Opin. Cell Biol.* **24**, 166–72.

Bai, H., Kang, P., Hernandez, A. M. and Tatar, M. (2013). Activin Signaling Targeted by Insulin/dFOXO Regulates Aging and Muscle Proteostasis in Drosophila. *PLoS Genet.* **9**, e1003941.

Baines, R. A. (2004). Synaptic strengthening mediated by bone morphogenetic protein-dependent retrograde signaling in the Drosophila CNS. *J. Neurosci.* **24**, 6904–11.

Baker, N. E. (2001). Cell proliferation, survival, and death in the Drosophila eye. *Semin. Cell Dev. Biol.* **12**, 499–507.

Ball, R. W., Warren-Paquin, M., Tsurudome, K., Liao, E. H., Elazzouzi, F., Cavanagh, C., An, B. S., Wang, T. T., White, J. H. and Haghighi, A. P. (2010). Retrograde BMP signaling controls synaptic growth at the NMJ by regulating trio expression in motor neurons. *Neuron* **66**, 536–549.

Ballard, S. L., Jarolimova, J. and Wharton, K. A. (2010). Gbb/BMP signaling is required to

maintain energy homeostasis in Drosophila. *Dev. Biol.* **337**, 375–85.

Belenkaya, T. Y., Han, C., Yan, D., Opoka, R. J., Khodoun, M., Liu, H. and Lin, X. (2004). Drosophila Dpp morphogen movement is independent of dynamin-mediated endocytosis but regulated by the glypican members of heparan sulfate proteoglycans. *Cell* **119**, 231–44.

Ben-Zvi, D., Pyrowolakis, G., Barkai, N. and Shilo, B.-Z. (2011). Expansion-repression mechanism for scaling the Dpp activation gradient in Drosophila wing imaginal discs. *Curr. Biol.* **21**, 1391–6.

Benkel, B. F. and Hickey, D. A. (1986). Glucose Repression of Amylase Gene Expression in DROSOPHILA MELANOGASTER. *Genetics* **114**, 137–44.

Berke, B., Wittnam, J., McNeill, E., Van Vactor, D. L. and Keshishian, H. (2013). Retrograde BMP signaling at the synapse: a permissive signal for synapse maturation and activity-dependent plasticity. *J Neurosci* **33**, 17937–17950.

Bertolino, P., Holmberg, R., Reissmann, E., Andersson, O., Berggren, P.-O. and Ibáñez, C. F. (2008). Activin B receptor ALK7 is a negative regulator of pancreatic β-cell function. *Proc. Natl. Acad. Sci. U. S. A.* **105**, 7246–7251.

Bickel, D., Shah, R., Gesualdi, S. C. and Haerry, T. E. (2008). Drosophila Follistatin exhibits unique structural modifications and interacts with several TGF-beta family members. *Mech. Dev.* **125**, 117–29.

Böhni, R., Riesgo-Escovar, J., Oldham, S., Brogiolo, W., Stocker, H., Andruss, B. F., Beckingham, K. and Hafen, E. (1999). Autonomous control of cell and organ size by CHICO, a Drosophila homolog of vertebrate IRS1-4. *Cell* **97**, 865–75.

Boulan, L., Milán, M. and Léopold, P. (2015). The Systemic Control of Growth. *Cold Spring Harb. Perspect. Biol.* **7**,.

Brakefield, P. M. (2006). Evo-devo and constraints on selection. *Trends Ecol. Evol.* **21**, 362–8.

Brogiolo, W., Stocker, H., Ikeya, T., Rintelen, F., Fernandez, R. and Hafen, E. (2001). An evolutionarily conserved function of the Drosophila insulin receptor and insulin-like peptides in growth control. *Curr. Biol.* **11**, 213–21.

Browder, M. H., D'Amico, L. J. and Nijhout, H. F. (2001). The role of low levels of juvenile hormone esterase in the metamorphosis of Manduca sexta. *J. Insect Sci.* **1**, 11.

Brummel, T. J., Twombly, V., Marqués, G., Wrana, J. L., Newfeld, S. J., Attisano, L., Massagué, J., O'Connor, M. B. and Gelbart, W. M. (1994). Characterization and relationship of Dpp receptors encoded by the saxophone and thick veins genes in Drosophila. *Cell* **78**, 251–61.

Brummel, T., Abdollah, S., Haerry, T. E., Shimell, M. J., Merriam, J., Raftery, L., Wrana, J. L. and O'Connor, M. B. (1999). The Drosophila Activin receptor Baboon signals through dSmad2 and controls cell proliferation but not patterning during larval development. *Genes Dev.* **13**, 98–111.

Bryant, P. J. and Simpson, P. (1984). Intrinsic and Extrinsic Control of Growth in Developing Organs. *Q. Rev. Biolgoy* **59**, 387–415.

Caldwell, P. E., Walkiewicz, M. and Stern, M. (2005). Ras activity in the Drosophila prothoracic gland regulates body size and developmental rate via ecdysone release. *Curr. Biol.* **15**, 1785–95.

Campbell, G. and Tomlinson, a (1999). Transducing the Dpp morphogen gradient in the wing of Drosophila: regulation of Dpp targets by brinker. *Cell* **96**, 553–62.

Chambers, A. P., Sandoval, D. A. and Seeley, R. J. (2013). Integration of satiety signals by the central nervous system. *Curr. Biol.* **23**, R379-88.

Chantranupong, L., Scaria, S. M., Saxton, R. A., Gygi, M. P., Shen, K., Wyant, G. A., Wang, T., Harper, J. W., Gygi, S. P. and Sabatini, D. M. (2016). The CASTOR Proteins Are Arginine Sensors for the mTORC1 Pathway. *Cell* **165**, 153–164.

Chen, C., Jack, J. and Garofalo, R. S. (1996). The Drosophila insulin receptor is required for normal growth. *Endocrinology* **137**, 846–856.

Chen, J., Honeyager, S. M., Schleede, J., Avanesov, A., Laughon, A. and Blair, S. S. (2012). Crossveinless d is a vitellogenin-like lipoprotein that binds BMPs and HSPGs, and is required for normal BMP signaling in the Drosophila wing. *Development* **139**, 2170–6.

Chien, S., Reiter, L. T., Bier, E. and Gribskov, M. (2002). Homophila: human disease gene cognates in Drosophila. *Nucleic Acids Res.* **30**, 149–51.

Chng, W. A., Sleiman, M. S. B., Schüpfer, F. and Lemaitre, B. (2014). Transforming growth factor β/activin signaling functions as a sugar-sensing feedback loop to regulate digestive enzyme expression. *Cell Rep.* **9**, 336–348.

Church, R. B. and Robertson, F. W. (1966). A biochemical study of the growth ofDrosophila melanogaster. *J. Exp. Zool.* **162**, 337–351.

Colombani, J., Raisin, S., Pantalacci, S., Radimerski, T., Montagne, J. and Léopold, P. (2003). A nutrient sensor mechanism controls Drosophila growth. *Cell* **114**, 739–49.

Colombani, J., Andersen, D. S. and Léopold, P. (2012). Secreted peptide Dilp8 coordinates Drosophila tissue growth with developmental timing. *Science* **336**, 582–5.

Conley, C. a, Silburn, R., Singer, M. a, Ralston, a, Rohwer-Nutter, D., Olson, D. J., Gelbart, W. and Blair, S. S. (2000). Crossveinless 2 contains cysteine-rich domains and is required for high levels of BMP-like activity during the formation of the cross veins in Drosophila. *Development* **127**, 3947–59.

Crick, F. (1970). Diffusion in Embryogenesis. *Nature* **225**, 420–422.

Curtiss, J. and Mlodzik, M. (2000). Morphogenetic furrow initiation and progression during eye development in Drosophila: the roles of decapentaplegic, hedgehog and eyes absent. *Development* **127**, 1325–36.

Dani, N. and Broadie, K. (2012). Glycosylated synaptomatrix regulation of trans-synaptic signaling. *Dev Neurobiol* **72**, 2–21.

Day, S. J. and Lawrence, P. A. (2000). Measuring dimensions: the regulation of size and shape. *Development* **127**, 2977–87.

de Celis, J. F. (2003). Pattern formation in the Drosophila wing: The development of the veins. *Bioessays* **25**, 443–51.

de Celis, J. F., Bray, S. and Garcia-Bellido, a (1997). Notch signalling regulates veinlet expression and establishes boundaries between veins and interveins in the Drosophila wing. *Development* **124**, 1919–28.

De Loof, A., Vandersmissen, T., Marchal, E. and Schoofs, L. (2015). Initiation of metamorphosis and control of ecdysteroid biosynthesis in insects: The interplay of absence of Juvenile hormone, PTTH, and Ca(2+)-homeostasis. *Peptides* **68**, 120–9.

Delanoue, R., Slaidina, M. and Léopold, P. (2010). The steroid hormone ecdysone controls systemic growth by repressing dMyc function in Drosophila fat cells. *Dev. Cell* **18**, 1012–21.

Demontis, F. and Perrimon, N. (2009). Integration of Insulin receptor/Foxo signaling and dMyc activity during muscle growth regulates body size in Drosophila. *Development* **136**, 983–93.

Demontis, F., Patel, V. K., Swindell, W. R. and Perrimon, N. (2014). Intertissue control of the nucleolus via a myokine-dependent longevity pathway. *Cell Rep.* **7**, 1481–1494.

Derynck, R., Gelbart, W. M., Harland, R. M., Heldin, C. H., Kern, S. E., Massagué, J., Melton, D. A., Mlodzik, M., Padgett, R. W., Roberts, A. B., et al. (1996). Nomenclature: vertebrate mediators of TGFbeta family signals. *Cell* **87**, 173.

Dickinson, M. H., Lehmann, F. O. and Sane, S. P. (1999). Wing rotation and the aerodynamic basis of insect flight. *Science* **284**, 1954–60.

Dickson, B. J. (2001). Rho GTPases in growth cone guidance. *Curr Opin Neurobiol* **11**, 103–110.

Droujinine, I. A. and Perrimon, N. (2016). Interorgan Communication Pathways in Physiology: Focus on Drosophila. *Annu. Rev. Genet.* **50**, 539–570.

Dutta, D., Anant, S., Ruiz-Gomez, M., Bate, M. and VijayRaghavan, K. (2004). Founder myoblasts and fibre number during adult myogenesis in Drosophila. *Development* **131**, 3761–3772.

Eaton, B. A. and Davis, G. W. (2005). LIM Kinase1 controls synaptic stability downstream of the type II BMP receptor. *Neuron* **47**, 695–708.

Eckel, R. H., Grundy, S. M. and Zimmet, P. Z. (2005). The metabolic syndrome. *Lancet* **365**, 1415–1428.

Eivers, E., Fuentealba, L. C., Sander, V., Clemens, J. C., Hartnett, L. and De Robertis, E. M. (2009). Mad is required for wingless signaling in wing development and segment patterning in Drosophila. *PLoS One* **4**, e6543.

Eivers, E., Demagny, H., Choi, R. H. and De Robertis, E. M. (2011). Phosphorylation of Mad controls competition between wingless and BMP signaling. *Sci. Signal.* **4**, ra68.

Elashry, M. I., Otto, A., Matsakas, A., El-Morsy, S. E. and Patel, K. (2009). Morphology and myofiber composition of skeletal musculature of the forelimb in young and aged wild type and myostatin null mice. *Rejuvenation Res.* **12**, 269–81.

Elkasrawy, M. N. and Hamrick, M. W. (2010). Myostatin (GDF-8) as a key factor linking muscle mass and bone structure. *J. Musculoskelet. Neuronal Interact.* **10**, 56–63.

Entchev, E. V, Schwabedissen, a and González-Gaitán, M. (2000). Gradient formation of the TGF-beta homolog Dpp. *Cell* **103**, 981–91.

Estella, C. and Mann, R. S. (2008). Logic of Wg and Dpp induction of distal and medial fates in the Drosophila leg. *Development* **135**, 627–36.

Estella, C., Voutev, R. and Mann, R. S. (2012). *A dynamic network of morphogens and transcription factors patterns the fly leg.* 1st ed. Elsevier Inc.

Estrada, B., Casares, F. and Sánchez-Herrero, E. (2003). Development of the genitalia in Drosophila melanogaster. *Differentiation* **71**, 299–310.

Ewing, A. W. (1964). The influence of wing area on the courtship behaviour of Drosophila melanogaster. *Anim. Behav.* **12**, 316–320.

Fan, X., Labrador, J. P., Hing, H. and Bashaw, G. J. (2003). Slit stimulation recruits Dock and Pak to the roundabout receptor and increases Rac activity to regulate axon repulsion at the CNS midline. *Neuron* **40**, 113–127.

Farkas, J. E. and Monaghan, J. R. (2017). A brief history of the study of nerve dependent regeneration. *Neurogenes. (Austin, Tex.)* **4**, e1302216.

Firth, L. C., Bhattacharya, A. and Baker, N. E. (2010). Cell cycle arrest by a gradient of Dpp signaling during Drosophila eye development. *BMC Dev. Biol.* **10**, 28.

Frankino, W. A., Emlen, D. J. and Shingleton, A. W. (2009). Experimental Approaches to Studying the Evolution of Animal Form. In *Experimental Evolution: Concepts, Methods and Applications of Selection Experiments*, pp. 419–478.

Fritsch, C., Sawala, A., Harris, R., Maartens, A., Sutcliffe, C., Ashe, H. L. and Ray, R. P. (2012). Different requirements for proteolytic processing of bone morphogenetic protein 5/6/7/8 ligands in Drosophila melanogaster. *J. Biol. Chem.* **287**, 5942–53.

Fuentes-Medel, Y., Ashley, J., Barria, R., Maloney, R., Freeman, M. and Budnik, V. (2012). Integration of a retrograde signal during synapse formation by glia-secreted TGF-beta ligand. *Curr Biol* **22**, 1831–1838.

Fujise, M., Takeo, S., Kamimura, K., Matsuo, T., Aigaki, T., Izumi, S. and Nakato, H. (2003). Dally regulates Dpp morphogen gradient formation in the Drosophila wing. *Development* **130**, 1515–1522.

Garland, T. and Carter, P. A. (1994). Evolutionary physiology. *Annu. Rev. Physiol.* **56**, 579–621.

Gesualdi, S. C. and Haerry, T. E. (2007). Distinct signaling of Drosophila Activin/TGF-beta family members. *Fly (Austin).* **1**, 212–21.

Ghosh, A. C. and O'Connor, M. B. (2014). Systemic Activin signaling independently regulates sugar homeostasis, cellular metabolism, and pH balance in Drosophila melanogaster. *Proc. Natl. Acad. Sci. U. S. A.* **111**, 5729–34.

Gibbens, Y. Y., Warren, J. T., Gilbert, L. I. and O'Connor, M. B. (2011). Neuroendocrine regulation of Drosophila metamorphosis requires TGFbeta/Activin signaling. *Development* **138**, 2693–2703.

Gilbert, L. I. (2004). Halloween genes encode P450 enzymes that mediate steroid hormone biosynthesis in Drosophila melanogaster. *Mol. Cell. Endocrinol.* **215**, 1–10.

Gilchrist, G. W. and Huey, R. B. (2004). Plastic and Genetic Variation in Wing Loading as a Function of Temperature Within and Among Parallel Clines in Drosophila subobscura. *Integr. Comp. Biol.* **44**, 461–70.

Gilchrist, A. S., Azevedo, R. B., Partridge, L. and O'Higgins, P. (2000). Adaptation and constraint in the evolution of Drosophila melanogaster wing shape. *Evol. Dev.* **2**, 114–24.

Goberdhan, D. C., Paricio, N., Goodman, E. C., Mlodzik, M. and Wilson, C. (1999). Drosophila tumor suppressor PTEN controls cell size and number by antagonizing the Chico/PI3-kinase signaling pathway. *Genes Dev.* **13**, 3244–58.

Gokhale, R. H. and Shingleton, A. W. (2015). Size control: the developmental physiology of body and organ size regulation. *Wiley Interdiscip. Rev. Dev. Biol.* **4**, 335–56.

Gokhale, R. H., Hayashi, T., Mirque, C. D. and Shingleton, A. W. (2016). Intra-organ growth coordination in Drosophila is mediated by systemic ecdysone signaling. *Dev. Biol.* **418**, 135–145.

Goold, C. P. and Davis, G. W. (2007). The BMP ligand Gbb gates the expression of synaptic homeostasis independent of synaptic growth control. *Neuron* **56**, 109–123.

Gould, S. J. (1966). Allometry and size in ontogeny and phylogeny. *Biol. Rev. Camb. Philos.*

Soc. **41**, 587–640.

Gramates, L. S., Marygold, S. J., Santos, G. Dos, Urbano, J.-M., Antonazzo, G., Matthews, B. B., Rey, A. J., Tabone, C. J., Crosby, M. A., Emmert, D. B., et al. (2017). FlyBase at 25: looking to the future. *Nucleic Acids Res.* **45**, D663–D671.

Grewal, S. S. (2012). Controlling animal growth and body size - does fruit fly physiology point the way? *F1000 Biol. Rep.* **4**, 12.

Grönke, S., Clarke, D.-F., Broughton, S., Andrews, T. D. and Partridge, L. (2010). Molecular evolution and functional characterization of Drosophila insulin-like peptides. *PLoS Genet.* **6**, e1000857.

Haerry, T. E., Khalsa, O., O'Connor, M. B. and Wharton, K. a (1998). Synergistic signaling by two BMP ligands through the SAX and TKV receptors controls wing growth and patterning in Drosophila. *Development* **125**, 3977–87.

Halder, G. and Johnson, R. L. (2011). Hippo signaling: growth control and beyond. *Development* **138**, 9–22.

Hales, K. G., Korey, C. A., Larracuente, A. M. and Roberts, D. M. (2015). Genetics on the Fly: A Primer on the Drosophila Model System. *Genetics* **201**, 815–42.

Hamaratoglu, F., de Lachapelle, A. M., Pyrowolakis, G., Bergmann, S. and Affolter, M. (2011). Dpp signaling activity requires Pentagone to scale with tissue size in the growing Drosophila wing imaginal disc. *PLoS Biol.* **9**, e1001182.

Hamaratoglu, F., Affolter, M. and Pyrowolakis, G. (2014). Dpp/BMP signaling in flies: from molecules to biology. *Semin. Cell Dev. Biol.* **32**, 128–36.

Hariharan, I. K. (2015). Organ Size Control: Lessons from Drosophila. *Dev. Cell* **34**, 255–65.

Hariharan, I. K., Wake, D. B. and Wake, M. H. (2015). Indeterminate Growth: Could It Represent the Ancestral Condition? *Cold Spring Harb. Perspect. Biol.* **8**, a019174.

Harmansa, S., Hamaratoglu, F., Affolter, M. and Caussinus, E. (2015). Dpp spreading is required for medial but not for lateral wing disc growth. *Nature* **527**, 317–22.

Hata, A. and Chen, Y.-G. (2016). TGF-β Signaling from Receptors to Smads. *Cold Spring Harb. Perspect. Biol.* **8**,.

Heitman, J., Movva, N. R. and Hall, M. N. (1991). Targets for cell cycle arrest by the immunosuppressant rapamycin in yeast. *Science* **253**, 905–9.

Heldin, C.-H. and Moustakas, A. (2016). Signaling Receptors for TGF-β Family Members. *Cold Spring Harb. Perspect. Biol.* **8**,.

Herboso, L., Oliveira, M. M., Talamillo, A., Pérez, C., González, M., Martín, D., Sutherland, J. D., Shingleton, A. W., Mirth, C. K. and Barrio, R. (2015). Ecdysone promotes growth of imaginal discs through the regulation of Thor in D. melanogaster. *Sci. Rep.* **5**, 12383.

Hevia, C. F. and de Celis, J. F. (2013). Activation and function of TGFβ signalling during Drosophila wing development and its interactions with the BMP pathway. *Dev. Biol.* **377**, 138–53.

Hevia, C. F., López-Varea, A., Esteban, N. and de Celis, J. F. (2017). A Search for Genes Mediating the Growth Promoting Function of TGFβ in the Drosophila melanogaster Wing Disc. *Genetics* **206**, genetics.116.197228.

Hickey, D. A. and Benkel, B. (1982). Regulation of amylase activity in drosophila melanogaster: effects of dietary carbohydrate. *Biochem. Genet.* **20**, 1117–29.

Hill, C. S. (2016). Transcriptional Control by the SMADs. *Cold Spring Harb. Perspect. Biol.* **8**,.

Hirschhorn, J. N. and Lettre, G. (2009). Progress in genome-wide association studies of human height. *Horm. Res.* **71 Suppl 2**, 5–13.

Horsfield, J., Penton, a, Secombe, J., Hoffman, F. M. and Richardson, H. (1998). decapentaplegic is required for arrest in G1 phase during Drosophila eye development. *Development* **125**, 5069–78.

Huang, J., Tian, L., Peng, C., Abdou, M., Wen, D., Wang, Y., Li, S. and Wang, J. (2011). DPP-mediated TGF signaling regulates juvenile hormone biosynthesis by activating the expression of juvenile hormone acid methyltransferase. *Development* **138**, 2283–2291.

Huxley, J. (1932). *Problems of Relative Growth*. London: Methuen & Co.

Ikeya, T., Galic, M., Belawat, P., Nairz, K. and Hafen, E. (2002). Nutrient-dependent expression of insulin-like peptides from neuroendocrine cells in the CNS contributes to growth regulation in Drosophila. *Curr. Biol.* **12**, 1293–300.

Inoue, H., Imamura, T., Ishidou, Y., Takase, M., Udagawa, Y., Oka, Y., Tsuneizumi, K., Tabata, T., Miyazono, K. and Kawabata, M. (1998). Interplay of signal mediators of decapentaplegic (Dpp): molecular characterization of mothers against dpp, Medea, and daughters against dpp. *Mol. Biol. Cell* **9**, 2145–56.

James, R. E. and Broihier, H. T. (2011). Crimpy inhibits the BMP homolog Gbb in motoneurons to enable proper growth control at the Drosophila neuromuscular junction. *Development* **138**, 3273–3286.

Jaźwińska, a, Kirov, N., Wieschaus, E., Roth, S. and Rushlow, C. (1999). The Drosophila gene brinker reveals a novel mechanism of Dpp target gene regulation. *Cell* **96**, 563–73.

Jensen, P. A., Zheng, X., Lee, T. and O'Connor, M. B. (2009). The Drosophila Activin-like ligand Dawdle signals preferentially through one isoform of the Type-I receptor Baboon. *Mech. Dev.* **126**, 950–7.

Jiang, H. and Edgar, B. A. (2009). EGFR signaling regulates the proliferation of Drosophila adult midgut progenitors. *Development* **136**, 483–93.

Johnston, L. A. and Gallant, P. (2002). Control of growth and organ size in Drosophila. *Bioessays* **24**, 54–64.

Kahlem, P. and Newfeld, S. J. (2009). Informatics approaches to understanding TGFbeta pathway regulation. *Development* **136**, 3729–40.

Kalidas, S. and Smith, D. P. (2002). Novel genomic cDNA hybrids produce effective RNA interference in adult Drosophila. *Neuron* **33**, 177–84.

Kamiya, Y., Miyazono, K. and Miyazawa, K. (2008). Specificity of the inhibitory effects of Dad on TGF-beta family type I receptors, Thickveins, Saxophone, and Baboon in Drosophila. *FEBS Lett.* **582**, 2496–500.

Karim, F. D. and Rubin, G. M. (1998). Ectopic expression of activated Ras1 induces hyperplastic growth and increased cell death in Drosophila imaginal tissues. *Development* **125**, 1–9.

Keshet, Y. and Seger, R. (2010). The MAP kinase signaling cascades: a system of hundreds of components regulates a diverse array of physiological functions. *Methods Mol. Biol.* **661**, 3–38.

Kicheva, A. and González-Gaitán, M. (2008). The Decapentaplegic morphogen gradient: a precise definition. *Curr. Opin. Cell Biol.* **20**, 137–43.

Kim, N. C. and Marques, G. (2012). The Ly6 neurotoxin-like molecule target of wit regulates spontaneous neurotransmitter release at the developing neuromuscular junction in Drosophila. *Dev Neurobiol* **72**, 1541–1558.

Kim, J., Johnson, K., Chen, H. J., Carroll, S. and Laughon, a (1997). Drosophila Mad binds to DNA and directly mediates activation of vestigial by Decapentaplegic. *Nature* **388**, 304–8.

Kim, M.-J., O'Connor, M. B. and O'Connor, M. B. (2014). Anterograde Activin signaling regulates postsynaptic membrane potential and GluRIIA/B abundance at the Drosophila neuromuscular junction. *PLoS One* **9**, e107443.

King-Jones, K. and Thummel, C. S. (2005). Nuclear receptors--a perspective from Drosophila. *Nat. Rev. Genet.* **6**, 311–23.

Koyama, T. and Mirth, C. K. (2018). Unravelling the diversity of mechanisms through which nutrition regulates body size in insects. *Curr. Opin. insect Sci.* **25**, 1–8.

Kretzschmar, M., Doody, J. and Massagué, J. (1997). Opposing BMP and EGF signalling pathways converge on the TGF-beta family mediator Smad1. *Nature* **389**, 618–22.

Kronenberg, H. M. (2003). Developmental regulation of the growth plate. *Nature* **423**, 332–6.

Künnapuu, J., Björkgren, I. and Shimmi, O. (2009). The Drosophila DPP signal is produced by cleavage of its proprotein at evolutionary diversified furin-recognition sites. *Proc. Natl. Acad. Sci. U. S. A.* **106**, 8501–6.

Künnapuu, J., Tauscher, P. M., Tiusanen, N., Nguyen, M., Löytynoja, A., Arora, K. and Shimmi, O. (2014). Cleavage of the Drosophila screw prodomain is critical for a dynamic BMP morphogen gradient in embryogenesis. *Dev. Biol.* **389**, 149–59.

Kuo, I. Y. and Ehrlich, B. E. (2015). Signaling in muscle contraction. *Cold Spring Harb. Perspect. Biol.* **7**, a006023.

Kuo, W.-J., Digman, M. A. and Lander, A. D. (2010). Heparan sulfate acts as a bone morphogenetic protein coreceptor by facilitating ligand-induced receptor hetero-oligomerization. *Mol. Biol. Cell* **21**, 4028–41.

Lamouille, S. and Derynck, R. (2007). Cell size and invasion in TGF-beta-induced epithelial to mesenchymal transition is regulated by activation of the mTOR pathway. *J. Cell Biol.* **178**, 437–51.

Lecuit, T. and Cohen, S. M. (1997). Proximal-distal axis formation in the Drosophila leg. *Nature* **388**, 139–45.

Lecuit, T., Brook, W., Ng, M., Calleja, M., Sun, H. and Cohen, S. (1996). Two distinct mechanisms for long-range patterning by Decapentaplegic in the Drosophila wing. *Nature* **381**, 387–393.

Lee-Hoeflich, S. T., Zhao, X., Mehra, A. and Attisano, L. (2005). The Drosophila type II receptor, Wishful thinking, binds BMP and myoglianin to activate multiple TGF?? family signaling pathways. *FEBS Lett.* **579**, 4615–4621.

Lee, J. Y., Hopkinson, N. S. and Kemp, P. R. (2011). Myostatin induces autophagy in skeletal muscle in vitro. *Biochem. Biophys. Res. Commun.* **415**, 632–6.

Leevers, S. J., Weinkove, D., MacDougall, L. K., Hafen, E. and Waterfield, M. D. (1996). The Drosophila phosphoinositide 3-kinase Dp110 promotes cell growth. *EMBO J.* **15**, 6584–94.

Letsou, A., Arora, K., Wrana, J. L., Simin, K., Twombly, V., Jamal, J., Staehling-Hampton, K., Hoffmann, F. M., Gelbart, W. M. and Massagué, J. (1995). Drosophila Dpp signaling is

mediated by the punt gene product: a dual ligand-binding type II receptor of the TGF beta receptor family. *Cell* **80**, 899–908.

Lo, P. C. and Frasch, M. (1999). Sequence and expression of myoglianin, a novel Drosophila gene of the TGF-beta superfamily. *Mech. Dev.* **86**, 171–5.

Lokireddy, S., Wijesoma, I. W., Sze, S. K., McFarlane, C., Kambadur, R. and Sharma, M. (2012). Identification of atrogin-1-targeted proteins during the myostatin-induced skeletal muscle wasting. *Am. J. Physiol. Cell Physiol.* **303**, C512-29.

Macias, M. J., Martin-Malpartida, P. and Massagué, J. (2015). Structural determinants of Smad function in TGF-β signaling. *Trends Biochem. Sci.* **40**, 296–308.

Madaan, U., Yzeiraj, E., Meade, M., Clark, J. F., Rushlow, C. A. and Savage-Dunn, C. (2018). BMP Signaling Determines Body Size via Transcriptional Regulation of Collagen Genes in Caenorhabditis elegans. *Genetics* **210**, 1355–1367.

Makhijani, K., Alexander, B., Rao, D., Petraki, S., Herboso, L., Kukar, K., Batool, I., Wachner, S., Gold, K. S., Wong, C., et al. (2017). Regulation of Drosophila hematopoietic sites by Activin-β from active sensory neurons. *Nat. Commun.* **8**, 15990.

Marqués, G., Bao, H., Haerry, T. E., Shimell, M. J., Duchek, P., Zhang, B. and O'Connor, M. B. (2002). The Drosophila BMP type II receptor Wishful Thinking regulates neuromuscular synapse morphology and function. *Neuron* **33**, 529–43.

Martín-Castellanos, C. and Edgar, B. a (2002). A characterization of the effects of Dpp signaling on cell growth and proliferation in the Drosophila wing. *Development* **129**, 1003–1013.

Martin, F. A., Herrera, S. C. and Morata, G. (2009). Cell competition, growth and size control in the Drosophila wing imaginal disc. *Development* **136**, 3747–3756.

Martín, F. a, Pérez-Garijo, A., Moreno, E. and Morata, G. (2004). The brinker gradient controls wing growth in Drosophila. *Development* **131**, 4921–4930.

Matsakas, A., Otto, A., Elashry, M. I., Brown, S. C. and Patel, K. (2010). Altered primary and secondary myogenesis in the myostatin-null mouse. *Rejuvenation Res.* **13**, 717–27.

Matsuda, S. and Shimmi, O. (2012). Directional transport and active retention of Dpp/BMP create wing vein patterns in Drosophila. *Dev. Biol.* **366**, 153–62.

Mattila, J., Havula, E., Suominen, E., Teesalu, M., Surakka, I., Hynynen, R., Kilpinen, H., Väänänen, J., Hovatta, I., Käkelä, R., et al. (2015). Mondo-Mlx Mediates Organismal Sugar Sensing through the Gli-Similar Transcription Factor Sugarbabe. *Cell Rep.* 350–364.

McBrayer, Z., Ono, H., Shimell, M., Parvy, J.-P., Beckstead, R. B., Warren, J. T., Thummel, C. S., Dauphin-Villemant, C., Gilbert, L. I. and O'Connor, M. B. (2007). Prothoracicotropic hormone regulates developmental timing and body size in Drosophila. *Dev. Cell* **13**, 857–71.

McCabe, J. and Partridge, L. (1997). AN INTERACTION BETWEEN ENVIRONMENTAL TEMPERATURE AND GENETIC VARIATION FOR BODY SIZE FOR THE FITNESS OF ADULT FEMALE DROSOPHILA MELANOGASTER. *Evolution (N. Y).* **51**, 1164–1174.

McCabe, B. D., Marqués, G., Haghighi, A. P., Fetter, R. D., Crotty, M. L., Haerry, T. E., Goodman, C. S. and O'Connor, M. B. (2003). The BMP homolog Gbb provides a retrograde signal that regulates synaptic growth at the Drosophila neuromuscular junction. *Neuron* **39**, 241–254.

McCabe, B. D., Hom, S., Aberle, H., Fetter, R. D., Marques, G., Haerry, T. E., Wan, H.,

O'Connor, M. B., Goodman, C. S. and Haghighi, A. P. (2004). Highwire regulates presynaptic BMP signaling essential for synaptic growth. *Neuron* **41**, 891–905.

McNabb, S. L., Baker, J. D., Agapite, J., Steller, H., Riddiford, L. M. and Truman, J. W. (1997). Disruption of a behavioral sequence by targeted death of peptidergic neurons in Drosophila. *Neuron* **19**, 813–23.

McPherron, A. C. and Lee, S. J. (1997). Double muscling in cattle due to mutations in the myostatin gene. *Proc. Natl. Acad. Sci. U. S. A.* **94**, 12457–61.

McPherron, A. C., Lawler, A. M. and Lee, S. J. (1997). Regulation of skeletal muscle mass in mice by a new TGF-beta superfamily member. *Nature* **387**, 83–90.

Milán, M., Campuzano, S. and García-Bellido, A. (1996). Cell cycling and patterned cell proliferation in the wing primordium of Drosophila. *Proc. Natl. Acad. Sci. U. S. A.* **93**, 640–5.

Minami, M., Kinoshita, N., Kamoshida, Y., Tanimoto, H. and Tabata, T. (1999). brinker is a target of Dpp in Drosophila that negatively regulates Dpp-dependent genes. *Nature* **398**, 242–6.

Mirth, C. K. and Shingleton, A. W. (2012). Integrating body and organ size in Drosophila: Recent advances and outstanding problems. *Front. Endocrinol. (Lausanne).* **3**, 1–13.

Mirth, C. K. and Shingleton, A. W. (2014). The roles of juvenile hormone, insulin/target of rapamycin, and ecydsone signaling in regulating body size in Drosophila. *Commun. Integr. Biol.* **7**,.

Mirth, C. K., Truman, J. W. and Riddiford, L. M. (2009). The Ecdysone receptor controls the post-critical weight switch to nutrition-independent differentiation in Drosophila wing imaginal discs. *Development* **136**, 2345–2353.

Mirth, C. K., Tang, H. Y., Makohon-Moore, S. C., Salhadar, S., Gokhale, R. H., Warner, R. D., Koyama, T., Riddiford, L. M. and Shingleton, A. W. (2014). Juvenile hormone regulates body size and perturbs insulin signaling in Drosophila. *Proc. Natl. Acad. Sci. U. S. A.* **111**, 7018–23.

Morata, G. and Lawrence, P. A. (1977). The development of wingless, a homeotic mutation of Drosophila. *Dev. Biol.* **56**, 227–40.

Morikawa, M., Derynck, R. and Miyazono, K. (2016). TGF-β and the TGF-β Family: Context-Dependent Roles in Cell and Tissue Physiology. *Cold Spring Harb. Perspect. Biol.* **8**, a021873.

Moss-Taylor, L., Upadhyay, A., Pan, X., Kim, M.-J. and O'Connor, M. B. (2019). Motoneuron-derived Activinβ regulates Drosophila body size and tissue-scaling during larval growth and adult development. *bioRxiv* 661363.

Müller, B., Hartmann, B., Pyrowolakis, G., Affolter, M. and Basler, K. (2003). Conversion of an extracellular Dpp/BMP morphogen gradient into an inverse transcriptional gradient. *Cell* **113**, 221–33.

Musselman, L. P., Fink, J. L., Narzinski, K., Ramachandran, P. V., Hathiramani, S. S., Cagan, R. L. and Baranski, T. J. (2011). A high-sugar diet produces obesity and insulin resistance in wild-type Drosophila. *Dis. Model. Mech.* **4**, 842–9.

Na, J., Musselman, L. P., Pendse, J., Baranski, T. J., Bodmer, R., Ocorr, K. and Cagan, R. (2013). A Drosophila model of high sugar diet-induced cardiomyopathy. *PLoS Genet.* **9**, e1003175.

Nahm, M., Kim, S., Paik, S. K., Lee, M., Lee, S., Lee, Z. H., Kim, J., Lee, D. and Bae, Y. C.

(2010). dCIP4 (Drosophila Cdc42-interacting protein 4) restrains synaptic growth by inhibiting the secretion of the retrograde Glass bottom boat signal. *J Neurosci* **30**, 8138–8150.

Nakae, J., Kido, Y. and Accili, D. (2001). Distinct and overlapping functions of insulin and IGF-I receptors. *Endocr. Rev.* **22**, 818–35.

Nellen, D., Burke, R., Struhl, G. and Basler, K. (1996). Direct and long-range action of a DPP morphogen gradient. *Cell* **85**, 357–68.

Ng, J. (2008). TGF-beta signals regulate axonal development through distinct Smad-independent mechanisms. *Development* **135**, 4025–35.

Ng, M., Diaz-Benjumea, F. J., Vincent, J. P., Wu, J. and Cohen, S. M. (1996). Specification of the wing by localized expression of wingless protein. *Nature* **381**, 316–8.

Nijhout, H. F. (2003). The control of body size in insects. *Dev. Biol.* **261**, 1–9.

Nijhout, H. F. and Callier, V. (2015). Developmental mechanisms of body size and wing-body scaling in insects. *Annu. Rev. Entomol.* **60**, 141–56.

Nijhout, H. F. and Grunert, L. W. (2010). The Cellular and Physiological Mechanism of Wing-Body Scaling in Manduca sexta. *Science (80-.).* **330**, 1693–1695.

Nijhout, H. F., Riddiford, L. M., Mirth, C., Shingleton, A. W., Suzuki, Y. and Callier, V. (2014). The developmental control of size in insects. *Wiley Interdiscip. Rev. Dev. Biol.* **3**, 113–134.

Norman, M., Vuilleumier, R., Springhorn, A., Gawlik, J. and Pyrowolakis, G. (2016). Pentagone internalises glypicans to fine-tune multiple signalling pathways. *Elife* **5**,.

Nylin, S. and Gotthard, K. (1998). Plasticity in Life-History Traits. *Annu. Rev. Entomol.* **43**, 63–83.

O'Connor, M. B., Umulis, D., Othmer, H. G. and Blair, S. S. (2006). Shaping BMP morphogen gradients in the Drosophila embryo and pupal wing. *Development* **133**, 183–93.

Oconnor-Giles, K. M., Ho, L. L. and Ganetzky, B. (2008). Nervous wreck interacts with thickveins and the endocytic machinery to attenuate retrograde BMP signaling during synaptic growth. *Neuron* **58**, 507–518.

Ogiso, Y., Tsuneizumi, K., Masuda, N., Sato, M. and Tabata, T. (2011). Robustness of the Dpp morphogen activity gradient depends on negative feedback regulation by the inhibitory Smad, Dad. *Dev. Growth Differ.* **53**, 668–78.

Oh, H. and Irvine, K. D. (2010). Yorkie: the final destination of Hippo signaling. *Trends Cell Biol.* **20**, 410–7.

Oh, H. and Irvine, K. D. (2011). Cooperative regulation of growth by Yorkie and Mad through bantam. *Dev. Cell* **20**, 109–22.

Oldham, S., Montagne, J., Radimerski, T., Thomas, G. and Hafen, E. (2000). Genetic and biochemical characterization of dTOR, the Drosophila homolog of the target of rapamycin. *Genes Dev.* **14**, 2689–94.

Park, D., Veenstra, J. A., Park, J. H. and Taghert, P. H. (2008). Mapping peptidergic cells in Drosophila: where DIMM fits in. *PLoS One* **3**, e1896.

Parker, N. F. and Shingleton, A. W. (2011). The coordination of growth among Drosophila organs in response to localized growth-perturbation. *Dev. Biol.* **357**, 318–25.

Parker, L., Ellis, J. E., Nguyen, M. Q. and Arora, K. (2006). The divergent TGF-β ligand Dawdle

utilizes an activin pathway to influence axon guidance in Drosophila. *Development* **133**, 4981–4991.

Pentek, J., Parker, L., Wu, A. and Arora, K. (2009). Follistatin preferentially antagonizes activin rather than BMP signaling in Drosophila. *Genesis* **47**, 261–73.

Penzo-Méndez, A. I. and Stanger, B. Z. (2015). Organ-Size Regulation in Mammals. *Cold Spring Harb. Perspect. Biol.* **7**,.

Pera, E. M., Ikeda, A., Eivers, E. and De Robertis, E. M. (2003). Integration of IGF, FGF, and anti-BMP signals via Smad1 phosphorylation in neural induction. *Genes Dev.* **17**, 3023–8.

Peterson, A. J. and O'Connor, M. B. (2013). Activin receptor inhibition by Smad2 regulates Drosophila wing disc patterning through BMP-response elements. *Development* **140**, 649–59.

Peterson, A. J. and O'Connor, M. B. (2014). Strategies for exploring TGF-β signaling in Drosophila. *Methods* **68**, 183–93.

Peterson, A. J., Jensen, P. A., Shimell, M., Stefancsik, R., Wijayatonge, R., Herder, R., Raftery, L. A. and O'Connor, M. B. (2012). R-Smad competition controls activin receptor output in Drosophila. *PLoS One* **7**, e36548.

Piccioli, Z. D. and Littleton, J. T. (2014). Retrograde BMP signaling modulates rapid activity-dependent synaptic growth via presynaptic LIM kinase regulation of cofilin. *J Neurosci* **34**, 4371–4381.

Pinal, N., Calleja, M. and Morata, G. (2019). Pro-apoptotic and pro-proliferation functions of the JNK pathway of Drosophila: roles in cell competition, tumorigenesis and regeneration. *Open Biol.* **9**, 180256.

Prober, D. A. and Edgar, B. A. (2000). Ras1 promotes cellular growth in the Drosophila wing. *Cell* **100**, 435–46.

Prokop, A. (2006). Organization of the efferent system and structure of neuromuscular junctions in Drosophila. *Int. Rev. Neurobiol.* **75**, 71–90.

Prokop, A. and Meinertzhagen, I. A. (2006). Development and structure of synaptic contacts in Drosophila. *Semin. Cell Dev. Biol.* **17**, 20–30.

Quianzon, C. C. and Cheikh, I. (2012). History of insulin. *J. community Hosp. Intern. Med. Perspect.* **2**,.

Ralston, A. and Blair, S. S. (2005). Long-range Dpp signaling is regulated to restrict BMP signaling to a crossvein competent zone. *Dev. Biol.* **280**, 187–200.

Ramírez-Weber, F. a and Kornberg, T. B. (1999). Cytonemes: cellular processes that project to the principal signaling center in Drosophila imaginal discs. *Cell* **97**, 599–607.

Rauskolb, C., Sun, S., Sun, G., Pan, Y. and Irvine, K. D. (2014). Cytoskeletal tension inhibits Hippo signaling through an Ajuba-Warts complex. *Cell* **158**, 143–156.

Rawson, J. M., Lee, M., Kennedy, E. L. and Selleck, S. B. (2003). Drosophila neuromuscular synapse assembly and function require the TGF-beta type I receptor saxophone and the transcription factor Mad. *J Neurobiol* **55**, 134–150.

Recasens-Alvarez, C., Ferreira, A. and Milán, M. (2017). JAK/STAT controls organ size and fate specification by regulating morphogen production and signalling. *Nat. Commun.* **8**, 13815.

Ren, X., Sun, J., Housden, B. E., Hu, Y., Roesel, C., Lin, S., Liu, L.-P., Yang, Z., Mao, D.,

Sun, L., et al. (2013). Optimized gene editing technology for Drosophila melanogaster using germ line-specific Cas9. *Proc. Natl. Acad. Sci. U. S. A.* **110**, 19012–7.

Restrepo, S., Zartman, J. J. and Basler, K. (2014). Coordination of patterning and growth by the morphogen DPP. *Curr. Biol.* **24**, R245–R255.

Rewitz, K. F., Yamanaka, N., Gilbert, L. I. and O'Connor, M. B. (2009). The insect neuropeptide PTTH activates receptor tyrosine kinase torso to initiate metamorphosis. *Science* **326**, 1403–5.

Rewitz, K. F., Yamanaka, N. and O'Connor, M. B. (2013). Developmental checkpoints and feedback circuits time insect maturation. *Curr. Top. Dev. Biol.* **103**, 1–33.

Riddiford, L. M. (1993). Hormone receptors and the regulation of insect metamorphosis. *Receptor* **3**, 203–9.

Riddiford, L. M., Truman, J. W., Mirth, C. K. and Shen, Y.-C. (2010). A role for juvenile hormone in the prepupal development of Drosophila melanogaster. *Development* **137**, 1117–26.

Rodgers, B. D. and Eldridge, J. A. (2015). Reduced circulating GDF11 is unlikely responsible for age-dependent changes in mouse heart, muscle, and brain. *Endocrinology* **156**, 3885–3888.

Rodriguez, J., Vernus, B., Chelh, I., Cassar-Malek, I., Gabillard, J. C., Hadj Sassi, A., Seiliez, I., Picard, B. and Bonnieu, A. (2014). Myostatin and the skeletal muscle atrophy and hypertrophy signaling pathways. *Cell. Mol. Life Sci.* **71**, 4361–71.

Rosenfeld, L. (2002). Insulin: discovery and controversy. *Clin. Chem.* **48**, 2270–88.

Roy, S., Hsiung, F. and Kornberg, T. B. (2011). Specificity of Drosophila cytonemes for distinct signaling pathways. *Science* **332**, 354–8.

Roy, S., Huang, H., Liu, S. and Kornberg, T. B. (2014). Cytoneme-mediated contact-dependent transport of the Drosophila decapentaplegic signaling protein. *Science* **343**, 1244624.

Rulifson, E. J., Kim, S. K. and Nusse, R. (2002). Ablation of insulin-producing neurons in flies: growth and diabetic phenotypes. *Science* **296**, 1118–20.

Ryoo, H. D., Gorenc, T. and Steller, H. (2004). Apoptotic cells can induce compensatory cell proliferation through the JNK and the Wingless signaling pathways. *Dev. Cell* **7**, 491–501.

Sabatini, D. M. (2017). Twenty-five years of mTOR: Uncovering the link from nutrients to growth. *Proc. Natl. Acad. Sci. U. S. A.* **114**, 11818–11825.

Saitoh, M., Shirakihara, T., Fukasawa, A., Horiguchi, K., Sakamoto, K., Sugiya, H., Beppu, H., Fujita, Y., Morita, I., Miyazono, K., et al. (2013). Basolateral BMP Signaling in Polarized Epithelial Cells. *PLoS One* **8**, e62659.

Sánchez, L. and Guerrero, I. (2001). The development of the Drosophila genital disc. *BioEssays* **23**, 698–707.

Sánchez, L., Gorfinkiel, N. and Guerrero, I. (2001). Sex determination genes control the development of the Drosophila genital disc, modulating the response to Hedgehog, Wingless and Decapentaplegic signals. *Development* **128**, 1033–1043.

Sander, V., Eivers, E., Choi, R. H. and De Robertis, E. M. (2010). Drosophila Smad2 opposes Mad signaling during wing vein development. *PLoS One* **5**, e10383.

Santabárbara-Ruiz, P., López-Santillán, M., Martínez-Rodríguez, I., Binagui-Casas, A., Pérez, L., Milán, M., Corominas, M. and Serras, F. (2015). ROS-Induced JNK and p38

Signaling Is Required for Unpaired Cytokine Activation during Drosophila Regeneration. *PLoS Genet.* **11**, e1005595.

Sartori, R., Schirwis, E., Blaauw, B., Bortolanza, S., Zhao, J., Enzo, E., Stantzou, A., Mouisel, E., Toniolo, L., Ferry, A., et al. (2013). BMP signaling controls muscle mass. *Nat. Genet.* **45**, 1309–18.

Saucedo, L. J., Gao, X., Chiarelli, D. A., Li, L., Pan, D. and Edgar, B. A. (2003). Rheb promotes cell growth as a component of the insulin/TOR signalling network. *Nat. Cell Biol.* **5**, 566–71.

Schindelin, J., Arganda-Carreras, I., Frise, E., Kaynig, V., Longair, M., Pietzsch, T., Preibisch, S., Rueden, C., Saalfeld, S., Schmid, B., et al. (2012). Fiji: an open-source platform for biological-image analysis. *Nat. Methods* **9**, 676–82.

Schmidt-Nielsen, K. (1984). *Scaling*. Cambridge: Cambridge University Press.

Schwank, G., Restrepo, S. and Basler, K. (2008). Growth regulation by Dpp: an essential role for Brinker and a non-essential role for graded signaling levels. *Development* **135**, 4003–4013.

Schwank, G., Dalessi, S., Yang, S.-F., Yagi, R., de Lachapelle, A. M., Affolter, M., Bergmann, S. and Basler, K. (2011). Formation of the long range Dpp morphogen gradient. *PLoS Biol.* **9**, e1001111.

Sebo, Z. L., Lee, H. B., Peng, Y. and Guo, Y. (2014). A simplified and efficient germline-specific CRISPR/Cas9 system for Drosophila genomic engineering. *Fly (Austin).* **8**, 52–7.

Serpe, M. and O'Connor, M. B. (2006). The metalloprotease tolloid-related and its TGF-beta-like substrate Dawdle regulate Drosophila motoneuron axon guidance. *Development* **133**, 4969–79.

Setiawan, L., Pan, X., Woods, A. L., O'Connor, M. B. and Hariharan, I. K. (2018). The BMP2/4 ortholog Dpp can function as an inter-organ signal that regulates developmental timing. *Life Sci. alliance* **1**, e201800216.

Sharma, R. P. and Chopra, V. L. (1976). Effect of the Wingless (wg1) mutation on wing and haltere development in Drosophila melanogaster. *Dev. Biol.* **48**, 461–5.

Shim, K. S. (2015). Pubertal growth and epiphyseal fusion. *Ann. Pediatr. Endocrinol. Metab.* **20**, 8–12.

Shimell, M., Pan, X., Martin, F. A., Ghosh, A. C., Leopold, P., O'Connor, M. B. and Romero, N. M. (2018). Prothoracicotropic hormone modulates environmental adaptive plasticity through the control of developmental timing. *Development* **145**,.

Shimmi, O., Umulis, D., Othmer, H. and O'Connor, M. B. (2005). Facilitated transport of a Dpp/Scw heterodimer by Sog/Tsg leads to robust patterning of the Drosophila blastoderm embryo. *Cell* **120**, 873–86.

Shingleton, A. W. and Frankino, W. A. (2013). New perspectives on the evolution of exaggerated traits. *Bioessays* **35**, 100–7.

Shingleton, A. W., Frankino, W. A., Flatt, T., Nijhout, H. F. and Emlen, D. J. (2007). Size and shape: the developmental regulation of static allometry in insects. *Bioessays* **29**, 536–48.

Shingleton, A. W., Estep, C. M., Driscoll, M. V and Dworkin, I. (2009). Many ways to be small: different environmental regulators of size generate distinct scaling relationships in Drosophila melanogaster. *Proceedings. Biol. Sci.* **276**, 2625–33.

Shlevkov, E. and Morata, G. (2012). A dp53/JNK-dependant feedback amplification loop is essential for the apoptotic response to stress in Drosophila. *Cell Death Differ.* **19**, 451–60.

Siegmund, T. and Korge, G. (2001). Innervation of the ring gland of Drosophila melanogaster. *J. Comp. Neurol.* **431**, 481–91.

Simpson, P. and Schneiderman, H. A. (1975). Isolation of temperature sensitive mutations blocking clone development inDrosophila melanogaster, and the effects of a temperature sensitive cell lethal mutation on pattern formation in imaginal discs. *Wilhelm Roux's Arch. Dev. Biol.* **178**, 247–275.

Simpson, P., Berreur, P. and Berreur-Bonnenfant, J. (1980). The initiation of pupariation in Drosophila: dependence on growth of the imaginal discs. *J. Embryol. Exp. Morphol.* **57**, 155–65.

Song, W., Cheng, D., Hong, S., Sappe, B., Hu, Y., Wei, N., Zhu, C., O'Connor, M. B., Pissios, P. and Perrimon, N. (2017a). Midgut-Derived Activin Regulates Glucagon-like Action in the Fat Body and Glycemic Control. *Cell Metab.* **25**, 386–399.

Song, W., Owusu-Ansah, E., Hu, Y., Cheng, D., Ni, X., Zirin, J. and Perrimon, N. (2017b). Activin signaling mediates muscle-to-adipose communication in a mitochondria dysfunction-associated obesity model. *Proc. Natl. Acad. Sci.* **114**, 8596–8601.

Sopko, R. and Perrimon, N. (2013). Receptor Tyrosine Kinases in Drosophila Development. *Cold Spring Harb. Perspect. Biol.* **5**, a009050–a009050.

Sopory, S., Kwon, S., Wehrli, M. and Christian, J. L. (2010). Regulation of Dpp activity by tissue-specific cleavage of an upstream site within the prodomain. *Dev. Biol.* **346**, 102–12.

Spence, A. J. (2009). Scaling in biology. *Curr. Biol.* **19**, R57-61.

Spencer, F. A., Hoffmann, F. M. and Gelbart, W. M. (1982). Decapentaplegic: a gene complex affecting morphogenesis in Drosophila melanogaster. *Cell* **28**, 451–61.

Stern, D. L. and Emlen, D. J. (1999). The developmental basis for allometry in insects. *Development* **126**, 1091–1101.

Stieper, B. C., Kupershtok, M., Driscoll, M. V and Shingleton, A. W. (2008). Imaginal discs regulate developmental timing in Drosophila melanogaster. *Dev. Biol.* **321**, 18–26.

Stocker, H., Radimerski, T., Schindelholz, B., Wittwer, F., Belawat, P., Daram, P., Breuer, S., Thomas, G. and Hafen, E. (2003). Rheb is an essential regulator of S6K in controlling cell growth in Drosophila. *Nat. Cell Biol.* **5**, 559–65.

Sulkowski, M., Kim, Y.-J. and Serpe, M. (2014). Postsynaptic glutamate receptors regulate local BMP signaling at the Drosophila neuromuscular junction. *Development* **141**, 436–47.

Swarup, S. and Verheyen, E. M. (2012). Wnt/Wingless signaling in Drosophila. *Cold Spring Harb. Perspect. Biol.* **4**,.

Sweeney, S. T. and Davis, G. W. (2002). Unrestricted synaptic growth in spinster-a late endosomal protein implicated in TGF-beta-mediated synaptic growth regulation. *Neuron* **36**, 403–416.

Tan, P. K., Wang, J., Littler, P.-L. H., Wong, K. K., Sweetnam, T. A., Keefe, W., Nash, N. R., Reding, E. C., Piu, F., Brann, M. R., et al. (2007). Monitoring interactions between receptor tyrosine kinases and their downstream effector proteins in living cells using bioluminescence resonance energy transfer. *Mol. Pharmacol.* **72**, 1440–6.

Tang, H. Y., Smith-Caldas, M. S. B., Driscoll, M. V, Salhadar, S. and Shingleton, A. W.

(2011). FOXO regulates organ-specific phenotypic plasticity in Drosophila. *PLoS Genet.* **7**, e1002373.

Teleman, A. A. (2009). Molecular mechanisms of metabolic regulation by insulin in Drosophila. *Biochem. J.* **425**, 13–26.

Teleman, a a and Cohen, S. M. (2000). Dpp gradient formation in the Drosophila wing imaginal disc. *Cell* **103**, 971–80.

Thomas, H. E., Stunnenberg, H. G. and Stewart, A. F. (1993). Heterodimerization of the Drosophila ecdysone receptor with retinoid X receptor and ultraspiracle. *Nature* **362**, 471–5.

Ting, C.-Y., Herman, T., Yonekura, S., Gao, S., Wang, J., Serpe, M., O'Connor, M. B., Zipursky, S. L. and Lee, C.-H. (2007). Tiling of r7 axons in the Drosophila visual system is mediated both by transduction of an activin signal to the nucleus and by mutual repulsion. *Neuron* **56**, 793–806.

Ting, C.-Y., McQueen, P. G., Pandya, N., Lin, T.-Y., Yang, M., Reddy, O. V., O'Connor, M. B., McAuliffe, M. and Lee, C.-H. (2014). Photoreceptor-derived activin promotes dendritic termination and restricts the receptive fields of first-order interneurons in Drosophila. *Neuron* **81**, 830–846.

Trendelenburg, A. U., Meyer, A., Rohner, D., Boyle, J., Hatakeyama, S. and Glass, D. J. (2009). Myostatin reduces Akt/TORC1/p70S6K signaling, inhibiting myoblast differentiation and myotube size. *Am. J. Physiol. Cell Physiol.* **296**, C1258-70.

Tsuneizumi, K., Nakayama, T., Kamoshida, Y., Kornberg, T. B., Christian, J. L. and Tabata, T. (1997). Daughters against dpp modulates dpp organizing activity in Drosophila wing development. *Nature* **389**, 627–31.

Tuck, S. (2014). The control of cell growth and body size in Caenorhabditis elegans. *Exp. Cell Res.* **321**, 71–6.

Twitty, V. C. and Schwind, J. L. (1931). The growth of eyes and limbs transplanted heteroplastically between two species of Amblystoma. *J. Exp. Zool.* **59**, 61–86.

Upadhyay, A., Moss-Taylor, L., Kim, M., Ghosh, A. C. and O'Connor, M. B. (2017). TGF-β Family Signaling in Drosophila. *Cold Spring Harb. Perspect. Biol.* **9**,.

Uyehara, C. M. and McKay, D. J. (2019). Direct and widespread role for the nuclear receptor EcR in mediating the response to ecdysone in Drosophila. *Proc. Natl. Acad. Sci.* 201900343.

Vuilleumier, R., Springhorn, A., Patterson, L., Koidl, S., Hammerschmidt, M., Affolter, M. and Pyrowolakis, G. (2010). Control of Dpp morphogen signalling by a secreted feedback regulator. *Nat. Publ. Gr.* **12**, 611–617.

Wang, S., Tsun, Z.-Y., Wolfson, R. L., Shen, K., Wyant, G. A., Plovanich, M. E., Yuan, E. D., Jones, T. D., Chantranupong, L., Comb, W., et al. (2015). The amino acid transporter SLC38A9 is a key component of a lysosomal membrane complex that signals arginine sufficiency to mTORC1. *Science* **347**, 188–94.

Wartlick, O., Mumcu, P., Kicheva, a, Bittig, T., Seum, C., Jülicher, F. and González-Gaitán, M. (2011a). Dynamics of Dpp signaling and proliferation control. *Science* **331**, 1154–1159.

Wartlick, O., Mumcu, P., Jülicher, F. and González-Gaitán, M. (2011b). Understanding morphogenetic growth control -- lessons from flies. *Nat. Rev. Mol. Cell Biol.* **12**, 594–604.

Weiss, A., Charbonnier, E., Ellertsdóttir, E., Tsirigos, A., Wolf, C., Schuh, R., Pyrowolakis, G. and Affolter, M. (2010). A conserved activation element in BMP signaling during

Drosophila development. *Nat. Struct. Mol. Biol.* **17**, 69–76.

Williams, E. K., Chang, R. B., Strochlic, D. E., Umans, B. D., Lowell, B. B. and Liberles, S. D. (2016). Sensory Neurons that Detect Stretch and Nutrients in the Digestive System. *Cell* **166**, 209–221.

Willsey, H. R., Zheng, X., Carlos Pastor-Pareja, J., Willsey, A. J., Beachy, P. A. and Xu, T. (2016). Localized JNK signaling regulates organ size during development. *Elife* **5**,.

Winbanks, C. E., Chen, J. L., Qian, H., Liu, Y., Bernardo, B. C., Beyer, C., Watt, K. I., Thomson, R. E., Connor, T., Turner, B. J., et al. (2013). The bone morphogenetic protein axis is a positive regulator of skeletal muscle mass. *J. Cell Biol.* **203**, 345–57.

Wolfman, N. M., McPherron, A. C., Pappano, W. N., Davies, M. V, Song, K., Tomkinson, K. N., Wright, J. F., Zhao, L., Sebald, S. M., Greenspan, D. S., et al. (2003). Activation of latent myostatin by the BMP-1/tolloid family of metalloproteinases. *Proc. Natl. Acad. Sci. U. S. A.* **100**, 15842–6.

Wolfson, R. L. and Sabatini, D. M. (2017). The Dawn of the Age of Amino Acid Sensors for the mTORC1 Pathway. *Cell Metab.* **26**, 301–309.

Wolfson, R. L., Chantranupong, L., Saxton, R. A., Shen, K., Scaria, S. M., Cantor, J. R. and Sabatini, D. M. (2016). Sestrin2 is a leucine sensor for the mTORC1 pathway. *Science* **351**, 43–8.

Wood, A. R., Esko, T., Yang, J., Vedantam, S., Pers, T. H., Gustafsson, S., Chu, A. Y., Estrada, K., Luan, J., Kutalik, Z., et al. (2014). Defining the role of common variation in the genomic and biological architecture of adult human height. *Nat. Genet.* **46**, 1173–86.

Wu, Q., Wen, T., Lee, G., Park, J. H., Cai, H. N. and Shen, P. (2003a). Developmental control of foraging and social behavior by the Drosophila neuropeptide Y-like system. *Neuron* **39**, 147–61.

Wu, S., Huang, J., Dong, J. and Pan, D. (2003b). hippo encodes a Ste-20 family protein kinase that restricts cell proliferation and promotes apoptosis in conjunction with salvador and warts. *Cell* **114**, 445–56.

Wu, Q., Zhang, Y., Xu, J. and Shen, P. (2005). Regulation of hunger-driven behaviors by neural ribosomal S6 kinase in Drosophila. *Proc. Natl. Acad. Sci. U. S. A.* **102**, 13289–94.

Wyant, G. A., Abu-Remaileh, M., Wolfson, R. L., Chen, W. W., Freinkman, E., Danai, L. V, Vander Heiden, M. G. and Sabatini, D. M. (2017). mTORC1 Activator SLC38A9 Is Required to Efflux Essential Amino Acids from Lysosomes and Use Protein as a Nutrient. *Cell* **171**, 642-654.e12.

Yamanaka, N., Rewitz, K. F. and O'Connor, M. B. (2013a). Ecdysone control of developmental transitions: lessons from Drosophila research. *Annu. Rev. Entomol.* **58**, 497–516.

Yamanaka, N., Romero, N. M., Martin, F. A., Rewitz, K. F., Sun, M., O'Connor, M. B. and Léopold, P. (2013b). Neuroendocrine control of Drosophila larval light preference. *Science* **341**, 1113–6.

Yao, T. P., Forman, B. M., Jiang, Z., Cherbas, L., Chen, J. D., McKeown, M., Cherbas, P. and Evans, R. M. (1993). Functional ecdysone receptor is the product of EcR and Ultraspiracle genes. *Nature* **366**, 476–9.

Yu, X. M., Gutman, I., Mosca, T. J., Iram, T., Ozkan, E., Garcia, K. C., Luo, L. and Schuldiner, O. (2013). Plum, an immunoglobulin superfamily protein, regulates axon pruning by facilitating TGF-β signaling. *Neuron* **78**, 456–68.

Zagorodnyuk, V. P., Chen, B. N. and Brookes, S. J. (2001). Intraganglionic laminar endings are mechano-transduction sites of vagal tension receptors in the guinea-pig stomach. *J. Physiol.* **534**, 255–68.

Zamani, N. and Brown, C. W. (2011). Emerging roles for the Transforming Growth Factor-β superfamily in regulating adiposity and energy expenditure. *Endocr. Rev.* **32**, 387–403.

Zecca, M. and Struhl, G. (2002). Control of growth and patterning of the Drosophila wing imaginal disc by EGFR-mediated signaling. *Development* **129**, 1369–76.

Zecca, M., Basler, K. and Struhl, G. (1995). Sequential organizing activities of engrailed, hedgehog and decapentaplegic in the Drosophila wing. *Development* **121**, 2265–78.

Zheng, X., Wang, J., Haerry, T. E., Wu, A. Y.-H., Martin, J., O'Connor, M. B., Lee, C.-H. J. and Lee, T. (2003). TGF-beta signaling activates steroid hormone receptor expression during neuronal remodeling in the Drosophila brain. *Cell* **112**, 303–315.

Zhou, X., Wang, J. L., Lu, J., Song, Y., Kwak, K. S., Jiao, Q., Rosenfeld, R., Chen, Q., Boone, T., Simonet, W. S., et al. (2010). Reversal of cancer cachexia and muscle wasting by ActRIIB antagonism leads to prolonged survival. *Cell* **142**, 531–43.

Zhou, S., Lo, W.-C., Suhalim, J. L., Digman, M. a, Gratton, E., Nie, Q. and Lander, A. D. (2012). Free extracellular diffusion creates the Dpp morphogen gradient of the Drosophila wing disc. *Curr. Biol.* **22**, 668–75.

Zhu, C. C., Boone, J. Q., Jensen, P. A., Hanna, S., Podemski, L., Locke, J., Doe, C. Q. and O'Connor, M. B. (2008). Drosophila Activin- and the Activin-like product Dawdle function redundantly to regulate proliferation in the larval brain. *Development* **135**, 513–521.